

THE RESISTANCE WELDING OF  
COATED STEELS

PHILIP NEIL WHATELEY

Master of Philosophy

THE UNIVERSITY OF ASTON IN BIRMINGHAM

July 1986

This copy of the thesis has been supplied on condition that anyone who consults it is understood to recognise that its copyright rests with its author and that no quotation from the thesis and no information derived from it may be published without the author's prior, written consent.

The University of Aston in Birmingham

The Resistance Welding of Coated Steels

Philip Neil Whateley

Master of Philosophy

July 1986

#### SUMMARY

Weldability and electrode life tests were performed on a range of spot welded zinc coated steels and it was concluded that variations in coating weight, composition and surface finish caused little significant change in either welding characteristics or electrode life.

Simple dynamic-resistance monitoring techniques were assessed and were found to be unacceptable for most of these materials when based on a single, maximum-deviation criterion for rejection.

However, a new method has been developed for the statistical assessment of monitor reliability.

#### Key Words

Coated Steels; Resistance Welding; Weld Monitoring.

## ACKNOWLEDGEMENTS

I would like to thank the members of the academic and technical staff of the University of Aston in Birmingham for their help and co-operation, in particular my supervisor, Dr.D.R.Andrews, for his guidance, and Mr.I.J.Wincup and Mr.K.Burt for their invaluable technical assistance.

I would also like to express my gratitude to Dr.N.T.Williams of British Steel Corporation Port Talbot, Mr.J.Broomhead of Rubery Owen Group Technology Ltd. and to Dr.David Hodgeson of the Department of Mechanical Engineering, University of Birmingham, and their colleagues.

Finally I would like to acknowledge the financial support of the Science and Engineering Research Council.

## CONTENTS

	Page
1 : INTRODUCTION	
1.1 : Resistance Welding and Quality Control	12
1.2 : Coated Steels and Resistance Welding	17
2 : LITERATURE SURVEY	20
3 : EXPERIMENTAL	
3.1 : Materials	23
3.2 : Welding Equipment	24
3.3 : Dynamic Resistance Monitoring	26
3.4 : Weldability Determination	29
3.5 : Electrode Life Determination	30
4 : RESULTS	
4.1 : Galvatite Normal Spangle Material	32
4.2 : Galvatite Iron - Zinc Material	60
4.3 : Electro zinc "Zintec" Material	81
4.4 : Metallography	91
5 : DISCUSSION	
5.1 : Weldability	94
5.2 : Electrode Life	96
5.3 : Monitor Reliability	103
6 : CONCLUSIONS	130
PLATES	132
REFERENCES	162

## FIGURES

Figure No.		Page
1	Resistance welding processes	15
2	Common Electrode Types	27
3	Schematic Dynamic Resistance Curve	28
4	Weldability Lobe, 0.5 mm Galvatite	33
5	Weldability Lobe, 0.9 mm Galvatite	33
6	Weldability Lobe, 1.2 mm Galvatite	34
7	Weldability Lobe, 1.2 mm Galvatite	35
8	Weldability Lobe, 1.2 mm Galvatite	35
9a	Pulled slug orientation	36
9b	Through weld crack	36
10a	Erichson fracture: Normal	37
10b	Erichson fracture: Oriented	37
11	Weldability Lobe : B.S.C.	39
12a	Tensile shear strength against weld current : W.C.M.J. G275	41
12b	Tensile shear strength against weld time : W.C.M.J. G275	41
13	Tensile shear strength against number of welds : W.C.M.J. G275	43
14	Variation in electrode tip diameter	44
15a	Number of defective welds against number of welds : W.C.M.J. G275	46
15b	Number of defective welds against number of welds : B.S.C. G275	46
16	Error number against weld number for W.C.M.J. G275	47

Figure No.		Page
17	Error number against weld strength for W.C.M.J. G275	48
18	Distribution of error numbers for good and bad welds	49
19	Weldability Lobes showing effect of tip spread	50
20	Weldability Lobes : B.S.C. G275	53
21	Weldability Lobe : B.S.C. G275	54
22	Weldability "carpet plot" B.S.C. G275	55
23	Variation in tensile shear strength with weld current and time : B.S.C. G275	56
24	Electrode tip diameter against number of welds : B.S.C. G275	57
25	Weld nugget diameter against number of welds : B.S.C. G275	58
26	Tensile shear strength against number of welds : B.S.C. G275	59
27	Variation in tensile shear strength with electrode life	61
28	Error number against weld number for B.S.C. G275	62
29	Error number against weld size for B.S.C. G275	63
30	Distribution of error numbers for good and bad welds	64
31	Weldability Lobes IZ	65
32	Weldability Lobe IZ	66

Figure No.		Page
33	Nugget diameter against number of welds : 1.0 mm IZ	67
34	Tip diameter against number of welds : 1.0 mm IZ	69
35	Weldability Lobes : B.S.C. IZ	70
36	Weldability Lobe : B.S.C. IZ	71
37	Weldability carpet plot : B.S.C. IZ	72
38	Number of defective welds against number of welds : B.S.C. IZ	73
39	Nugget diameter against number of welds : 1.2 mm IZ	74
40	Tip diameter against number of welds 1.2 mm IZ	75
41	Error number against number of welds for 1.2 mm IZ	76
42	Error number against weld diameter for 1.2 mm IZ	77
43	Distribution of error numbers for good and bad welds	78
44	Weldability Lobes : Zintec	83
45	Weld diameter against number of welds for 1.2 mm W.C.M.J. Zintec	85
46	Electrode tip diameter against number of welds	86
47	Number of defective welds for 1.2 mm Zintec	87
48	Error number against weld number for 1.2 mm Zintec	88

Figure No.		Page
49	Error number against weld size for Zintec	89
50	Distribution of error numbers between good and bad welds	90
51	Copper - zinc equilibrium diagram	100
52	Phases present on electrode tips	101
53	Error number against number of welds (schematic)	105
54	Error number against weld quality (schematic)	107
55	Acceptance and rejection levels for W.C.M.J. G275	110
56	Acceptance and rejection for B.S.C. G275	111
57	Acceptance and rejection for Galvatite IZ	112
58	Acceptance and rejection for Zintec	113
59	Normal distribution curves for W.C.M.J. G275	118
60	Normal distribution curves for B.S.C. G275	119
61	Normal distribution curves for B.S.C. IZ	120
62	Normal distribution curves for W.C.M.J. Zintec	121
63	Confidence intervals for W.C.M.J. G275	123
64	Confidence intervals for B.S.C. G275	124
65	Confidence intervals for B.S.C. IZ	125
66	Confidence intervals for W.C.M.J. Zintec	126

## TABLES

Table No.		Page
1	Analysis of W.C.M.J. G275	40
2	Welding conditions for G275 materials	42
3	Analysis of B.S.C. G275	52
4	Welding conditions for B.S.C. IZ	79
5	Analysis of B.S.C. IZ	80
6	Analysis of W.C.M.J. Zintec	82
7	Welding conditions for W.C.M.J. Zintec	84
8	Electrode lives	98
9	Microhardness in Cu - Zn diffusion couple	102
10	Monitor error numbers for 95% rejection of bad welds	114
11	Monitor reliability percentages	115
12	Mean and standard deviations for good and bad welds	116
13	Selected values of $Z_{\alpha/2}$	122
14	Percentage reliabilities for weld monitor	127

## PLATES

Plate No.		Page
1	British Federal single-phase pedestal welder	133
2	British Federal S3 HUD/3 control panel	133
3	Position of voltage terminals on electrodes	135
4	Position of Hall-effect probe	135
5	Resistance welding monitor	137
6	Pulled slug type failure	137
7	Interface shear type failure	139
8	Pulled slug failure with expulsion	139
9	Acceptable weld in spangle material	141
10	Commercially produced acceptable weld	141
11	Weld with low penetration	143
12	Weld with no fusion	143
13	Expulsion from weld	145
14	Expulsion from weld with extreme indentation	145
15	Surface crack in high heat weld	147
16	Structure of Matthey 328 electrode material	149
17	Surface of electrode	149
18	Cracking and spalling of electrode surface	151
19	Mechanism of tip spread	153
20	Mechanism of tip spread (electron image)	155
21	Surface of electrode tip (electron image)	155
22	Position of line scan across electrode surface	157
23	Zinc line concentration profile	157
24	Copper line concentration profile	159

Plate No.		Page
25	Iron line concentration profile	159
26	Coating morphology for galvanised steel	161
27	Coating morphology for electrozinc steel	161

## 1 INTRODUCTION

### 1.1 Resistance Welding and Quality Control

Resistance welding was discovered in 1877 by Professor Elihu Thompson in the U.S.A. when he was experimenting with high current discharges from Leyden jars. Patents were taken out in 1886 and the spot welding process was developed in 1898. Resistance welding processes were only slowly adopted by industry and there was little use of the process prior to the First World War. The years during and since the Second World War have seen tremendous progress in the development of resistance welding processes, due largely to increased demands and to improvements in electrical circuitry and timing devices.

Resistance welding is a general term used to describe a group of welding processes which depend on the passage of a high electric current for the generation of heat.

Resistance welding is defined as any welding process in which, at some stage, force is applied to surfaces in contact and in which the heat for welding is produced by the passage of an electric current through the electrical resistance at, or adjacent to, these surfaces. No filler metal is used (except in resistance brazing) and fluxes and protective atmospheres are seldom used.

The amount of heat produced is determined by the relationship between the electrical resistance and the current

being passed and by the time for which the current is allowed to flow;

$$Q \propto I^2 R t$$

where  $Q$  = heat,  $I$  = current,  $R$  = resistance,  $t$  = the duration of current flow.

The resistance values are commonly very low and the weld time is required to be very short. This results in the need for exceptionally high welding currents up to about 20,000 Amps. Equipment capable of delivering such high currents for closely controlled brief intervals of time is expensive and resistance welding processes are therefore particularly suitable for mass production applications where the expense is justified.

Most metals can be resistance welded provided that correct conditions of current and time are selected. Pure copper and silver present difficulties because of their very high thermal and electrical conductivities. These difficulties can be overcome to a certain extent with good equipment or by alloying the metal to increase its resistance.

The main advantages of the resistance welding processes may be summarised as follows:

- i) Suitability for mass production
- ii) accurate controls which can be pre-set
- iii) no need for filler metal, fluxes or atmosphere
- iv) applicability to thin materials and complex shapes

- v) ability to join dissimilar metals
- vi) negligible metal loss - an economic advantage when joining precious metals.

There are three main resistance welding processes in common use.

In spot welding (Fig.1a), a weld nugget is formed between the electrodes, the melting being localised by the shape of the electrodes. Two or more welds may be produced simultaneously by using multiple sets of electrodes.

Projection welding is a process (Fig.1c) using raised projections or embossments on one surface to locate the nugget, multiple welds may be produced using one set of electrodes.

Seam welding is a method which uses two rotating disc-electrodes to produce a series of overlapping nuggets giving a gas tight seam between the two parts to be joined (Fig.1b). There is also a variant of this last process, known as roll-spot welding, in which the current, instead of being continuous, is intermittent, hence producing a row of spot welds which may, or may not, be discrete.

The quality of welds produced by these processes can be somewhat variable. The most important factors that affect weld quality are as follows:

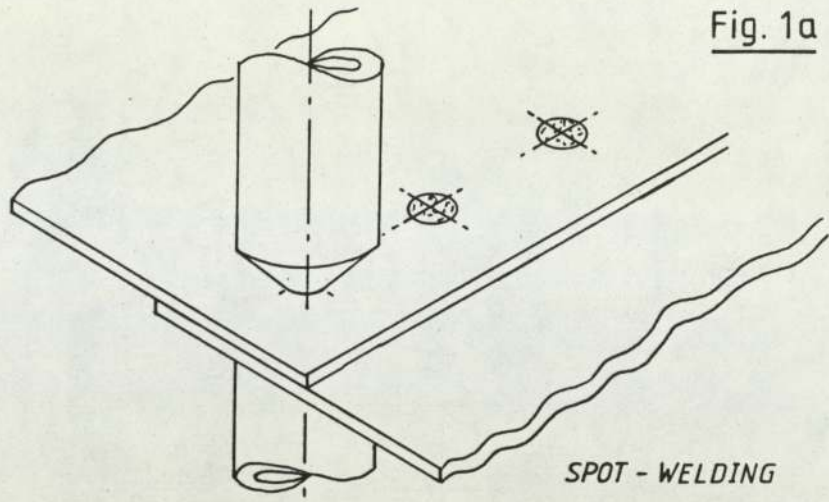


Fig. 1a

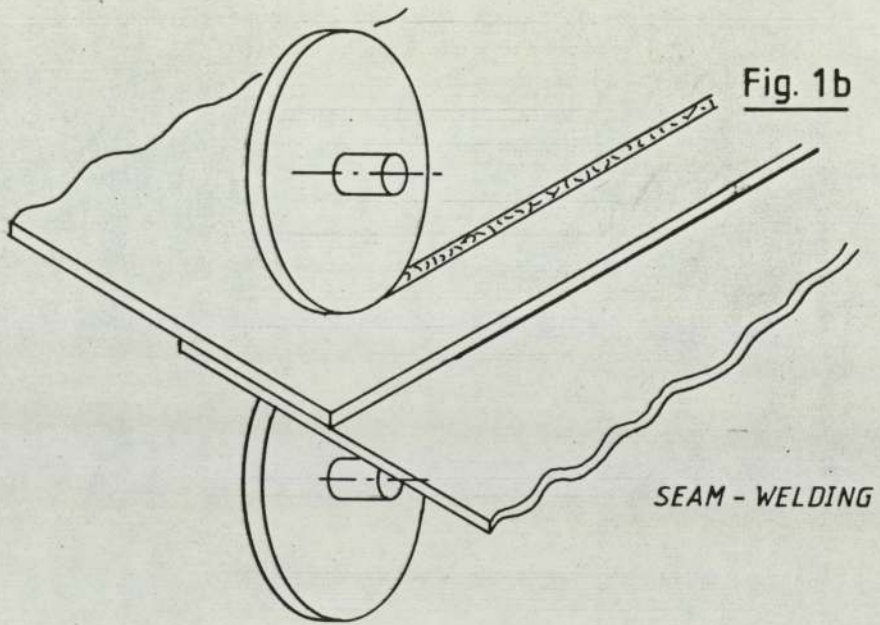


Fig. 1b

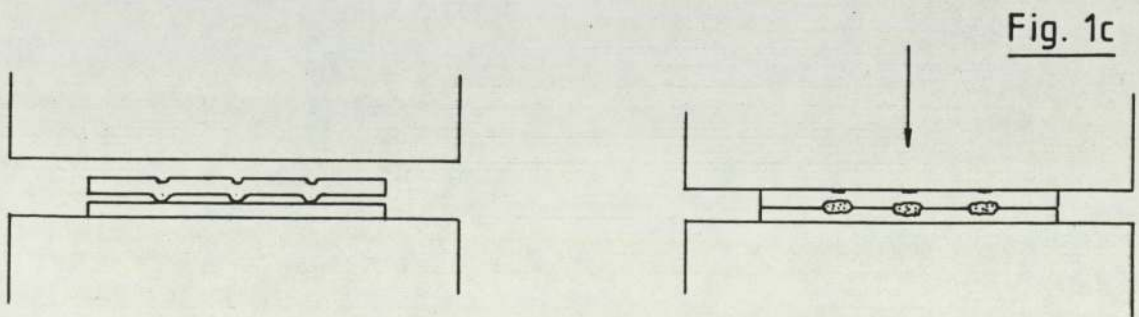


Fig. 1c

PROJECTION - WELDING

1. Surface appearance
2. Weld size
3. Weld penetration
4. Strength and ductility
5. Internal discontinuities
6. Sheet separation and expulsion
7. Weld consistency.

The surface appearance of a resistance weld gives an indication of the conditions under which the weld was made, and provides evidence of such things as electrode misalignment and deterioration. However it cannot be used as a criterion for the strength, size or internal soundness of a weld. The diameter or width of the fused zone must meet the requirements of the appropriate specification or design criteria, since the strength and in-service reliability of the weld will be directly related to the weld size. The presence of internal discontinuities such as cracks and cavities, resulting from excessive weld heat, may have deleterious effects on weld strength, fatigue strength and corrosion resistance.

A major problem in the use of resistance welding as a manufacturing technique has been quality assurance. In the absence, until recently, of in-process monitoring techniques, the only method suitable for quality control of spot welded products was the destructive examination of a sample of welds produced. This involves either the loss of a proportion of fabricated components, or the use of test

samples such as peel test coupons or tensile-shear specimens, which are less representative of normal production. This problem has always meant that resistance welding has been limited to applications which are only moderately safety critical, or to materials such as mild steel, which exhibit a high degree of consistency in the quality of welds. Alternatively, for more safety critical applications, such as automotive sub-frame assembly, the use of safety factors has led to a penalty in labour and energy costs due to increases in the number of welds used. The need to extend the process to more critical applications, such as aerospace, has resulted in the development of many types of in-process monitoring instruments. These range from the earliest types which measured electrode displacement during the weld, through devices which measure the voltage across the electrodes during the weld, to instruments based on dynamic resistance measurements formed by the monitoring of current and voltage simultaneously. It is a device of this latter type which is used in this thesis, and further details of its operation are given in the section on experimental procedures and equipment.

## 1.2 Coated Steels and Resistance Welding

The use of metallic coatings on steel for corrosion protection and decoration has been common for many years, with zinc coating being the most common method of sacrificially protecting steel. The use of cadmium and lead has now fallen into disfavour due to their toxicity whilst

tin coatings, until recently widely used in the food canning industry, only provide a barrier to corrosion and are, in any case, being superseded by aluminium two-piece cans having inherent corrosion resistance.

The normal practice with zinc coating is to hot dip galvanise the completed fabrication. In recent years, however, automotive engineers in particular have realised that the use of thinner HSLA steels for body shell construction in order to reduce vehicle weights and improve fuel economy, will result in a considerable reduction in the corrosion life of the vehicle. As a result of this there is increasing demand for pre-coated steels, in particular hot dipped galvanized and electroplated zinc coated steels. Hot dipped material is used mainly for truck and bus applications whereas electro zinc is used more for private vehicles where the quality of finish is more important, but in both cases, and in other applications outside the automotive industries, the zinc coating causes severe problems when fabricating using resistance welding.

The zinc coating itself is often uneven which causes variation in electrical properties, but, more significantly, the coating has a low melting point and rapidly alloys with the copper-base welding electrodes leading to a rapid deterioration in the quality of welds produced. These problems make it all the more important to use some form of in-process monitoring to ensure that welds are produced to adequate quality.

The dynamic resistance weld monitor, developed by Aston University in cooperation with Rubery Owen Ltd. has been investigated and has proved satisfactory for quality assessment of welds in mild steel and many aluminium alloys. However, in the light of comments in the literature, and the limited amount of information available, especially on the subject of electrozinc materials, it was felt that an in-depth study of welding behaviour and monitoring characteristics would prove valuable.

## 2 LITERATURE SURVEY

A survey of the literature relating to resistance welding of coated steels in particular reveals both the enormous number of factors believed to influence the quality of welds, and the level of disagreement between workers on the importance of each of these factors. However, one area in which there is general agreement is the need for increased current and weld time resulting from the zinc coating on the surface of the mild steel. (W.Glaze,1971), (F.C.Porter, 1983), (N.T.Williams,1973). These workers also report the reduction in electrode life when welding these materials.

Most authors suggest that the increase in weld heat, in terms of both time and current, is due to the need to overcome the inherently lower contact resistance of the zinc coating surface (F.C.Porter op.cit.). Freytag (1967), on studying the welding of single side coated steels, discovered that significant increases in current and weld time were only required when welds were produced with the coating at the faying surfaces. Freytag (op.cit.) is one of many workers to report the influence of electrode contamination on accelerated electrode wear, but he suggests that the primary factor in reducing electrode life is the higher temperature reached during the weld cycle due to zinc at the faying interface. However, Freytag also states that :

"There is no apparent correlation between surface contact resistance and the weldability of various galvanised steels".

In addition to conflicting with Porter (op.cit.) this also

contradicts other statements by Freytag in the same paper to the effect that the lower contact resistance necessitates higher welding currents which lead directly to a shorter electrode life. He also states that the increase in welding current results from a decrease in coating hardness, which is dependent on the iron content of the coating, and which, although associated with less electrode wear, does not necessarily result in a longer electrode life (!).

In contrast, work by Williams (1977) and by Williams and Lavery (1970) on the use of iron-zinc alloy coatings suggests that the use of these, IZ, coatings results in electrode lives comparable to uncoated mild steel of around 8000 to 15000 welds with Cu - Zr - Cr electrodes.

Ganowski and Williams (1973) and Williams (1977) also discuss the use of "pimpel" type electrodes which are reported as giving an increase in electrode life of two times for IZ and from seven to eight times for normal spangle, although in the June 1977 paper N.T. Williams mentions the sensitivity of the pimpel type electrodes to welding conditions.

Evrard (1967) has studied the effect of welding rate on electrode life. He reported that welding rates which do not allow the tip temperature to return to room temperature between welds will limit the electrode life for galvanised material to around 2000 welds. However, slow welding rates of less than twelve welds per minute allow an electrode

life of 3500 to 4000 welds. However, no information was given in this paper on the rate of flow of coolant water or the efficiency of cooling. Most British and American workers conform to the requirements of the relevant standards (see, for example, BS 1140: 1980) for a minimum coolant flow rate of seven litres per minute. Whilst workers such as Porter (1983) have stressed the importance of maintaining this as a minimum level of cooling, one worker (Holásek (1974)) has reported similar electrode lives with coolant flow rates as low as four litres per minute.

### 3 EXPERIMENTAL PROCEDURES AND MATERIALS

#### 3.1 Materials

The zinc coated materials investigated in this work may be categorised as follows:

##### i. Hot dipped materials

The materials in this group consisted of spangle galvanised mild steel sheet mainly of 1.2 mm thickness, although limited supplies of thinner materials were obtained. The nominal coating thickness on these materials was  $275 \text{ gm}^{-2}$  and the materials were therefore of the type known as "Galvatile G275 NS" where "NS" stands for normal spangle. This type of material was obtained from two main sources: British Steel Corporation at Port Talbot and a steel stockholder, W.C.M. James (Successors) Ltd., of Birmingham.

##### ii. Alloy coated material

This material is a hot dip galvanised material which is subsequently heat treated to produce diffusion alloying of the zinc coating with the iron in the substrate material. This material may also be produced directly by using a base steel with a high silicon content although this is less suitable for resistance welding since silicon increases the hardenability of the steel. This material was used in 1.2 mm and 1.0 mm thicknesses although small quantities of thinner gauge material was obtained. Calvatite IZ, as this material is known, was only obtained from B.S.C. Port Talbot.

### iii. Electro-zinc materials

This material, known by the B.S.C. trade name of "Zintec" is a mild steel sheet on which a deposit of zinc is formed by electrodeposition. Supplies of this material were obtained from B.S.C. Port Talbot, W.C.M. James, and from Motor Panels (Coventry) Ltd. This material is available in many different thicknesses although 1.2 mm thickness was chosen to standardise the results. Other thicknesses were also used in preliminary tests as was a sample of single sided zintec.

In general the thicker, hot dip coatings are used where a high degree of corrosion resistance is required throughout the life of the component, whereas the much thinner electro-zinc coatings provide protection during transport and subsequent fabrication but only provide long term protection as a substrate for an organic coating. The iron-zinc alloy coating was developed in an attempt to combine the corrosion protection of the thicker hot dipped galvanised materials with the superior weldability of the thin electro-zinc materials.

### 3.2 Welding Equipment

The majority of the welding tests were performed on a  
X British Federal 210 kVA, modified series PA.2 type projection welding machine (see plate 1). A projection welding machine was used because it is of more rigid construction, having a shallower throat than a normal spot

welding machine. This reduced potential variations due to mechanical flexing of the machine arms and head friction to a minimum.

The welding controller used was a British Federal type S3HUD/2 as shown in plate 2. This allowed precise, repeatable control of weld time, upslope and current together with squeeze and hold times. The controller also had the facility for two impulse welding and post-weld heat-treatment. Whilst it would have been desirable to investigate impulse welding and post weld annealing, especially for material found to be brittle following welding, insufficient time and material were available.

The flow of coolant water to the electrodes was monitored using flowmeters and was kept constant at seven litres per minute for each electrode.

The electrode force was originally determined by calibration of the air supply pressure using a statimeter. The use of a calibrated strain gauge assembly attached to the upper arm of the welding machine allowed monitoring of a voltage value proportional to the electrode force during the weld cycle so that the relationship between squeeze and weld initiation could be assessed.

The welding current was measured using a British Federal digital weld monitor, type DWM/2, giving readings to four significant figures.

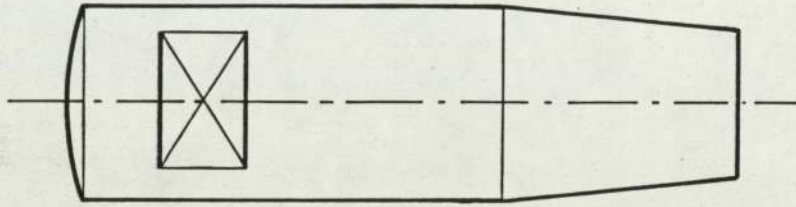
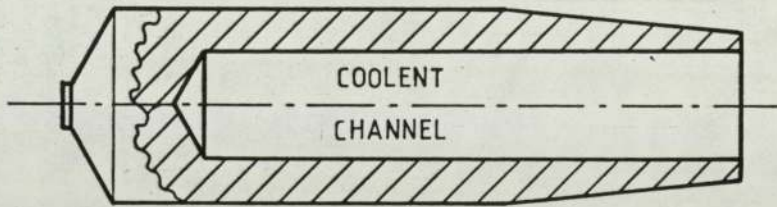
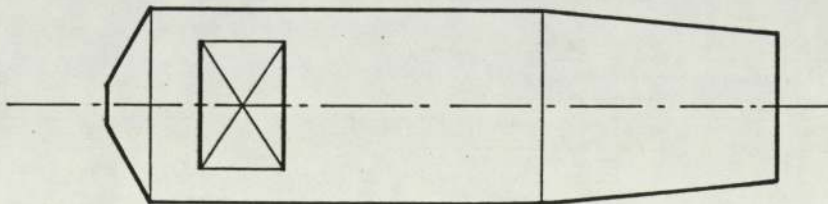
The resistance spot welding electrodes used were manufactured from Matthey 328 material obtained from Johnson Matthey Metals. This is a copper base 1% chrome, 0.1% zirconium alloy having a higher softening point than the standard 1% chrome-copper used for welding uncoated steel. The electrodes used were all of the vertical centre type, rather than offset or cranked. Three types of tip profile are in use for resistance welding in the U.K. These are truncated cone, domed and "pimpel" (Fig.2). Domed electrodes are considered totally unsuited for welding of coated steels and were not investigated in this work. Truncated cone and "pimpel" type electrodes were machined to the required tip diameters ( $5 \times \sqrt{\text{sheet thickness}}$ ) with included angles of  $120^\circ$ . The flow of coolant within the electrode conformed to B.S.4215: 1967 section 2.4.

### 3.3 Dynamic Resistance Monitoring

The importance of dynamic resistance monitoring for in-process quality control was emphasized in the introduction. The technique relies on dividing the instantaneous voltage across the welding electrodes by the instantaneous current in the secondary loop during the weld. This gives a curve known as the dynamic resistance curve for the weld (Fig.3). The voltage signal is taken directly from terminals on the electrodes (Plate 3). The current was determined using a Hall effect probe placed in the throat of the welding machine, (Plate 4), which generated a voltage signal proportional to the current.

## COMMON ELECTRODE TYPES

— APPROX. FULL SIZE

DOMED ELECTRODES'PIMPEL' ELECTRODESTRUNCATED-CONE ELECTRODES

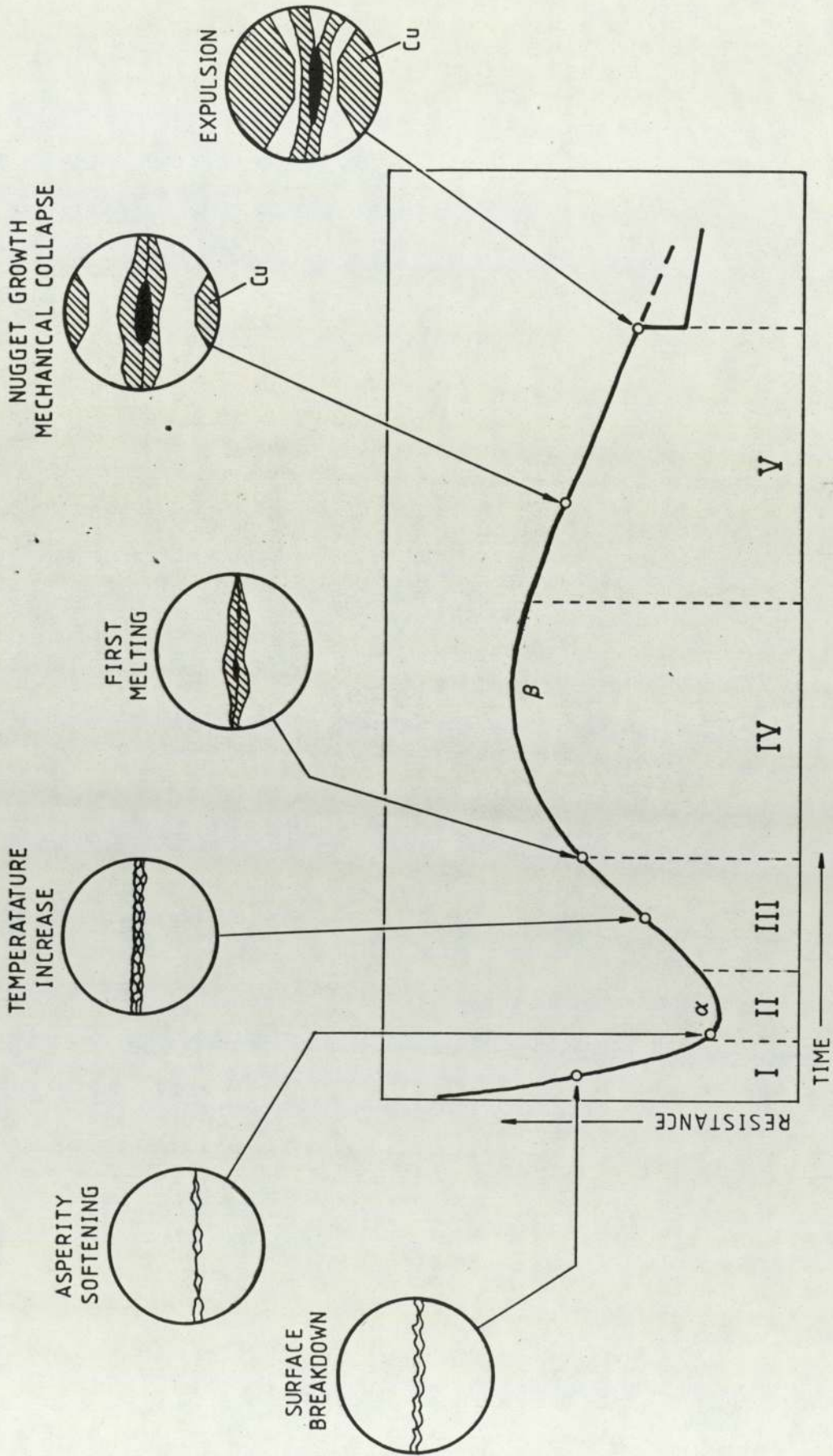


Fig. 3 THEORETICAL DYNAMIC RESISTANCE CURVE ( After Dickinson *et al.* ( 1980 ) )

The voltage and "current" signals are fed into the dynamic resistance monitor (Plate 5) where, after signal conditioning they are passed to two parallel analogue to digital (A/D) converters. These produce a numerical value corresponding to the peaks of the alternating signals for voltage and current for each half-cycle of the weld current. A microprocessor is then used to divide the stored voltage and current values to produce the dynamic resistance characteristics for the weld.

By storing the dynamic resistance characteristics for a good weld it is possible to compare all subsequent welds to this "master" weld. This comparison is achieved by subtracting corresponding values of the master weld from the test weld. The largest of the values thus obtained is known as the "monitor error number" and can be used as an acceptance/rejection criterion or in experimental work as a numerical measure of the deviation of the dynamic resistance characteristic of the test weld from the master.

#### 3.4 Weldability Determination

The weldability of a material is best shown in the form of a weldability lobe for the material. These are determined by producing welded test coupons for a range of weld currents and weld times at a given pressure and then peeling apart the coupons to determine the quality of the weld.

Both British Standards (BS 1140:1980) and American standards

define the minimum acceptable weld as one having a weld nugget diameter of  $4 \times \sqrt{\text{sheet thickness}}$ , and this was taken as a suitable criterion for these tests, independent of whether the peel test failed by pulling a slug (Plate 6) or by fracturing at the original faying surface (Plate 7) (see N.T.Williams 1981).

The upper limit of weld quality was taken as the point at which evidence of expulsion of molten metal from the weld is found (Plate 8). If the current and weld-time coordinates of these upper and lower limits are plotted a lobe is obtained which shows the range of weld currents and weld durations for which acceptable welds will be obtained at the weld pressure used and for the particular machine and set of conditions in force when the test was performed. (See, for example, Fig.4.).

### 3.5 Electrode Life Determination

The electrode deterioration characteristics were determined for each material by means of endurance tests. Welds were produced on plates of material at a rate varying between sixty and thirty welds per minute. At regular intervals, the spacing of which varied from twenty five to one hundred welds according to the expected electrode life, test welds were made on coupons for peel test or tensile shear test (see BS 1140:1980). The current and voltage signals for these welds were recorded for independent analysis at Birmingham University whilst the "monitor error number" was

noted. The test welds were examined destructively with occasional confirmation by metallographic sectioning. This allowed determination of the electrode lives for the materials whilst the error number allowed a statistical analysis to be performed to determine monitor reliability.

Metallographic sections were cut using a diamond edged "Isomet" cutting blade to minimise distortion, mounted in bakelite and polished using a "Minimet" polisher to prevent edge damage. The samples were etched using a dilute (0.5%) solution of nitric acid in ethanol to reveal grain structure without excessive attack to the zinc coating.

## 4 RESULTS

### 4.1 Galvatite Normal Spangle

Weldability lobes were produced for Galvatite-spangle for sheet thicknesses 0.5 mm, 0.9 mm and 1.2 mm using electrode forces of 1.1 kN, 2.0 kN and 2.3 kN respectively. (Figs. 4, 5 and 6). These show clearly that the lobes increase in width and shift to higher currents with increasing sheet thickness and electrode force.

Weldability tests on samples of 1.2 mm Galvatite normal spangle obtained from a steel stockholder (W.C.M. James (Successors) Ltd.) showed that, at the welding force recommended in British Standard 1140 (1980) of 2.8 kN, the weldability lobe was very narrow (Fig.7). Visual examination of peel-tested welds showed that a higher than normal proportion of welds having a nugget diameter greater than  $4\sqrt{t}$  exhibited interface failure so that the correct nugget diameter was only revealed by examination of the fracture surface morphology under optical stereo-microscopy. In addition, many through-thickness cracks were observed in the weld nugget where this had been bent during the destructive test (Fig.9). On the few occasions where pulled slug failure was present the plugs, instead of being circular, had a marked rectangular appearance, indicative of rolling texture in the sheet. This was confirmed by performing a modified Erichsen cupping test which showed marked directionality of fracture (Figs.10a, 10b) (BS1449:

### WELDABILITY LOBES

Fig. 4

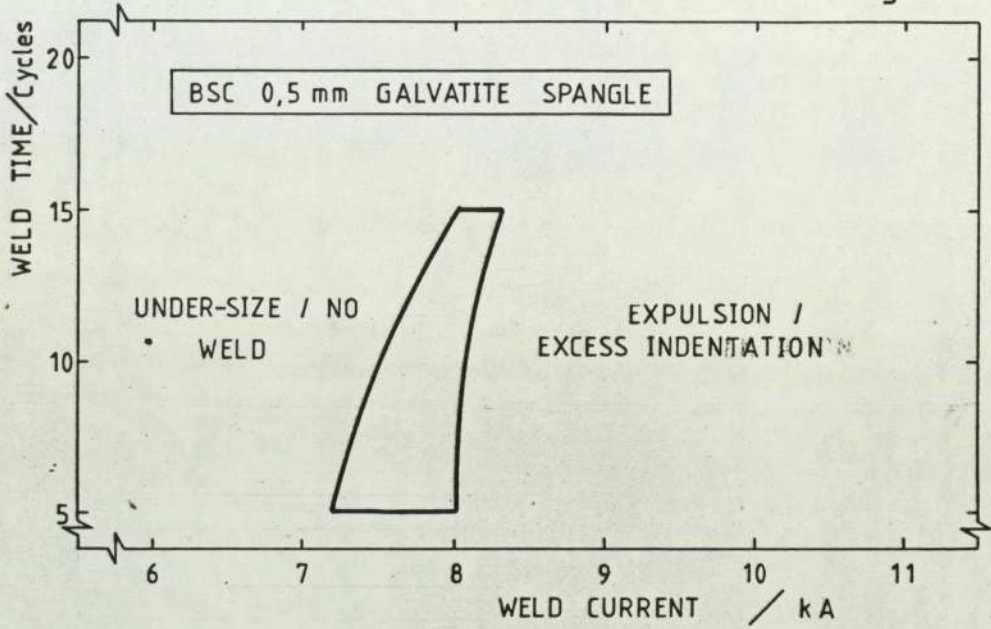


Fig. 5

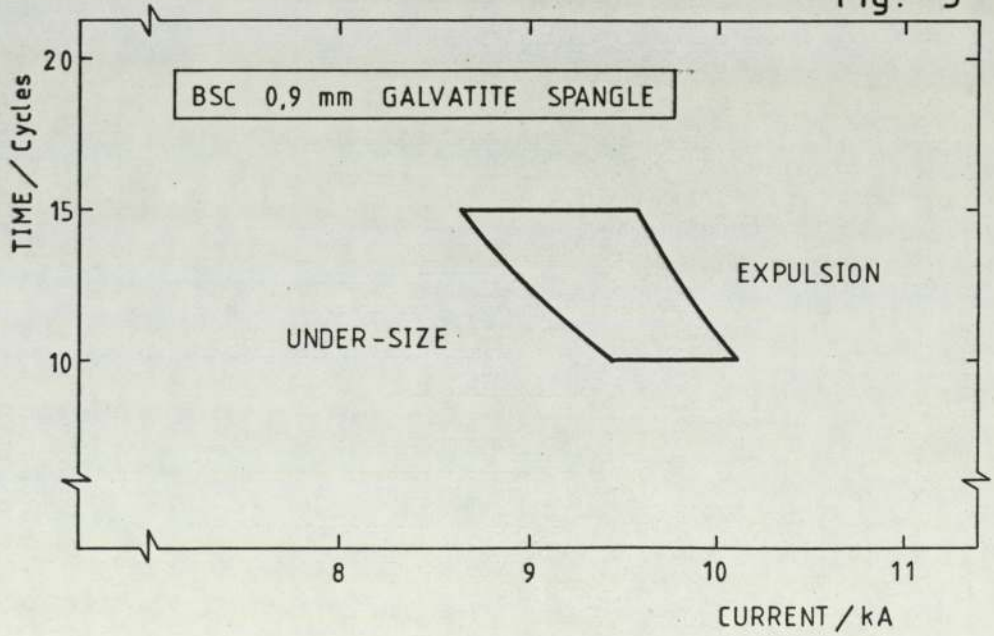
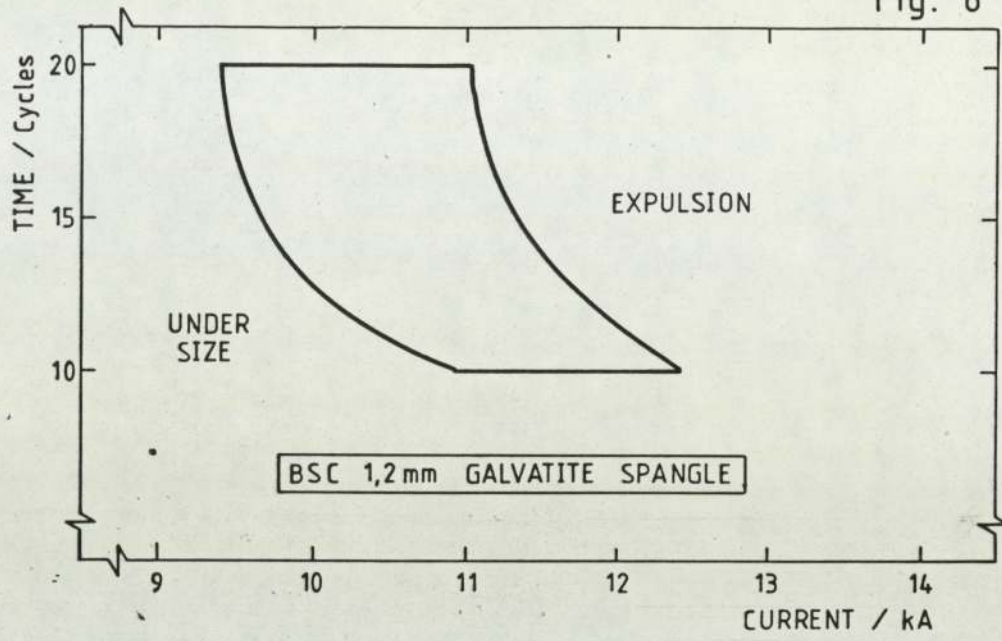


Fig. 6



## WELDABILITY LOBES

Fig. 7

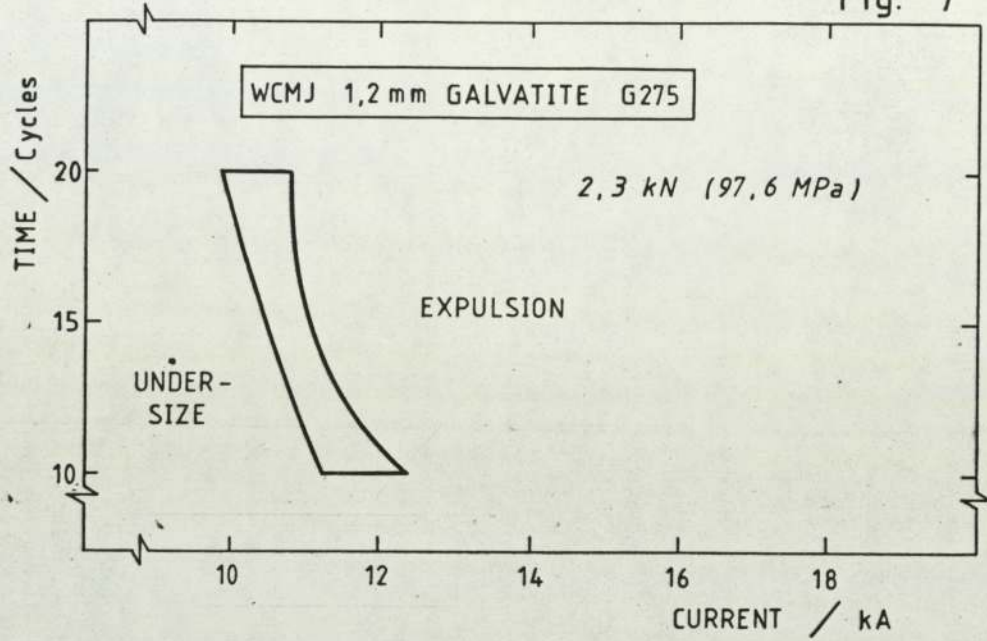
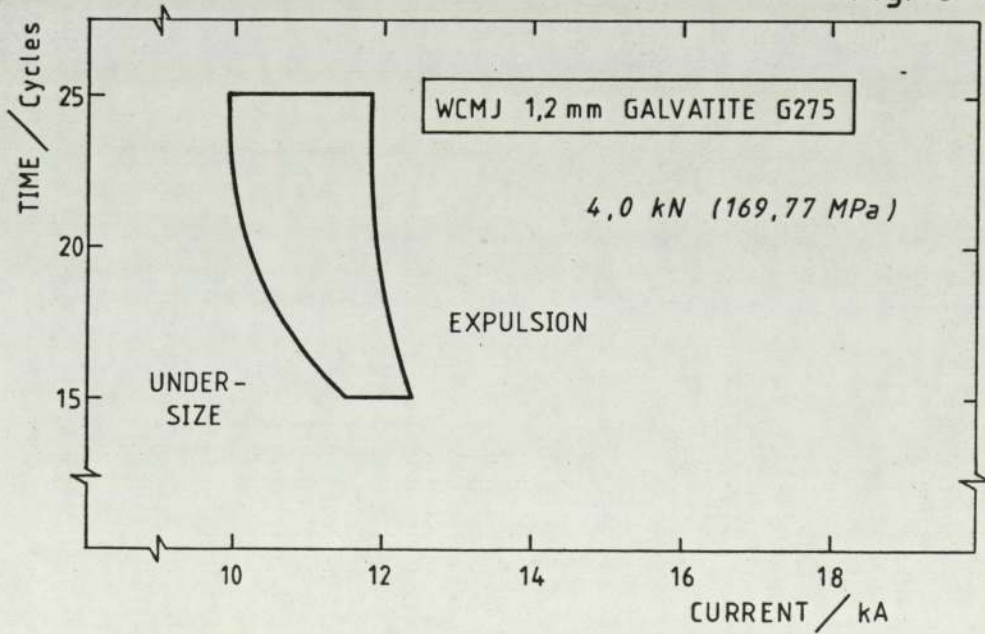


Fig. 8



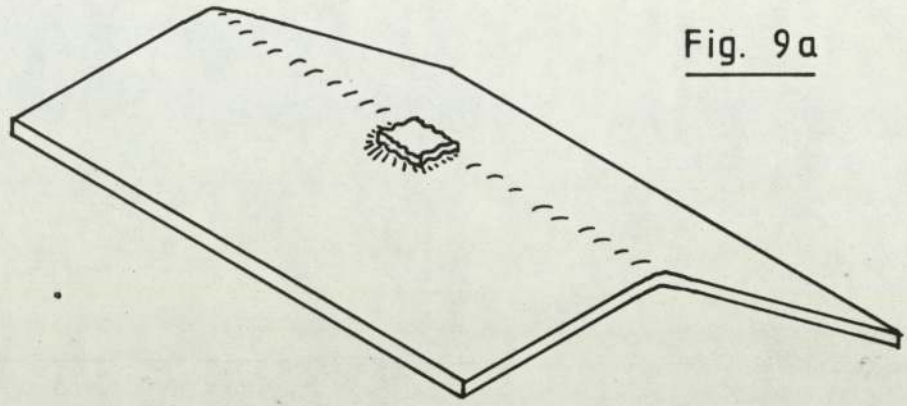


Fig. 9a

SHOWING PARTIAL SLUG WITH ANISOTROPIC FRACTURES

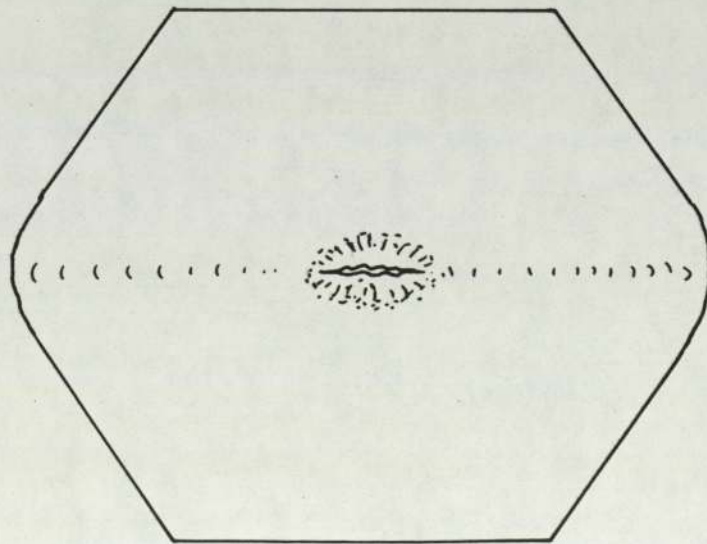
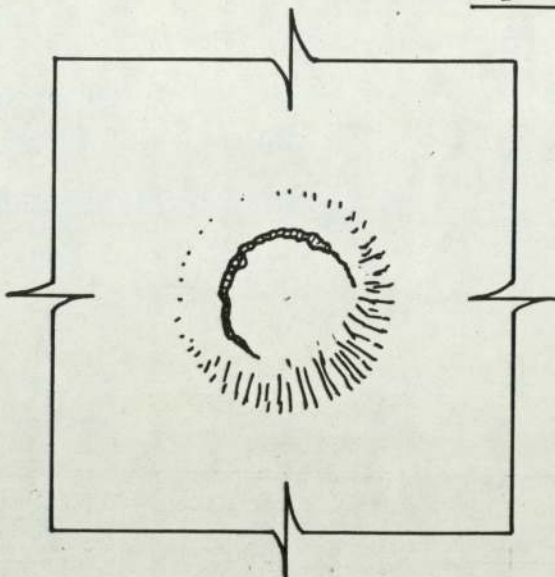


Fig. 9b

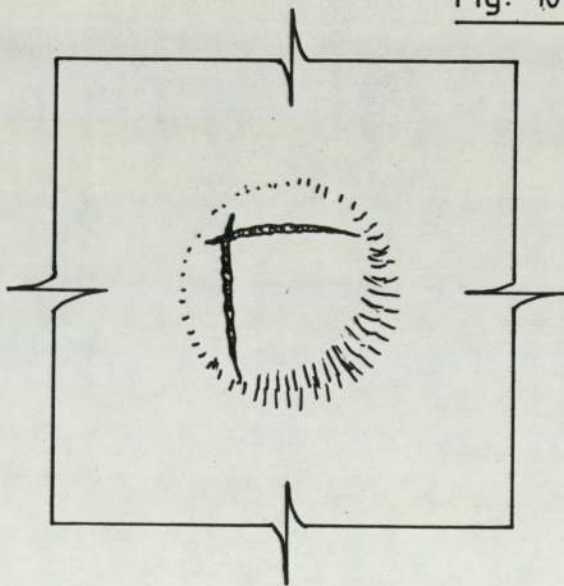
SHOWING THROUGH-THICKNESS CRACK

Fig. 10 a



SHOWING NORMAL ERICHSEN CUPPING TEST

Fig. 10 b

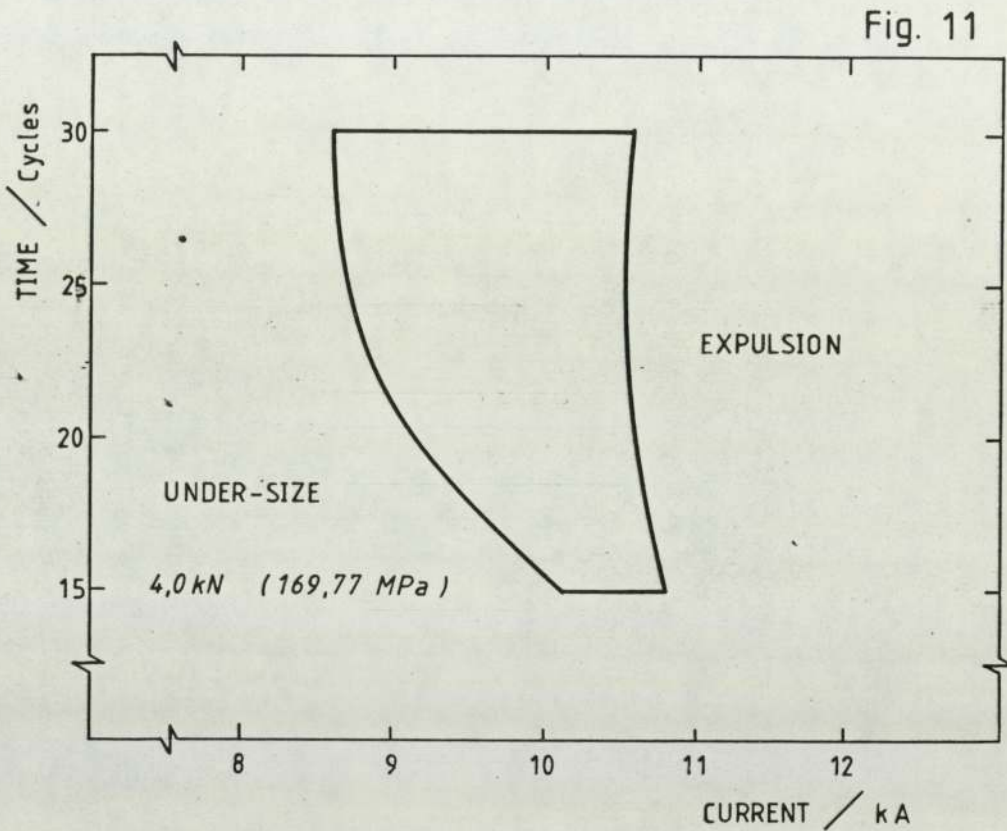


SHOWING ANISOTROPY IN ERICHSEN CUPPING TEST

Part 1 : 1972 section 1.21). A weldability lobe produced with an electrode force of 4 kN showed a considerable increase in width (Fig.8). This was confirmed by lobes produced at B.S.C. Port Talbot (Fig.11). Chemical analysis of this material was also performed by B.S.C. Port Talbot. (Table 1). Although the weldability lobe obtained at 4 kN was wide enough to use as a basis for electrode life tests, there were still a large number of welds which, although satisfactory, exhibited interface failure on destructive testing. This produced difficulty in judging whether or not a weld was satisfactory on peel tests. It was decided, therefore, to investigate the possibility of using tensile shear tests as a criterion of weld acceptability. The variation in weld strength with weld current and weld time at an electrode force of 4 kN was investigated in order to determine the minimum acceptable weld strength (See BS1140 : 1980 and AWS : 1980). The results of the investigation are plotted in Figs 12a and 12b. It was decided to use a tensile shear strength of 9 kN as the minimum acceptable strength for welds in this material.

Electrode life tests were carried out using an electrode force of 4 kN, an electrode tip diameter of 5.5 mm, a weld time of 20 cycles and an initial current of  $(10.16 \pm 0.5)$  kA (Table 2a).

The variation in tensile shear strength and electrode tip diameter with number of welds was determined (Figs.13 and 14). The electrode life was determined from a plot of the number



WELDABILITY LOBE FOR WCMJ GALVATITE G275 SPANGLE  
PRODUCED BY K. CHATERGEE, BSC PORT TALBOT

Table 1

Analysis of 1.2 mm W.C.M.James Galvatite G275 Base Metal

(Composition by Weight)

Carbon	0.142 %
Silicon	0.031 %
Phosphorous	0.018 %
Manganese	0.46 %
(Carbon equivalent	0.219 % )

## Coatings

- i)  $280 \text{ gm}^{-2}$  of zinc including both sides  
(equivalent to approximately  $20 \mu\text{m}$  of zinc on each side)
- ii) No evidence of phosphate or chromate coating
- iii) The coating was wavier than the specification for the material allowed, with differences in zinc grain size between sides
- iv) The coating contained considerable dross.

TENSILE SHEAR STRENGTH AGAINST WELD CURRENT (AT 15 Cycles) AND AGAINST WELD TIME  
 (AT [10,15 ± 0,15] kA) FOR WCMJ 1,2 mm GALVANITTE G275. ● - PULLED SLUG, ○ - INTERFACE FAILURE

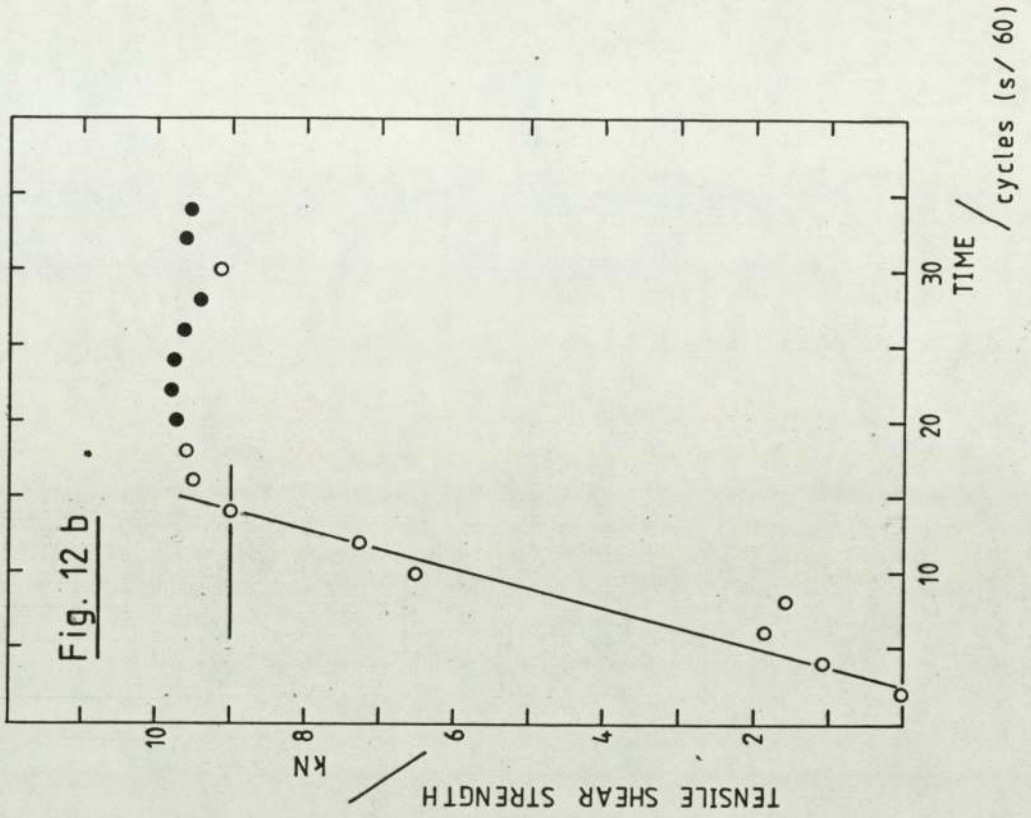
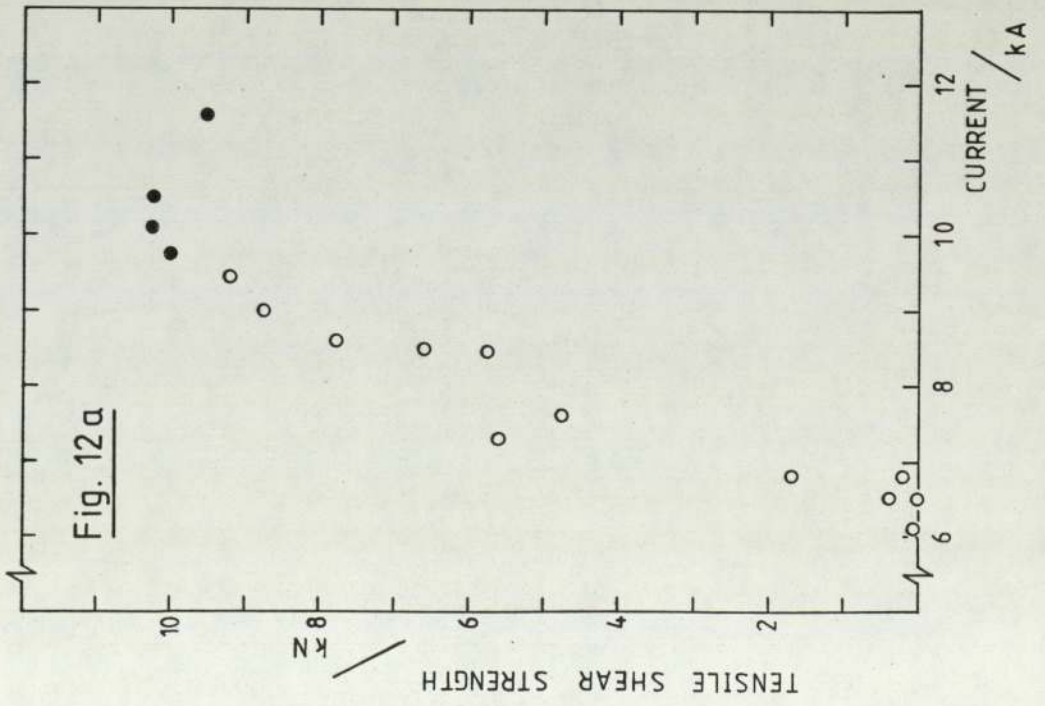


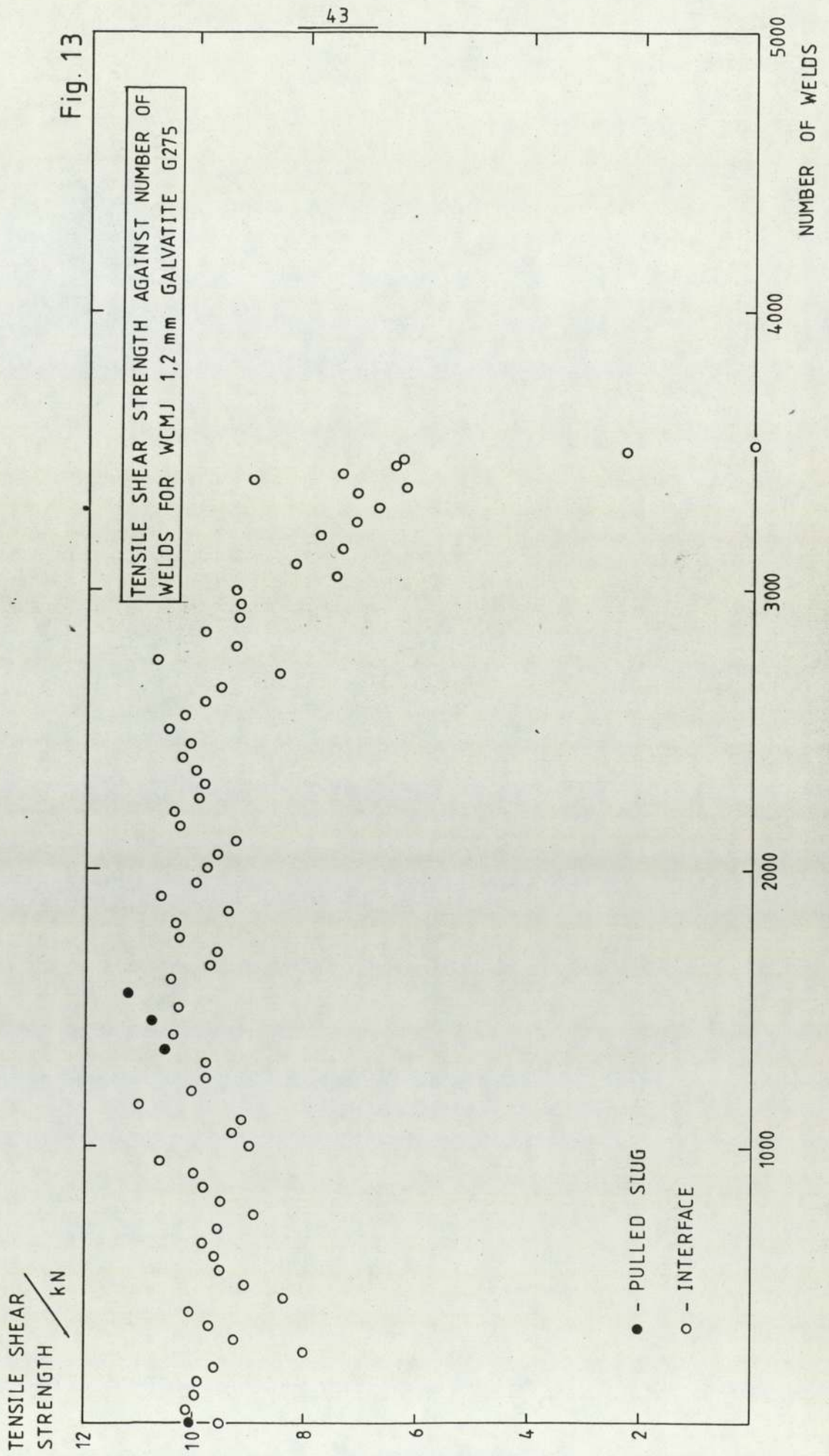
Table 2

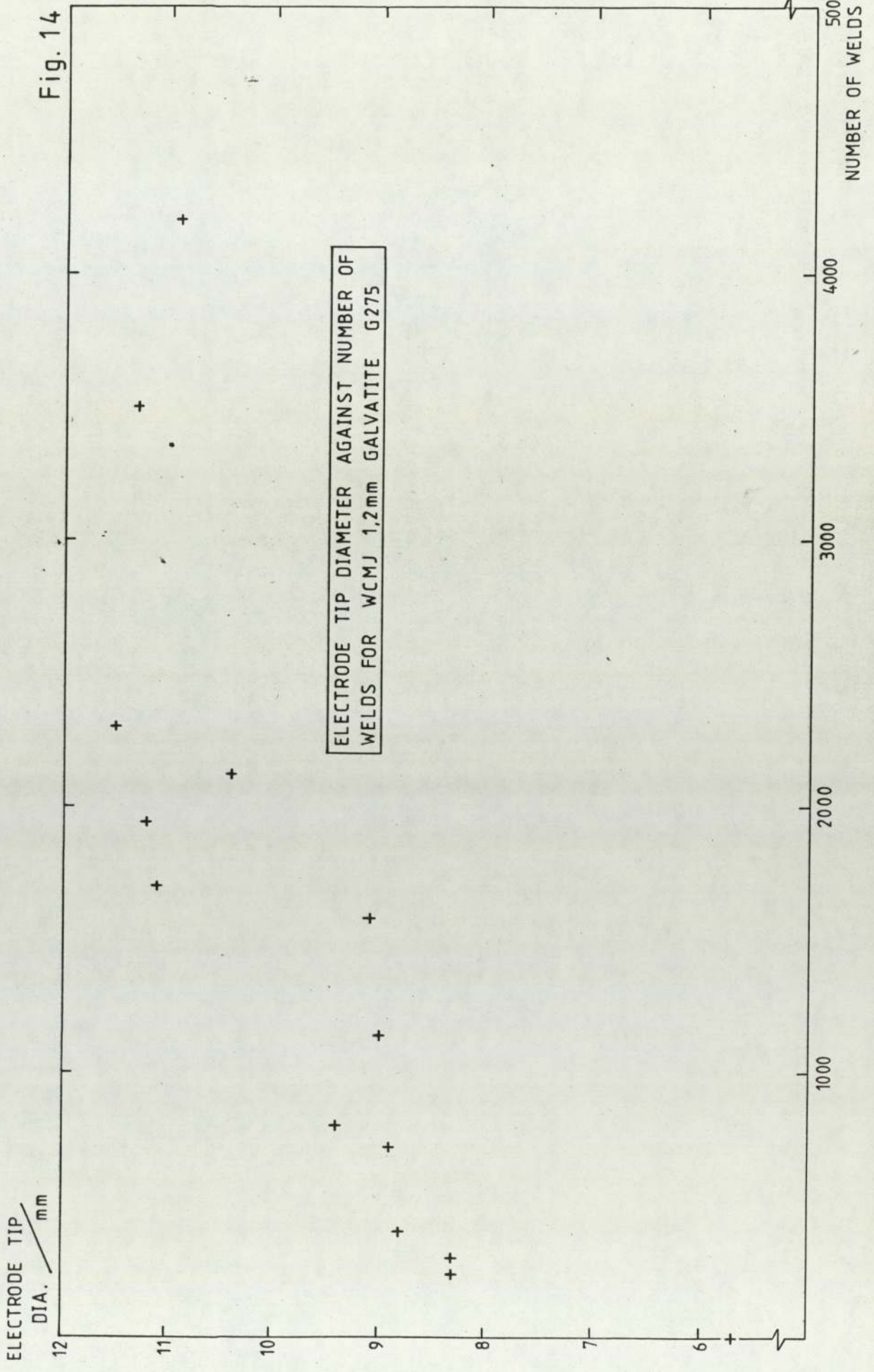
## Initial Conditions for Electrode Life Tests

a) W.C.M. James 1.2 mm Galvatite G275

b) B.S.C. 1.2 mm Galvatite G275

Material	(a)	(b)
Electrode Force / kN :	4.0	3.5
Electrode tip diameter / mm :	5.5	5.5
Inter electrode gap / mm :	10	10
Squeeze time / cycles :	20	40
Up Slope / cycles :	3	3
Weld time / cycles :	20	20
Weld current / kA :	$10.2 \pm 0.5 \sigma_{n-1}$	$11.2 \pm 0.1 \sigma_{n-1}$
Hold time / cycles :	40	60
Weld frequency :	varied from 25 to 40 welds/min	
Coolant flow / $1 \text{ min}^{-1}$ :	$\sim 7$	$\sim 7$





of defective welds against the total number of welds, shown as the sample number, (Fig.15a). The usable electrode life was found to be 2975 welds with approximately 9% of the welds in the useful life faulty.

In addition to the other data obtained, the monitor error numbers for each weld were recorded and these are plotted against the number of welds produced, hence showing the variation in error number with electrode life, in Fig.16, and plotted against weld strength in Fig.17. The distribution of error numbers between good and bad welds is given in Fig.18.

Weldability lobes produced after 4200 welds show the effect of increasing electrode tip diameter on weldability. Figure 19a shows the shift in weldability lobe position to a higher current, whilst Figure 19b gives the same weldability lobes but plotted in terms of current density, rather than current, against weld time. Note that whilst higher currents are required to produce satisfactory welds, the current density required (in other words corrected for electrode spread) is much lower.

The material obtained from W.C.M.James differed in both substrate material composition (Carbon Equivalent = 0.219%), and in coating quality, from the nominal specification adhered to by B.S.C. Since this affected both the conditions required to produce good welds and the methods used to assess weld quality it was decided that, in order to confirm

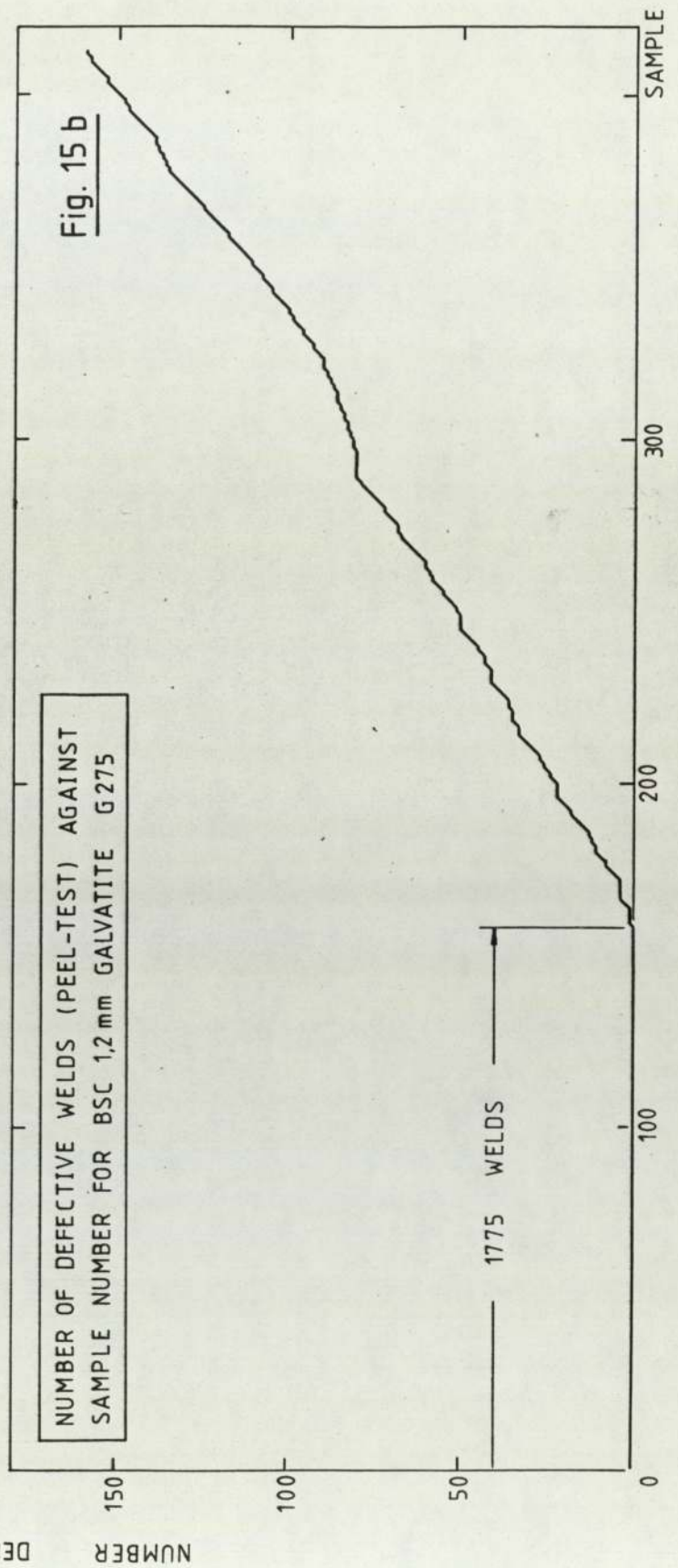
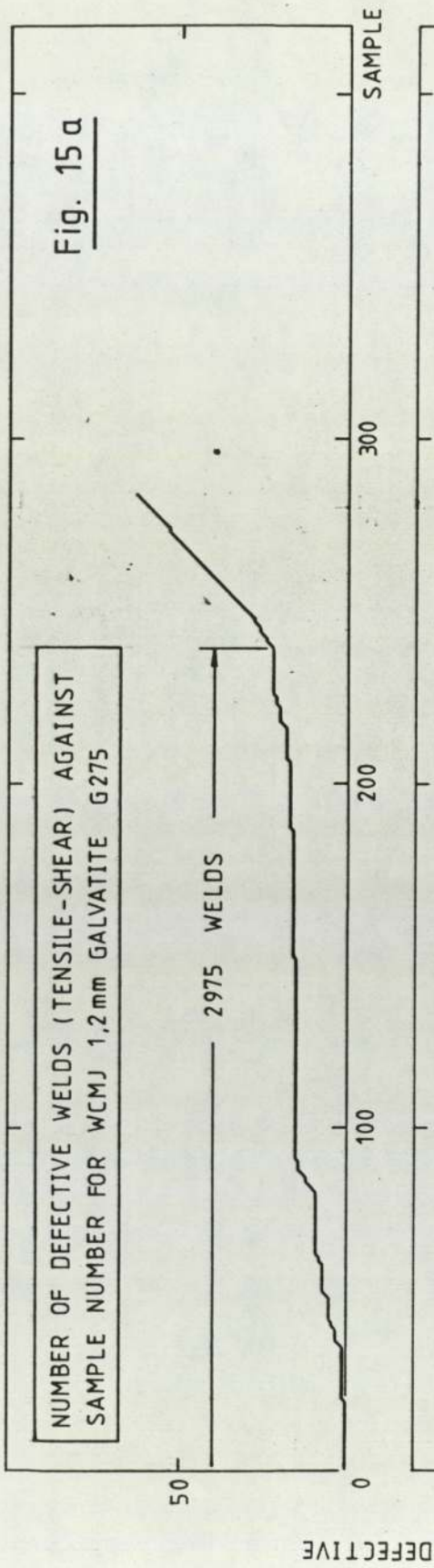


Fig. 16

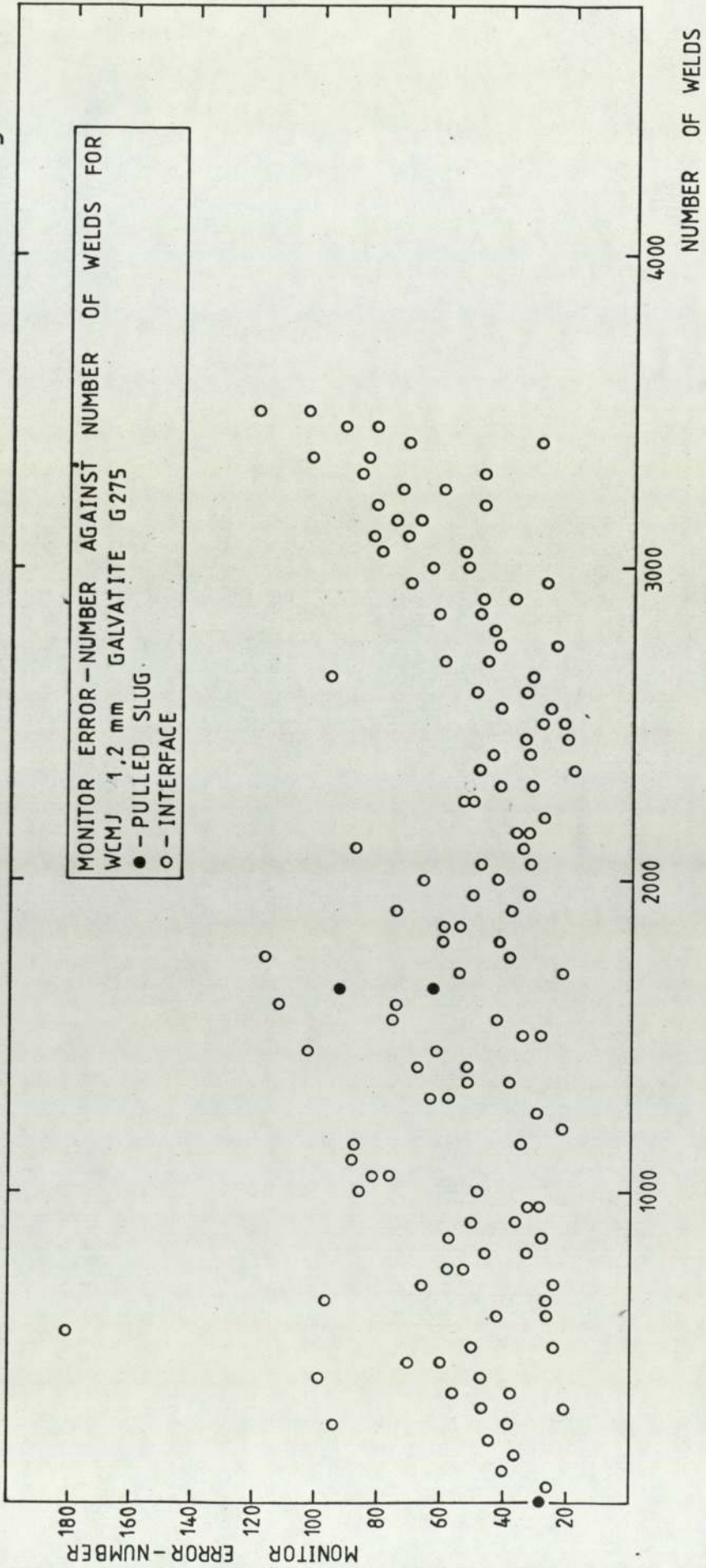


Fig. 17

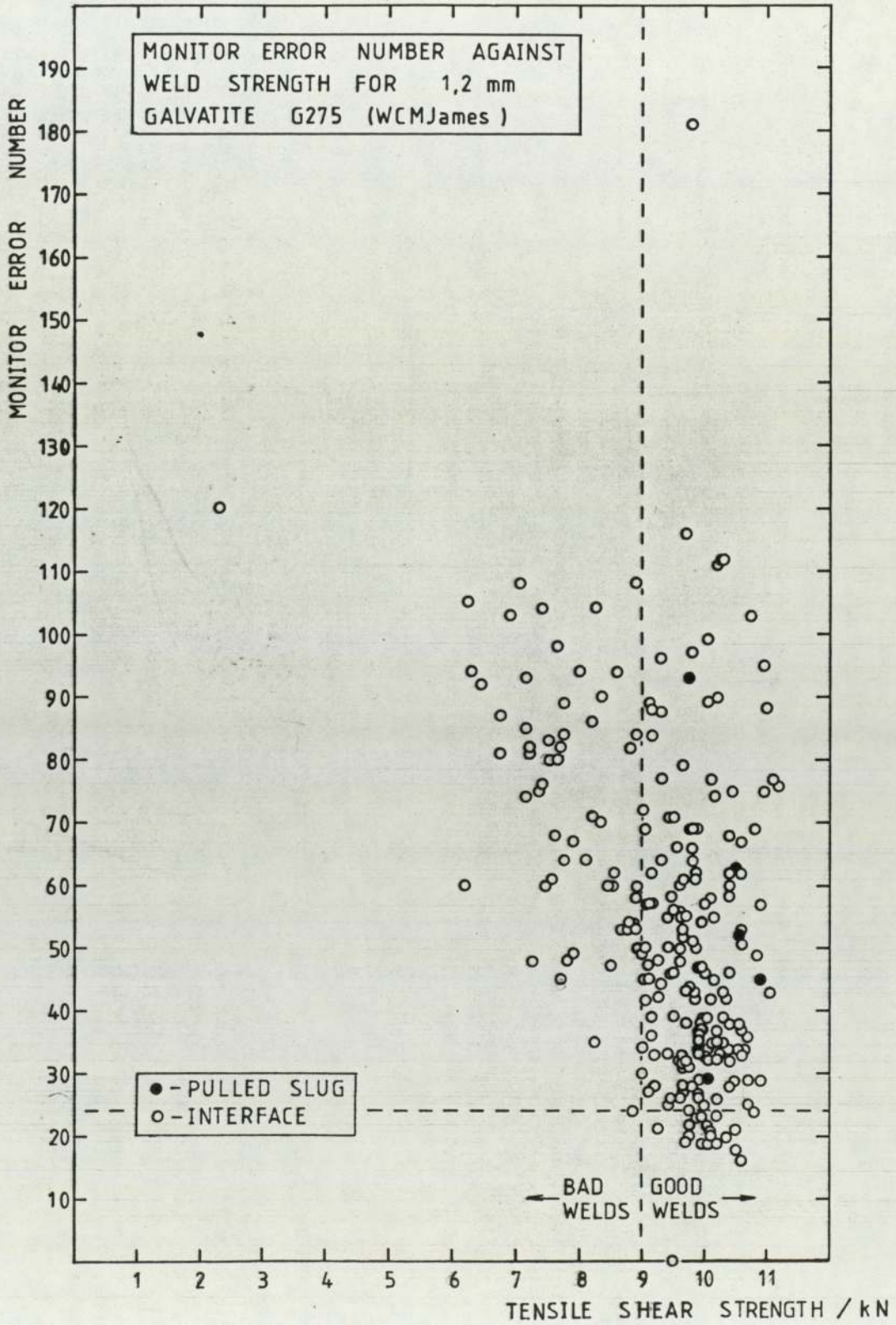
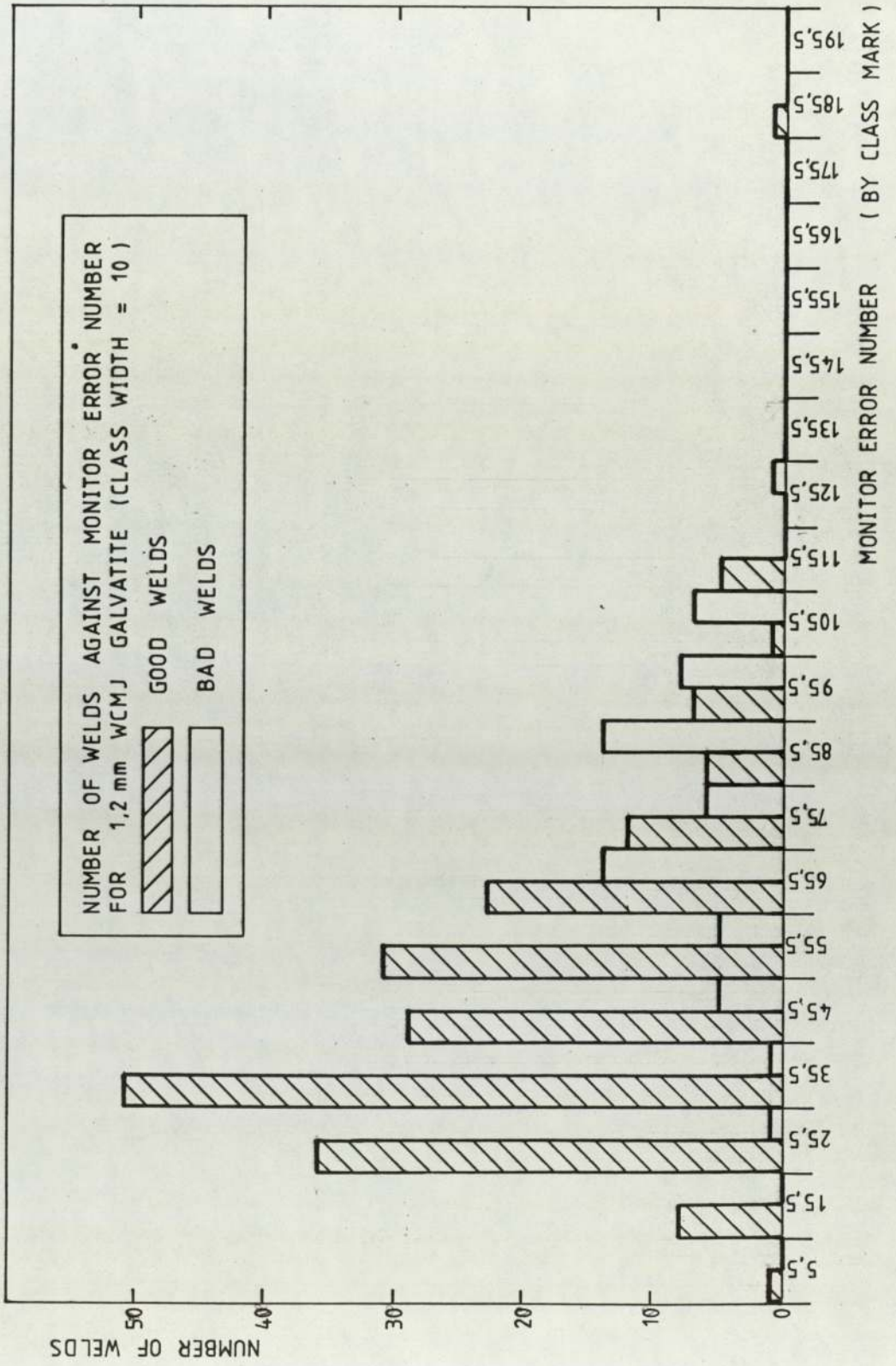
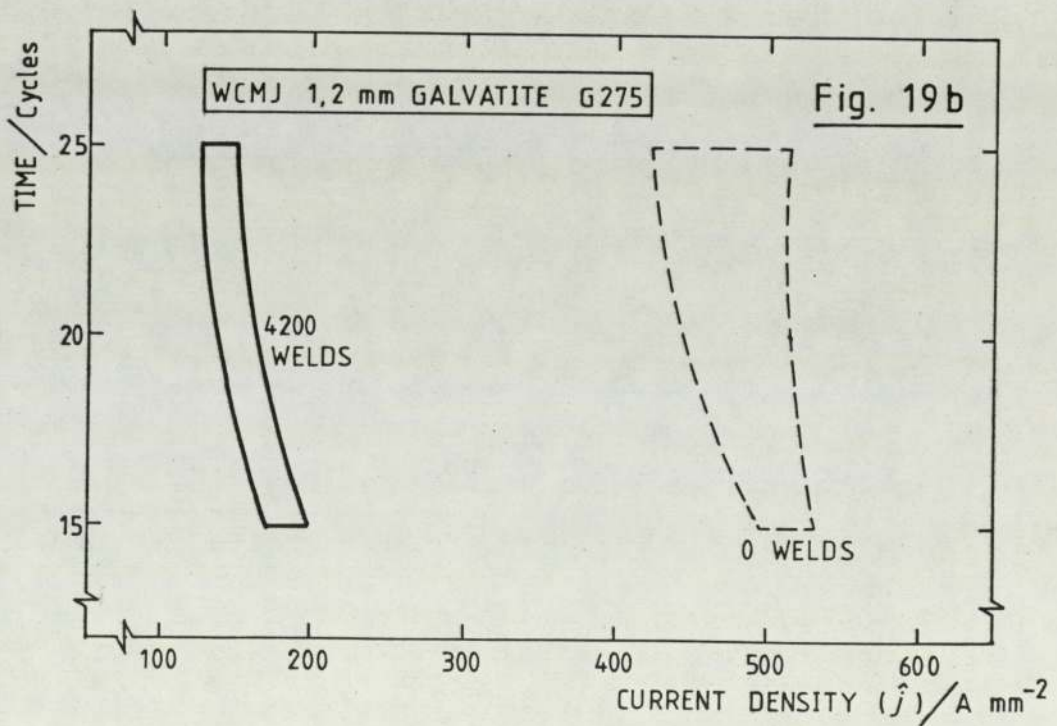
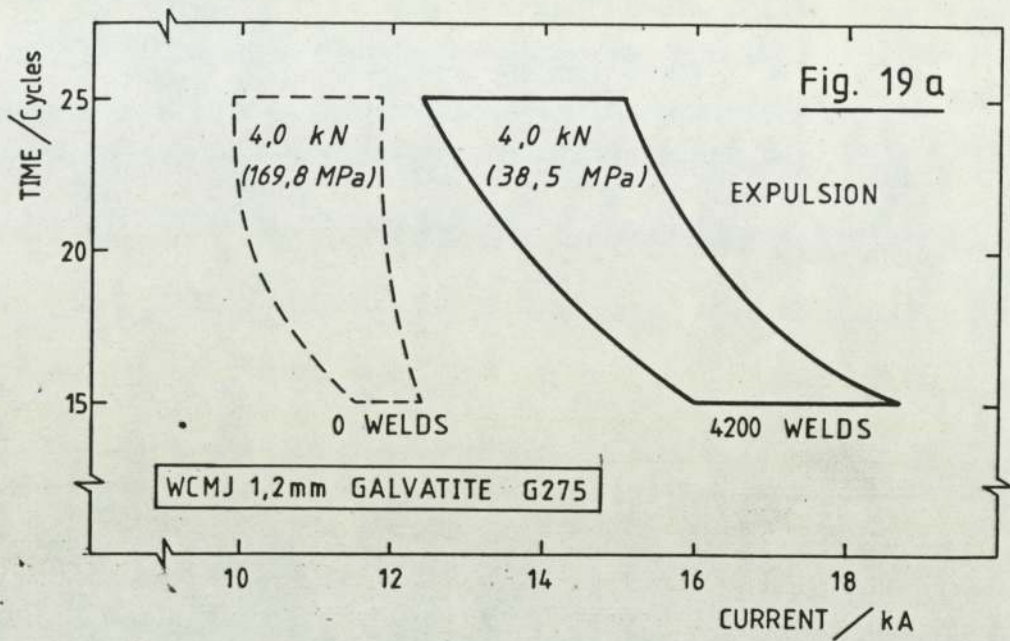


Fig. 18



WELDABILITY LOBES SHOWING THE EFFECT OF INCREASE IN ELECTRODE TIP DIAMETER FROM 5,5mm TO 11,5 mm AFTER 4200 WELDS



the validity of the results, further supplies of 1.2 mm Galvatite G275 be obtained from British Steel for the purpose of assessing the influence of any variation between batches, (Table 3).

Weldability lobes were determined at three different pressures for the new batch of material and these are given in Figures 20a, 20b and 21. In addition to these lobes a composite "carpet" plot (see B.J.Brinkworth 1973) is given (Fig.22). This presents the same information as the three weldability lobes, but in a form which allows interpolation of lobes at different pressures, together with assessment of the effect of welding pressure, current and time on the same graph.

Whilst it was now possible to assess weld quality by measuring the diameter of welds on peel tests, tensile shear tests were also carried out in order to confirm the tests performed on the material obtained from W.C.M.James. Initial tests were carried out to determine the variation in tensile shear strength with weld current and weld time, and hence decide upon a minimum acceptable weld strength of 9.0 kN (Figures 23a, 23b).

From data obtained during electrode life tests graphs were plotted showing the variation in electrode tip diameter (Fig.24), variation in weld nugget diameter and variation in tensile shear strength with number of welds produced (Figs.25 and 26). In addition data was obtained allowing a

Table 3

Analysis of 1.2 mm B.S.C. Galvatite G275 Base Metal

	(By Weight)
Carbon	0.035 %
Sulphur	0.012 %
Phosphorous	0.006 %
Manganese	0.30 %
Soluble Aluminium	< 0.01 %
Nitrogen	0.0028%
Silicon	0.001 %
(Carbon Equivalent	0.085 % )

## Coating

- i)  $313 \text{ gm}^{-2}$  of zinc including both sides  
(equivalent to approximately  $22 \mu\text{m}$  of zinc on each side)
- ii) No evidence of phosphate or chromate coatings

## WELDABILITY LOBES

Fig. 20 a

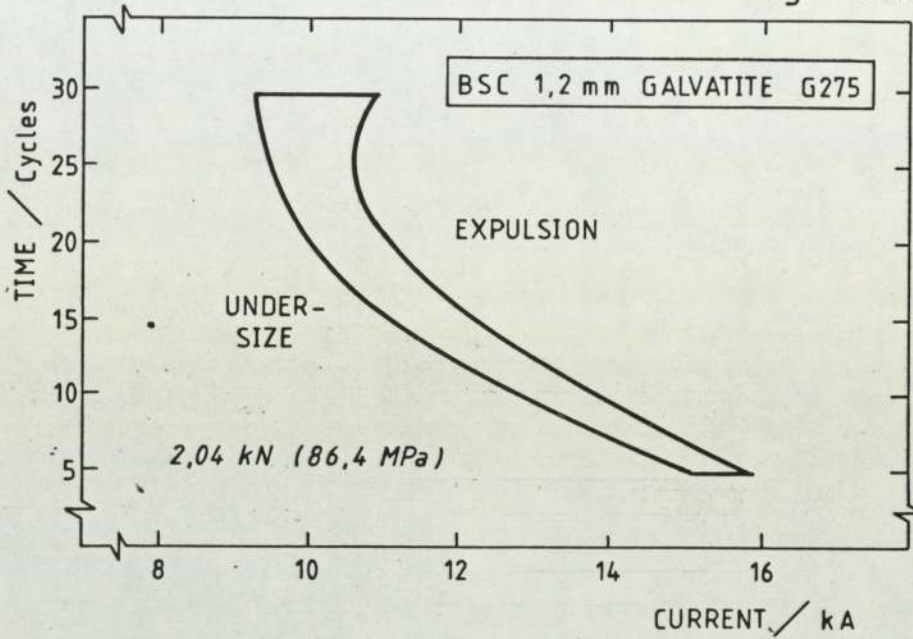


Fig. 20 b

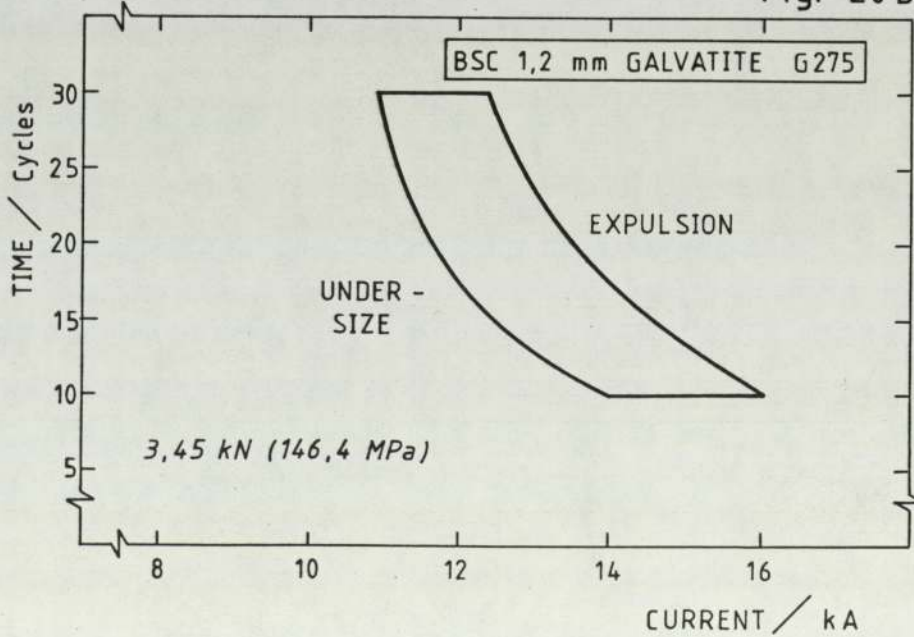


Fig. 21

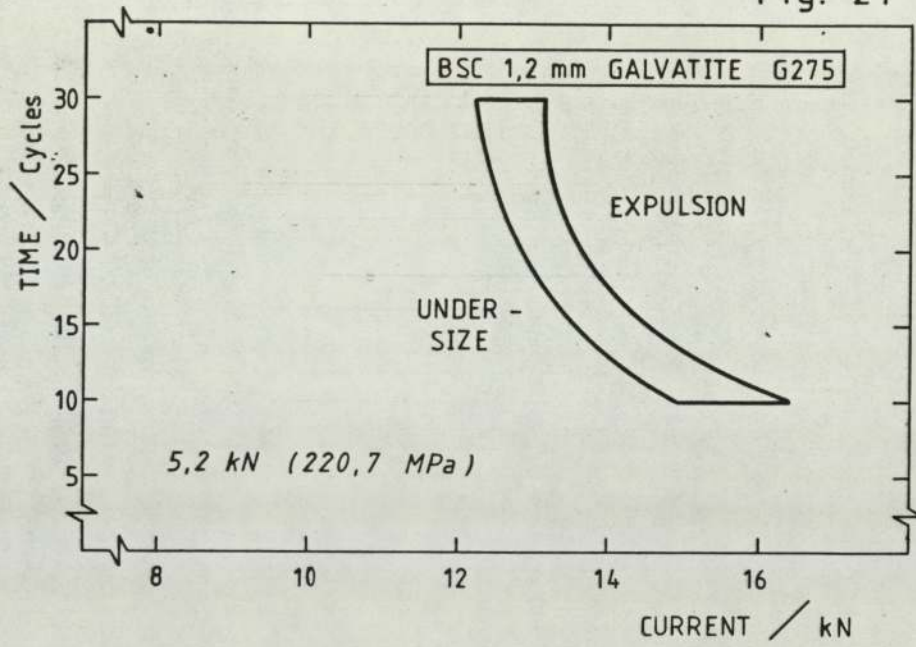
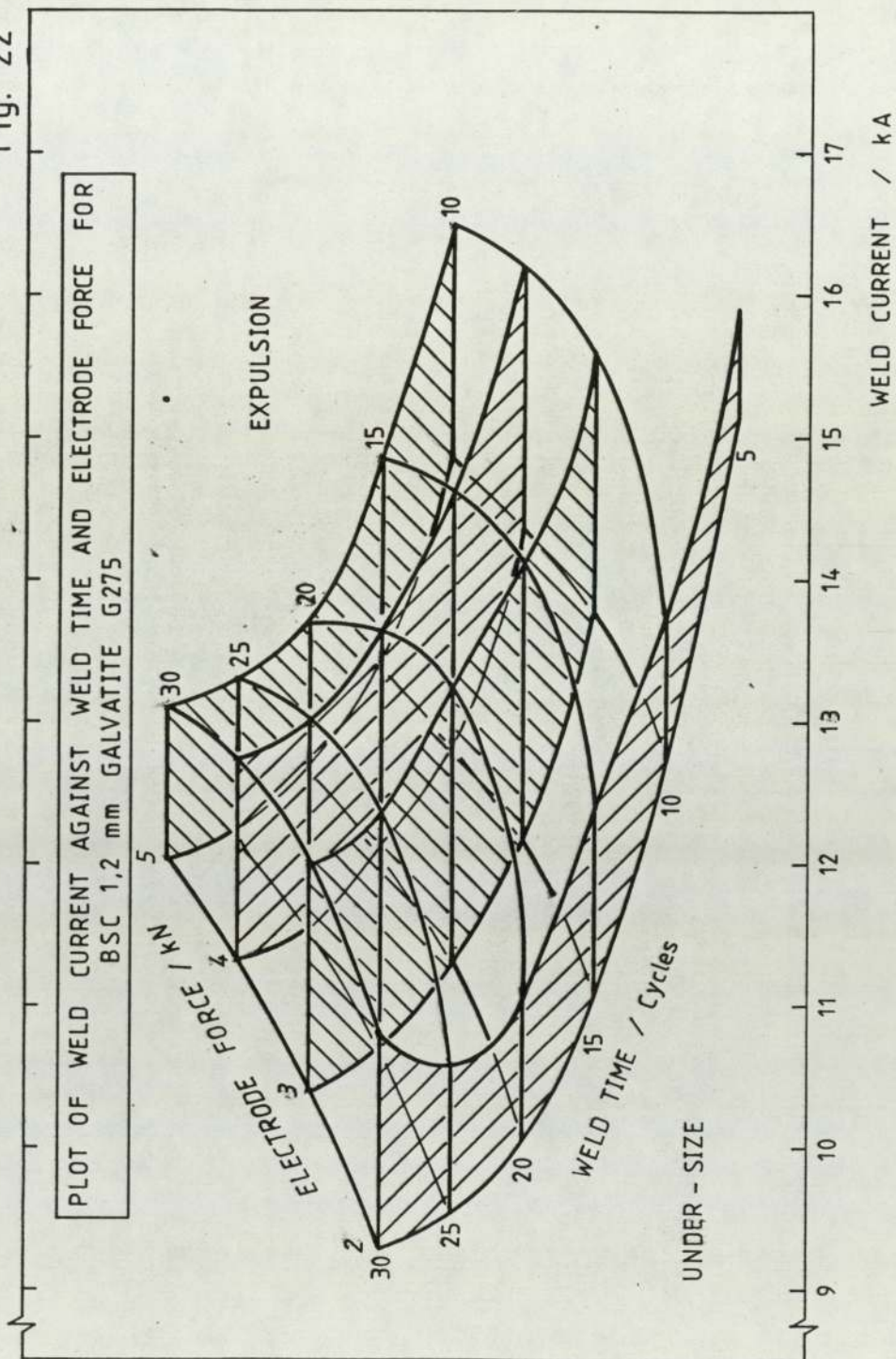
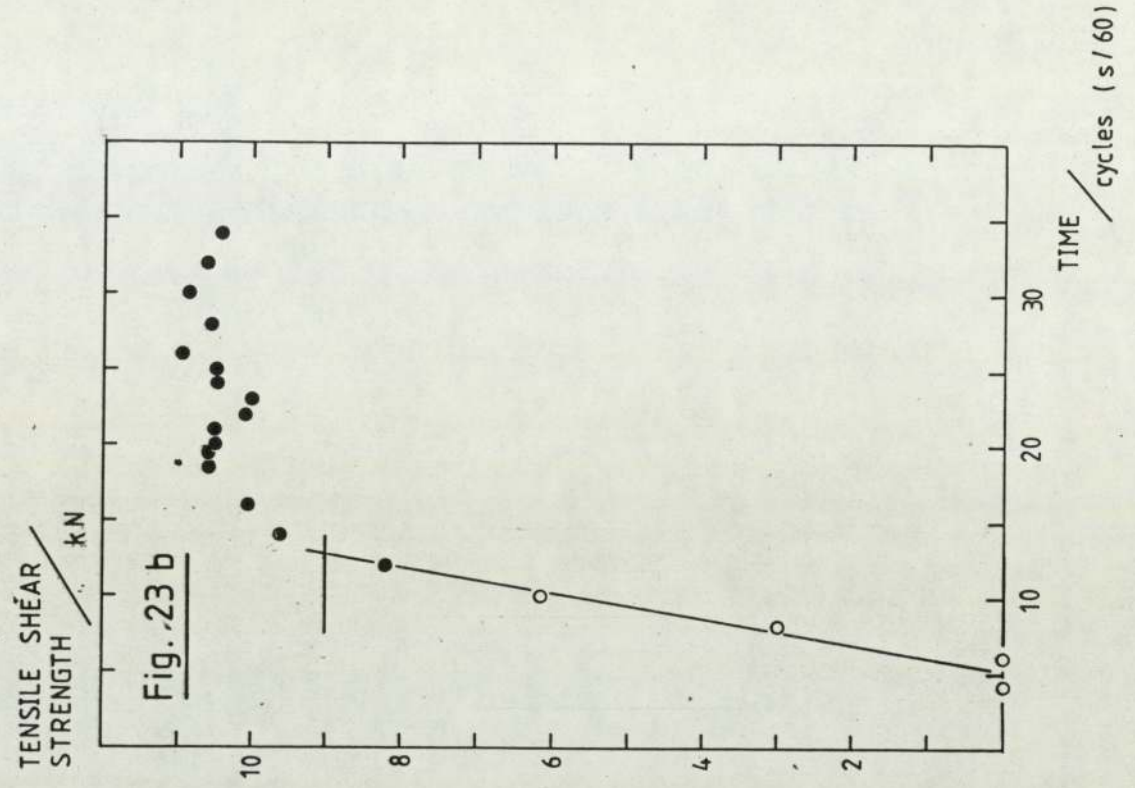
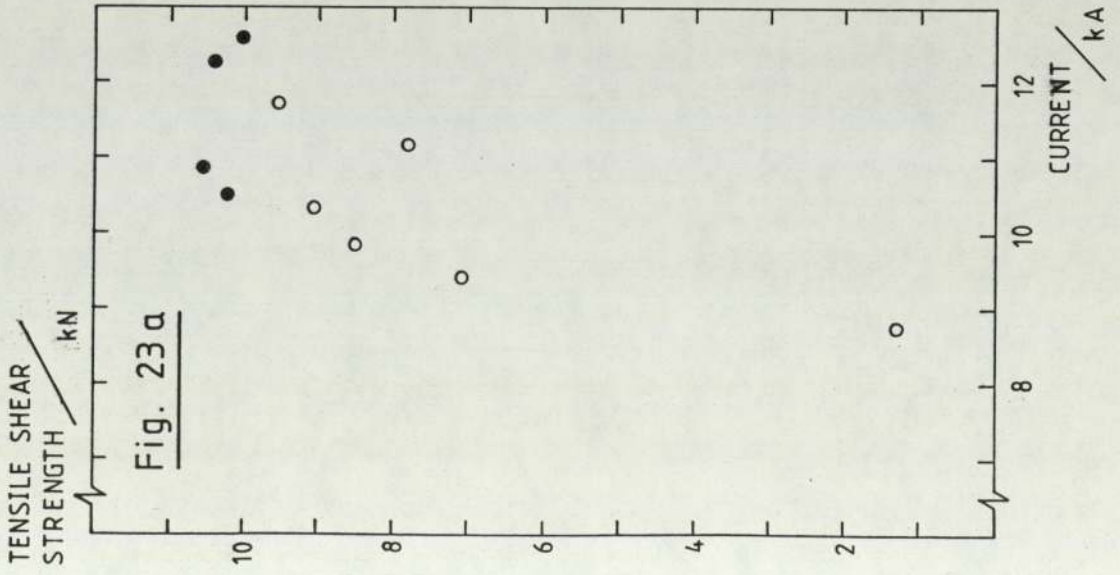


Fig. 22



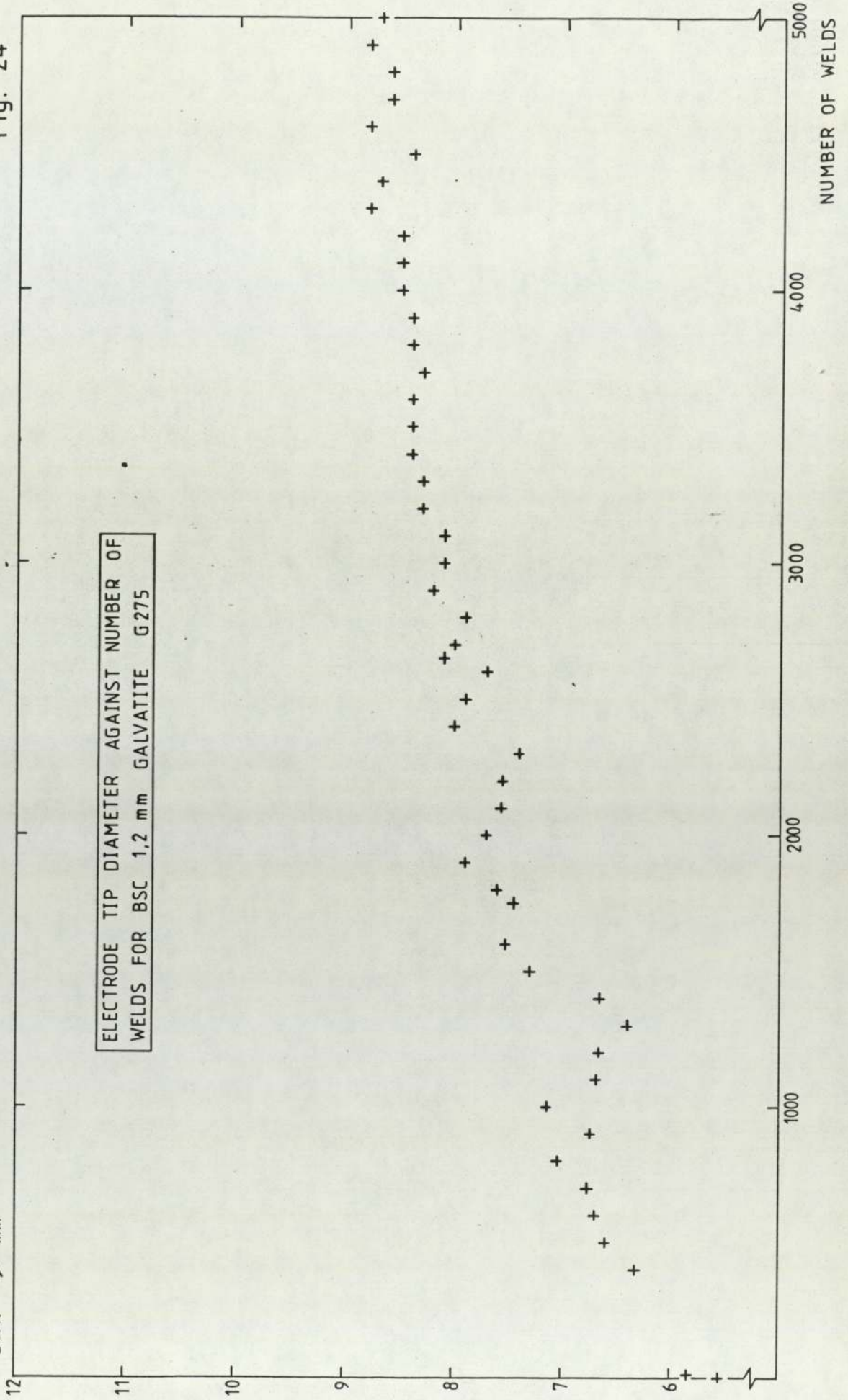
TENSILE SHEAR STRENGTH AGAINST WELD CURRENT (20 Cycles) AND AGAINST WELD TIME  
 ((11,6 ± 0,5)kA) FOR BSC 1,2 mm GALVANIZED G275 . ● - PULLED SLUG / ○ - INTERFACE FAILURE



ELECTRODE TIP  
DIA. / mm

Fig. 24

ELECTRODE TIP DIAMETER AGAINST NUMBER OF  
WELDS FOR BSC 1,2 mm GALVATITE G275



WELD NUGGET  
DIAMETER / mm

Fig. 25

WELD NUGGET DIAMETER AGAINST NUMBER OF  
WELDS FOR BSC 1,2 mm GALVANITE G 275

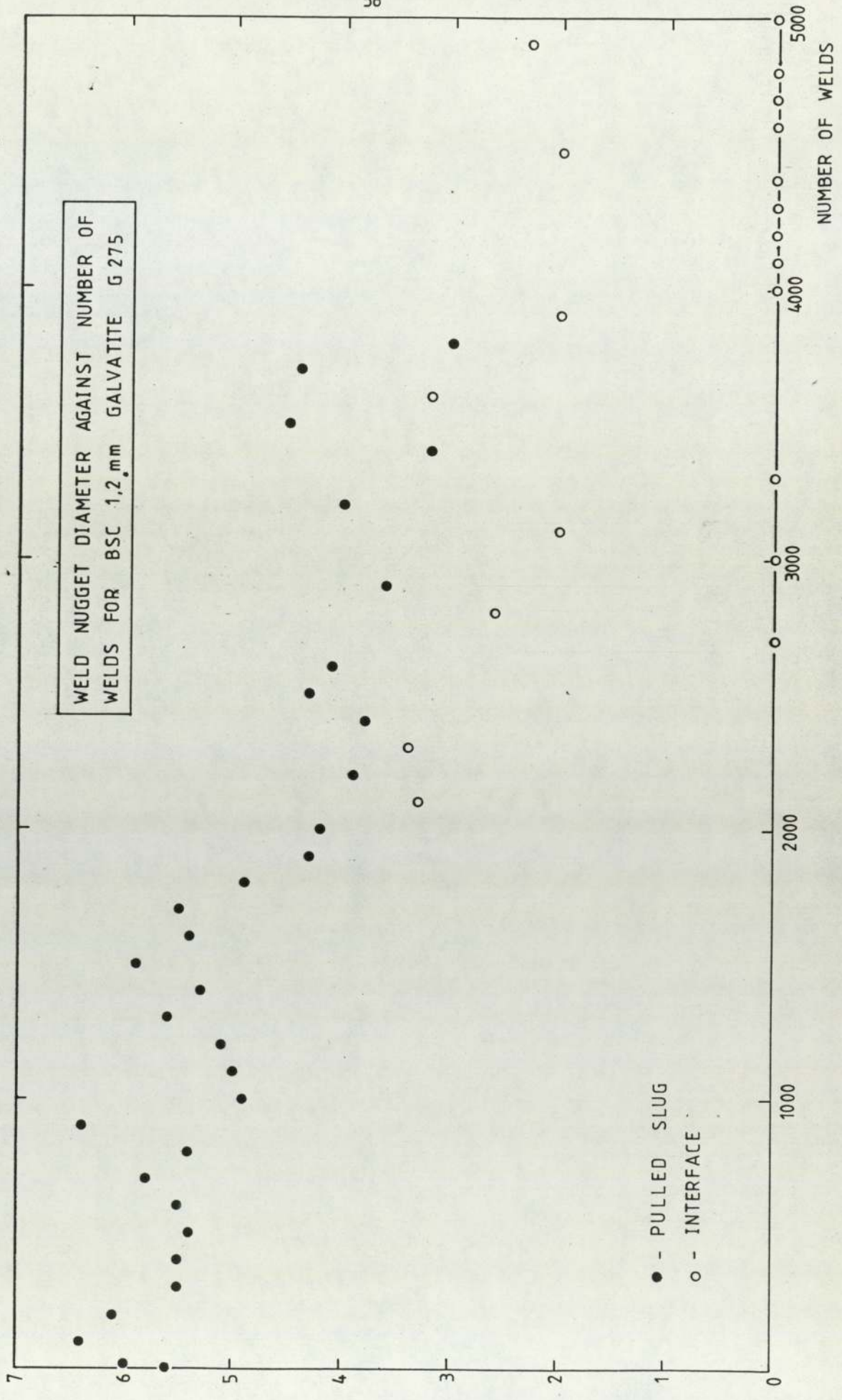
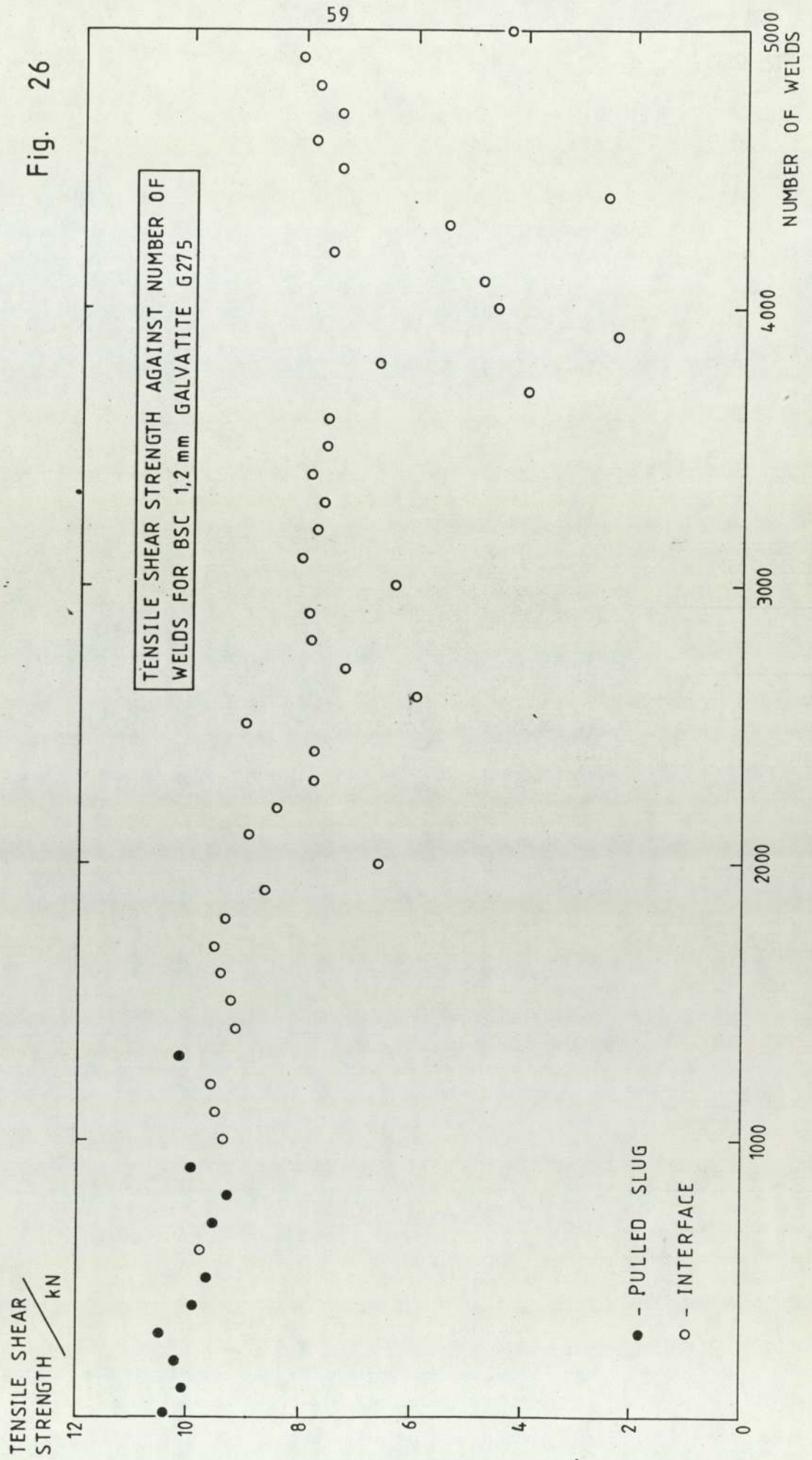


Fig. 26



comparison between the variation in tensile shear strength with current for new electrodes and with electrodes after 5000 welds (Fig.27).

Recording of the monitor error number during welding enabled the production of graphs showing the variation in error number with number of welds produced and with weld size (Figs.28 and 29). The distribution of error numbers between good and bad welds is given in a histogram (Fig.30).

Electrode life tests were carried out using the initial conditions given in table 2b.

#### 4.2 Galvatite Iron-Zinc

A selection of samples of iron-zinc alloy coated steel (Galvatite IZ) were obtained in a range of sizes from 0.5 mm to 1.0 mm. Weldability lobes were produced for B.S.C. Galvatite IZ in thicknesses 0.5 mm (Fig.31a), 0.87 mm (Fig.31b) and 1.0 mm (Fig.32).

A brief electrode endurance test was performed to assess the relative electrode durability of truncated cone ( $120^{\circ}$  included angle) and "pimpel" type electrodes (see section 3.2), using 1.0 mm Galvatite IZ. The variation in weld size with number of welds produced for the two types of electrodes is given in Figure 33. The electrode life for truncated cone electrodes may be estimated at around 2000 welds and for pimpel type electrodes at around 250 welds. The variation in electrode tip diameter with electrode life is also plotted

TENSILE SHEAR STRENGTH AGAINST WELD CURRENT FOR BSC  
1,2 mm GALVANITE G275

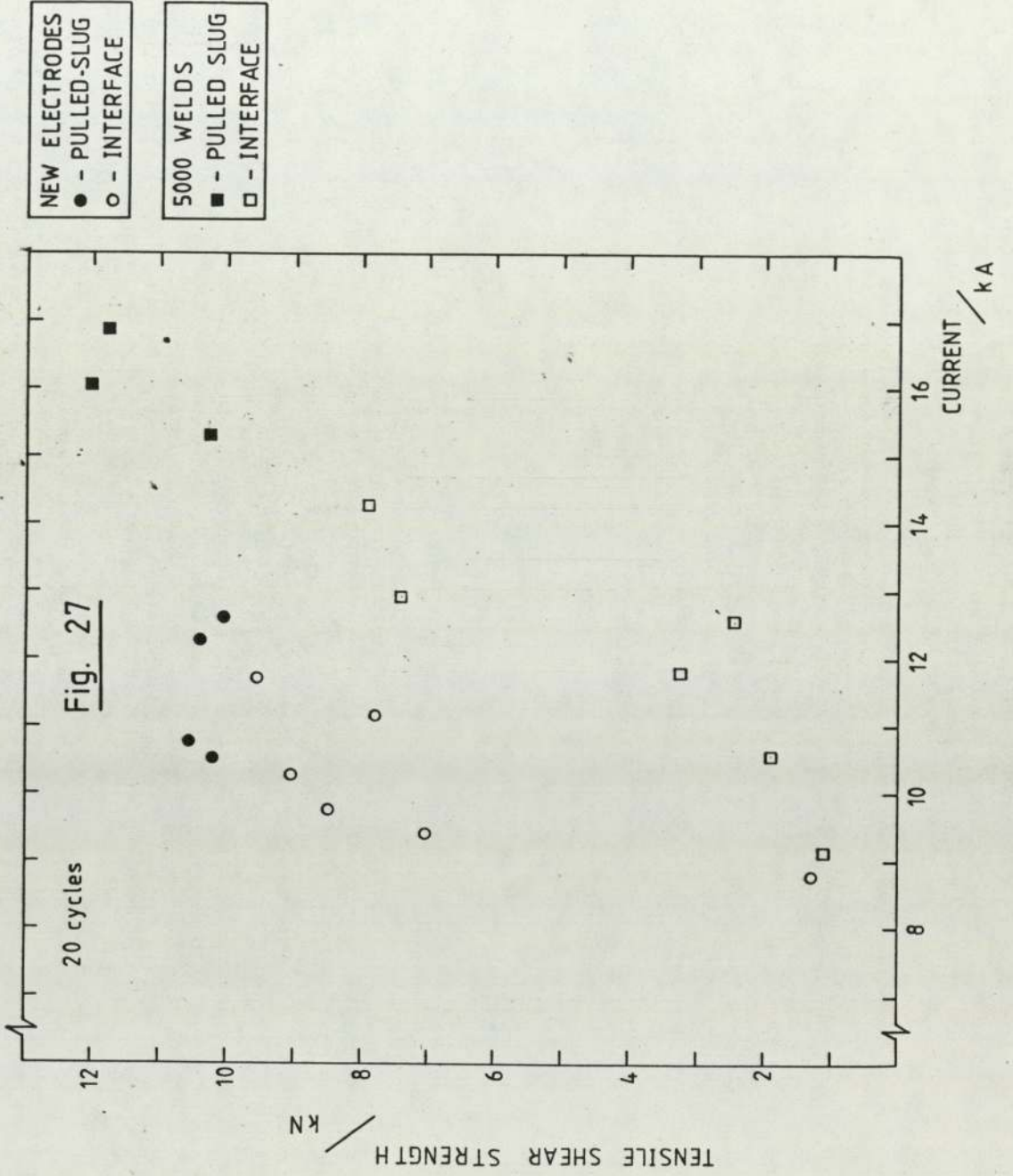


Fig. 28

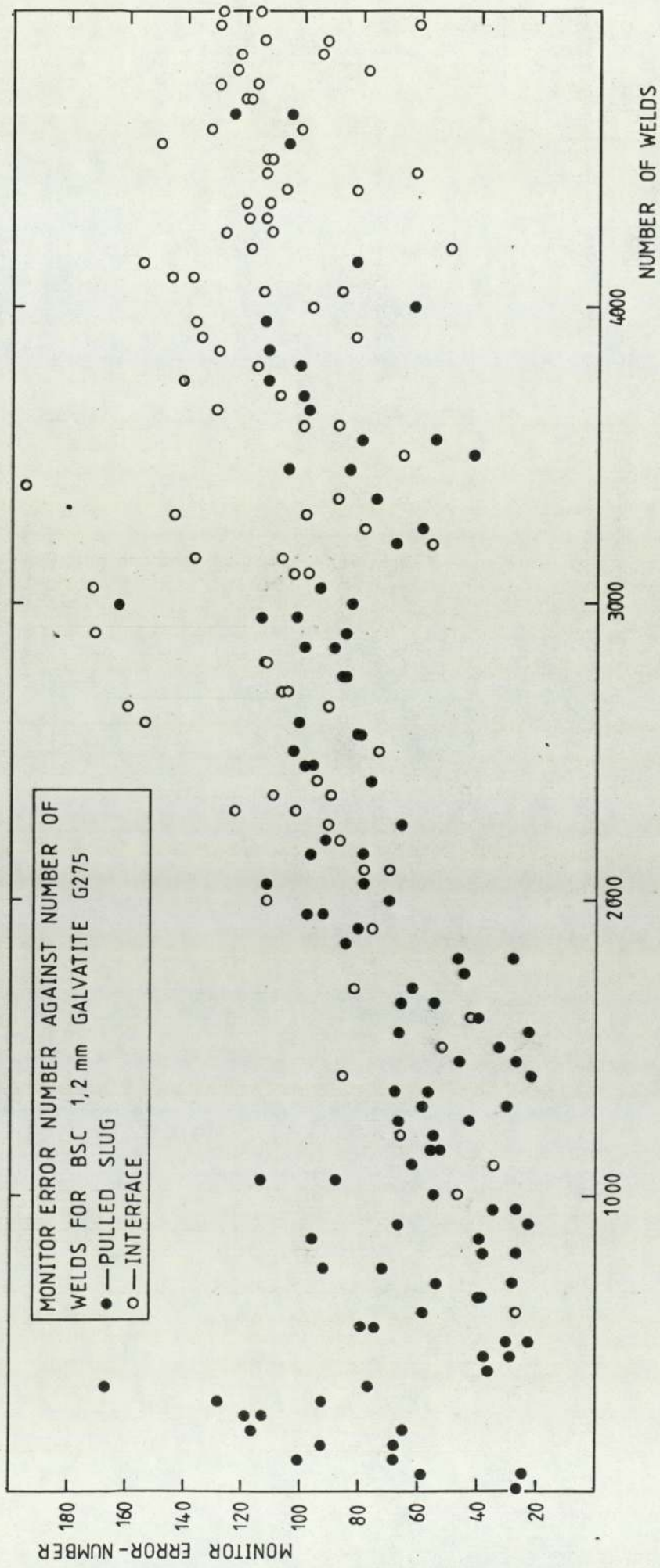


Fig. 29

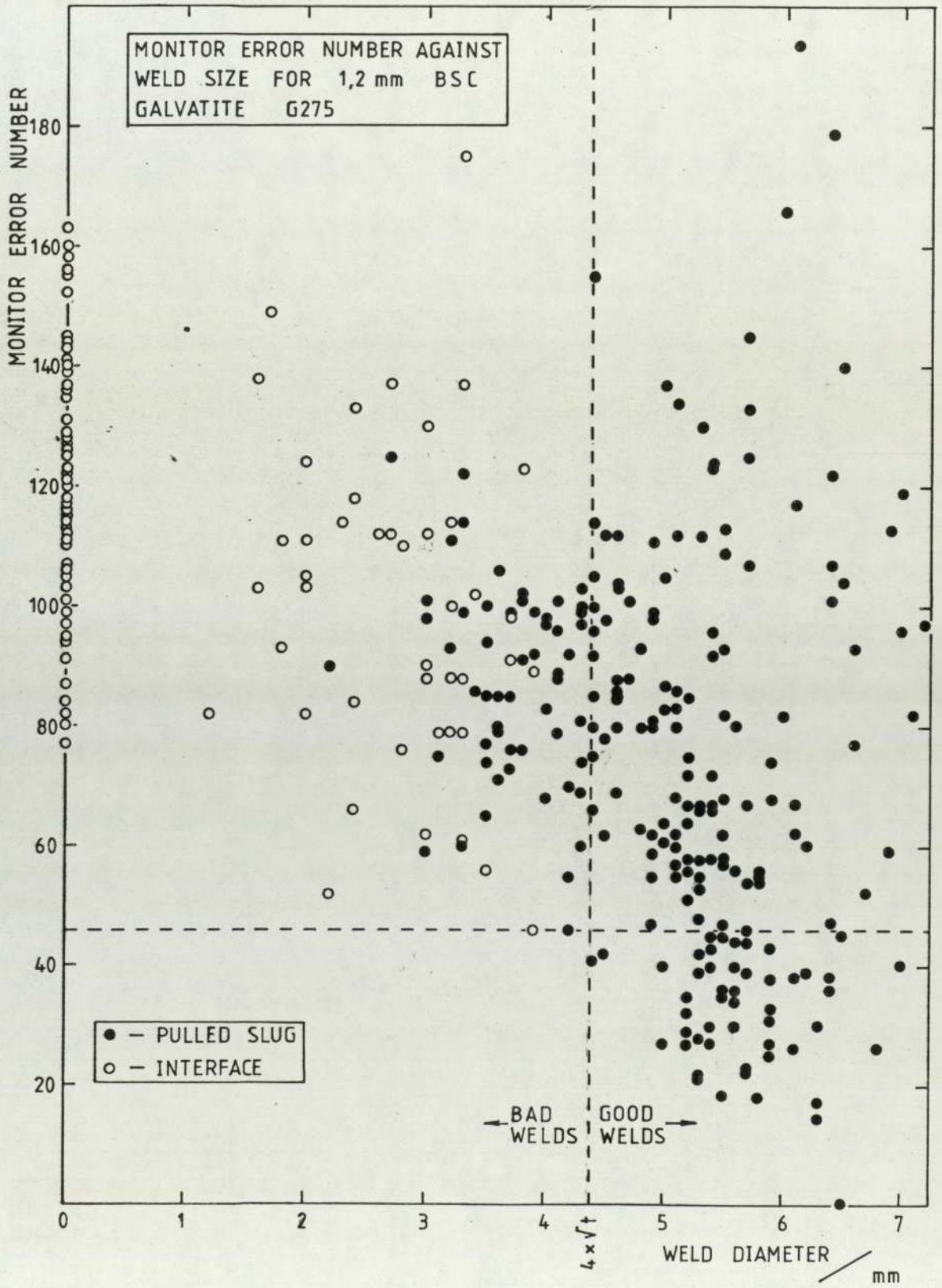
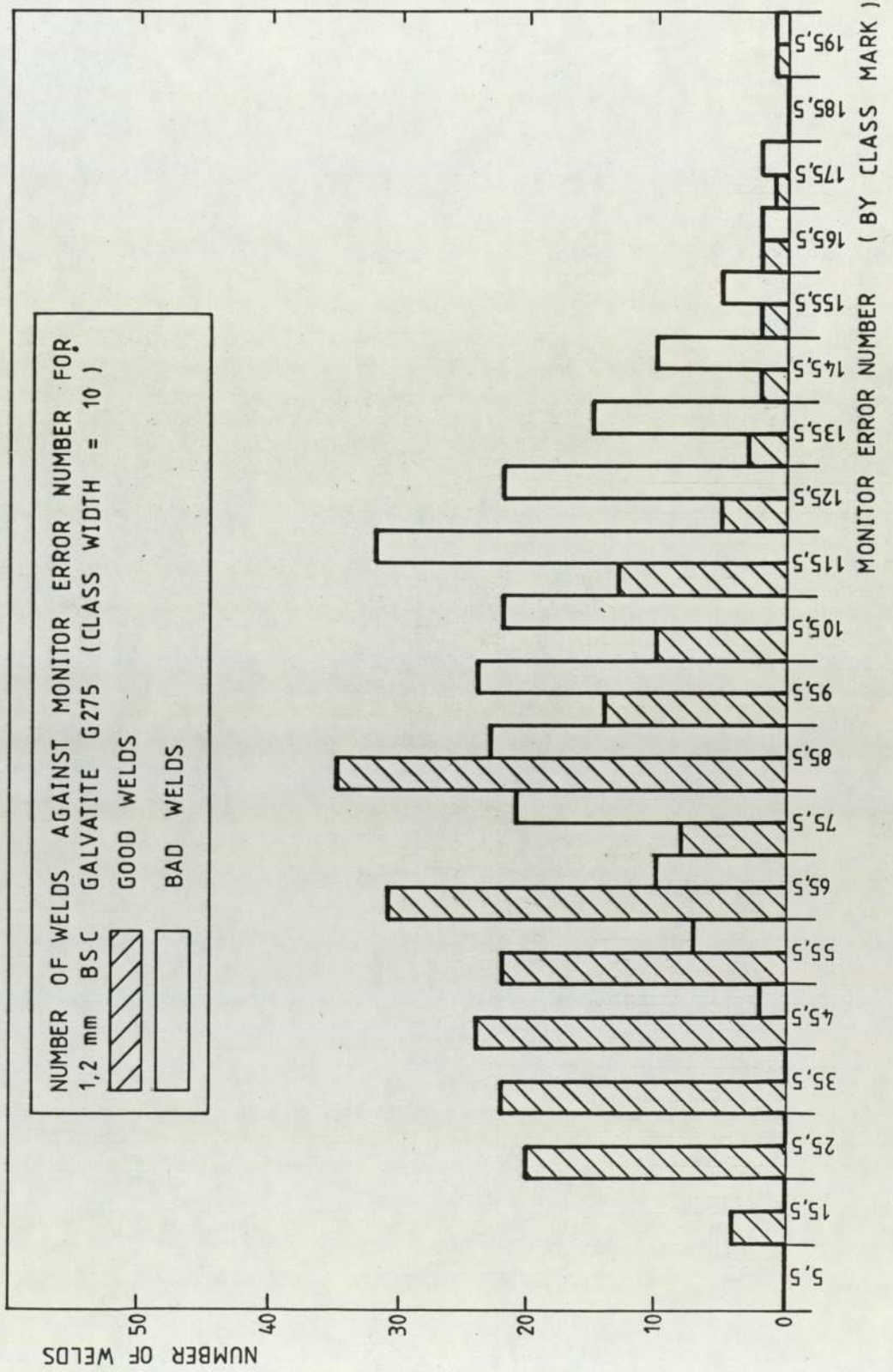


Fig. 30



## WELDABILITY LOBES

Fig. 31 a

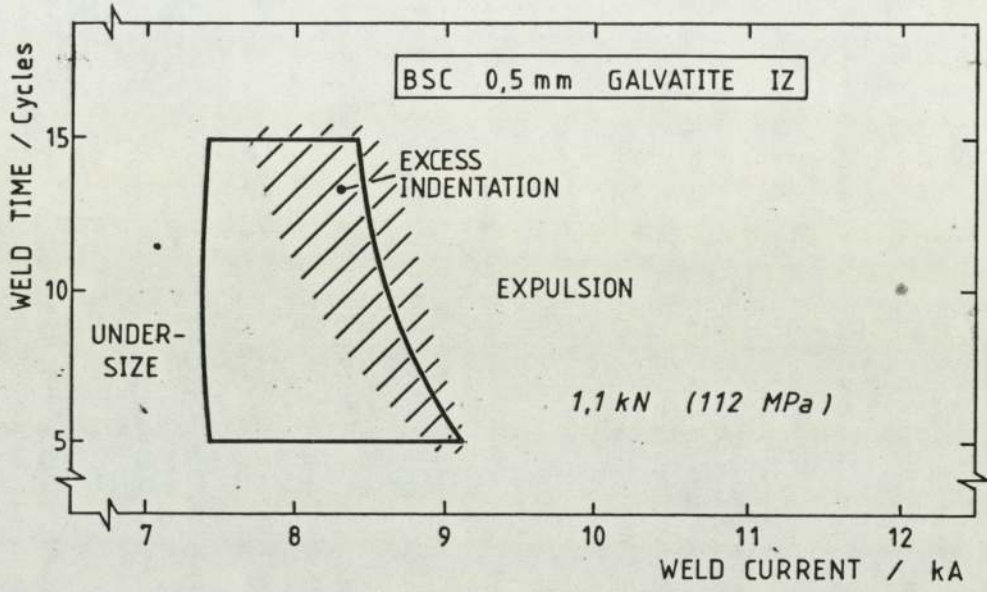


Fig. 31 b

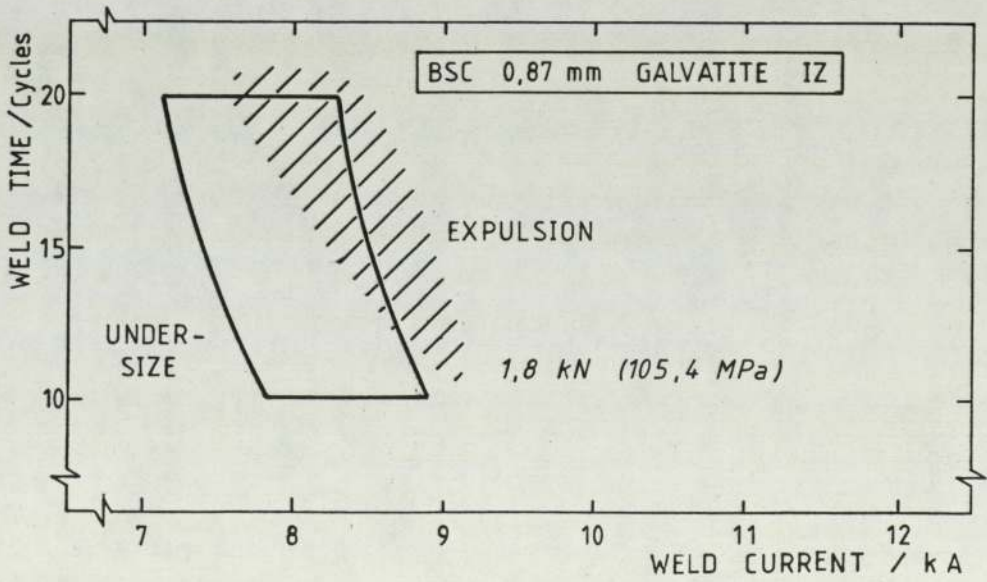


Fig. 32

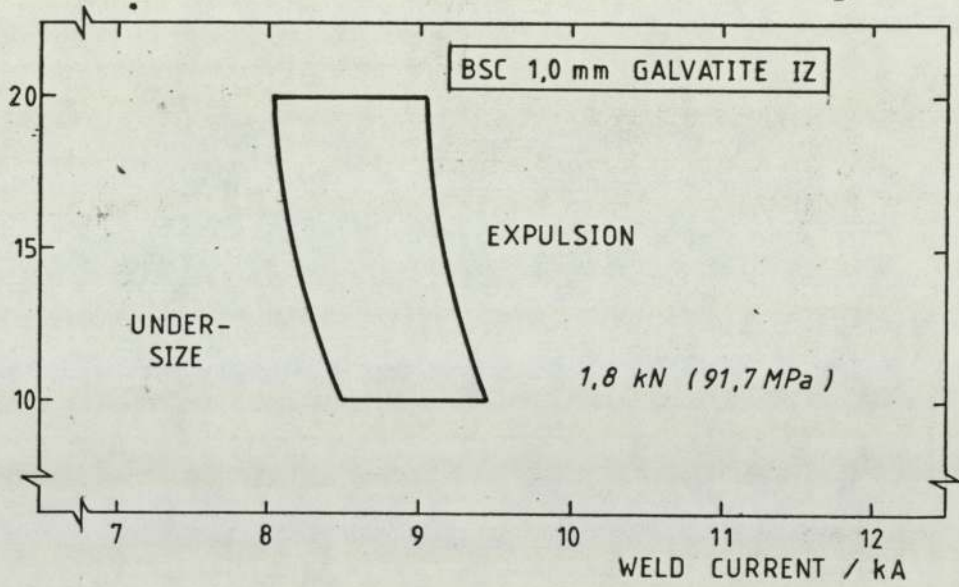
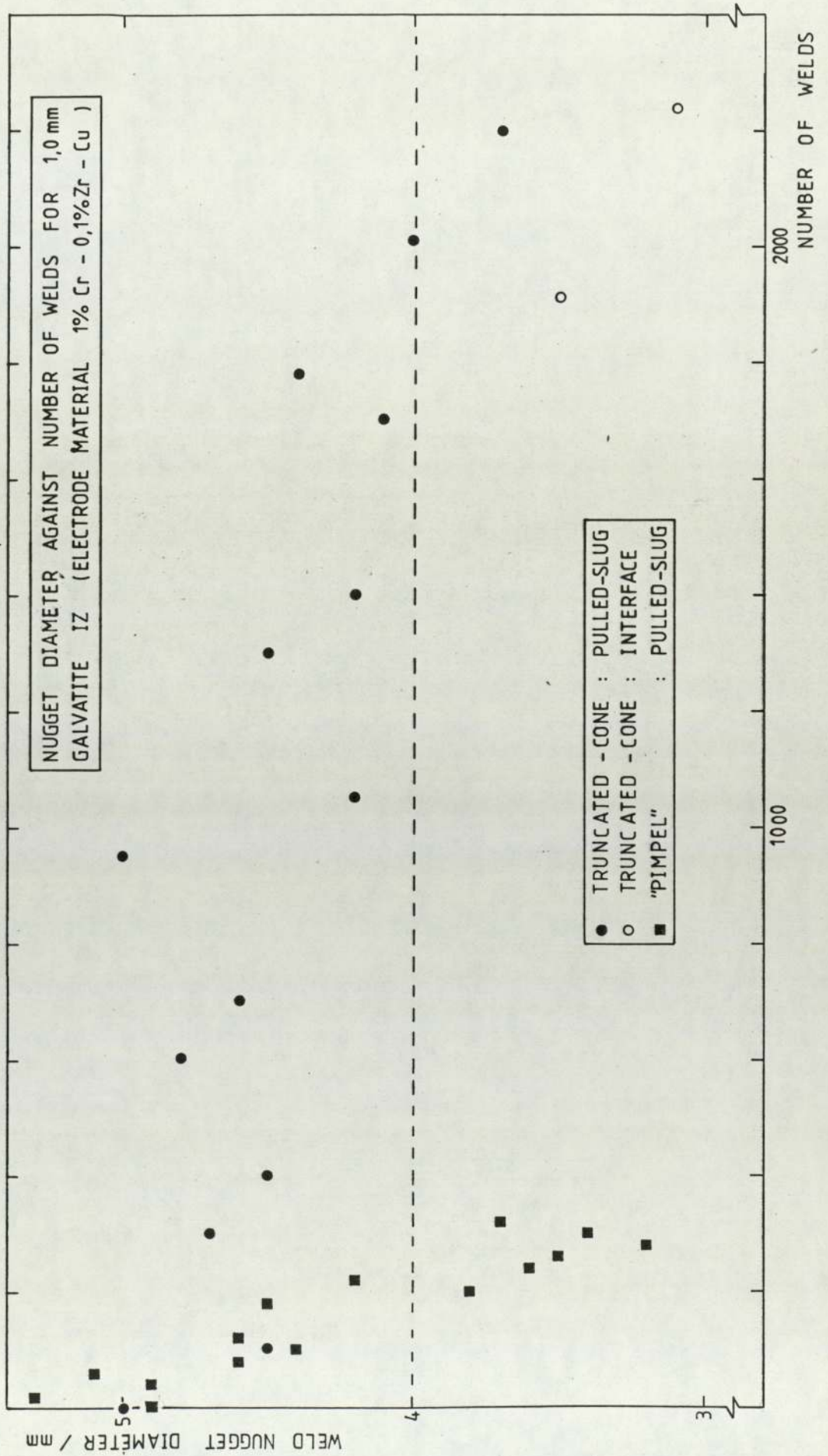


Fig. 33



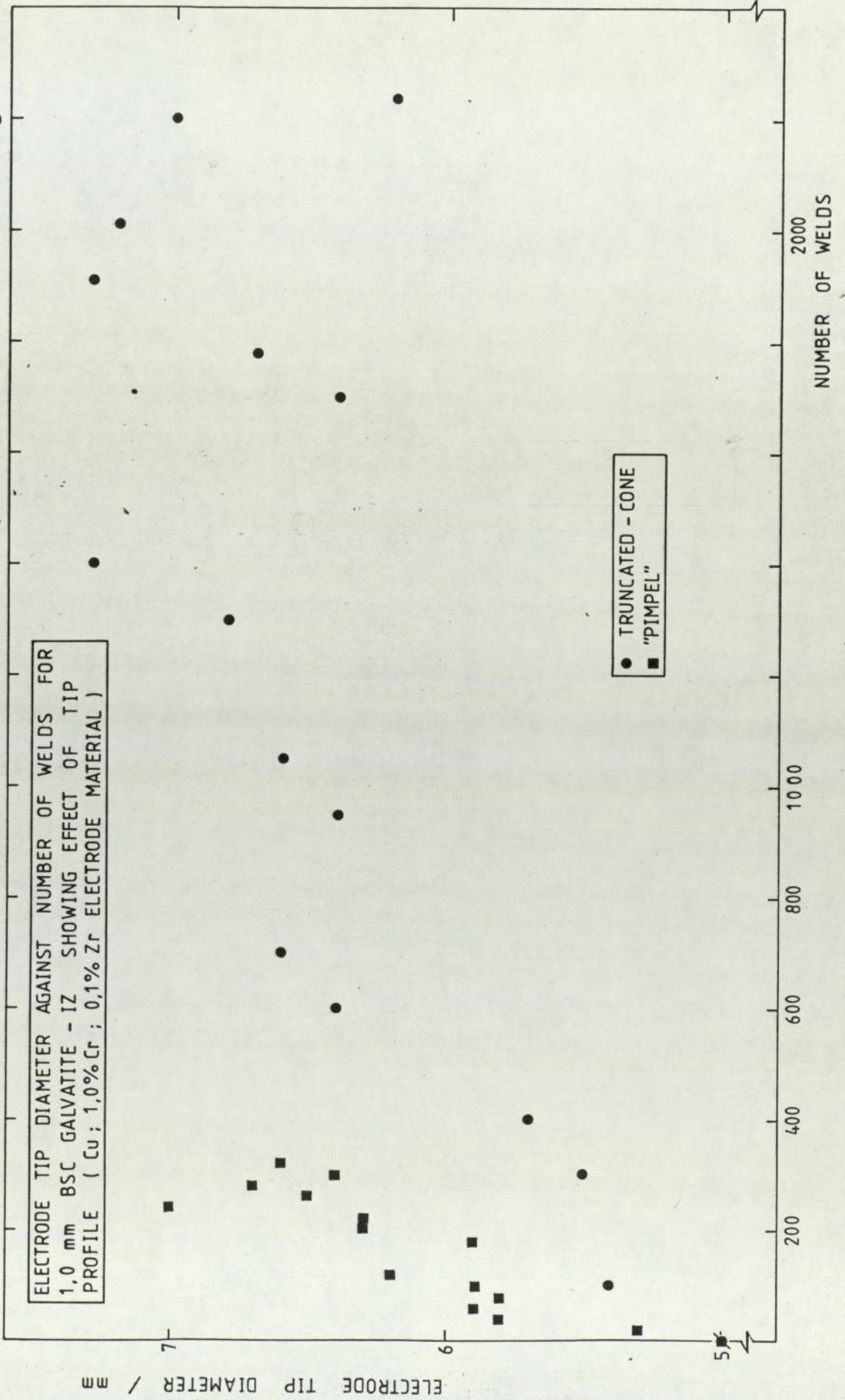
(Figure 34) for the two types of electrodes. It can be seen from the two graphs that there is good correlation between the increase in electrode tip size and the decrease in weld size for the two electrode profiles.

In order to ensure comparability between results for different materials (for example, Galvatite spangle and zintec) quantities of 1.2mm Galvatite IZ were obtained from British Steel. Weldability lobes for this material were produced at a range of pressures (Figures 35a and 35b and 36). A carpet plot was also produced showing the variation in weld current with both weld time and electrode force, (Figure 37).

The results of the electrode endurance test for this material are given in Figures 38 to 43. Figure 38 is a plot of the number of defective welds against the number of welds produced. From the point at which the slope increases sharply, the electrode life may be determined as 2800 welds, with approximately 12% of welds produced during the electrode life being faulty. Figures 39 and 40 show the change in weld size and electrode tip size with number of welds produced. Figure 41 is a plot of the change in monitor error number during the life of the electrodes. The change in monitor error number with weld size is plotted in Figure 42 and the distribution of error numbers between good and bad welds is given in the form of a histogram (Figure 43).

The initial conditions for the electrode life test are given in Table 4.

Fig. 34



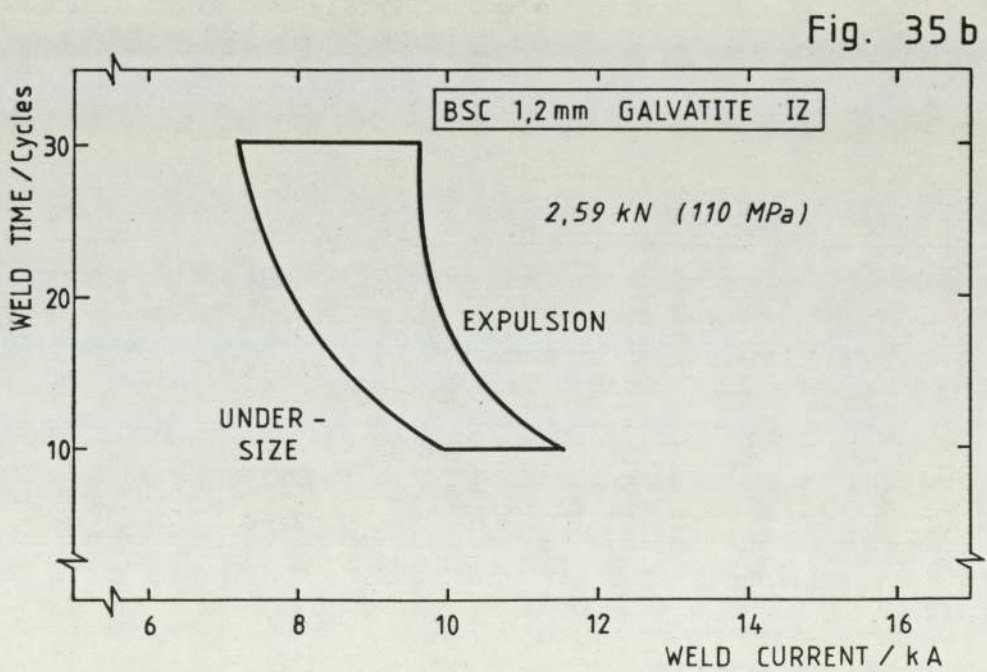
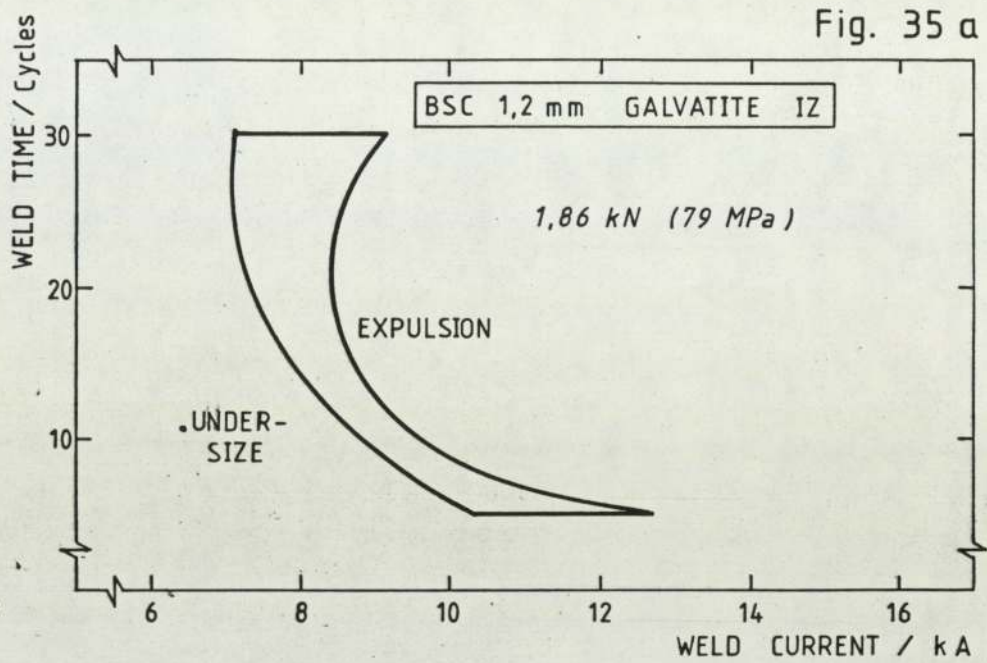
WELDABILITY LOBES

Fig. 36

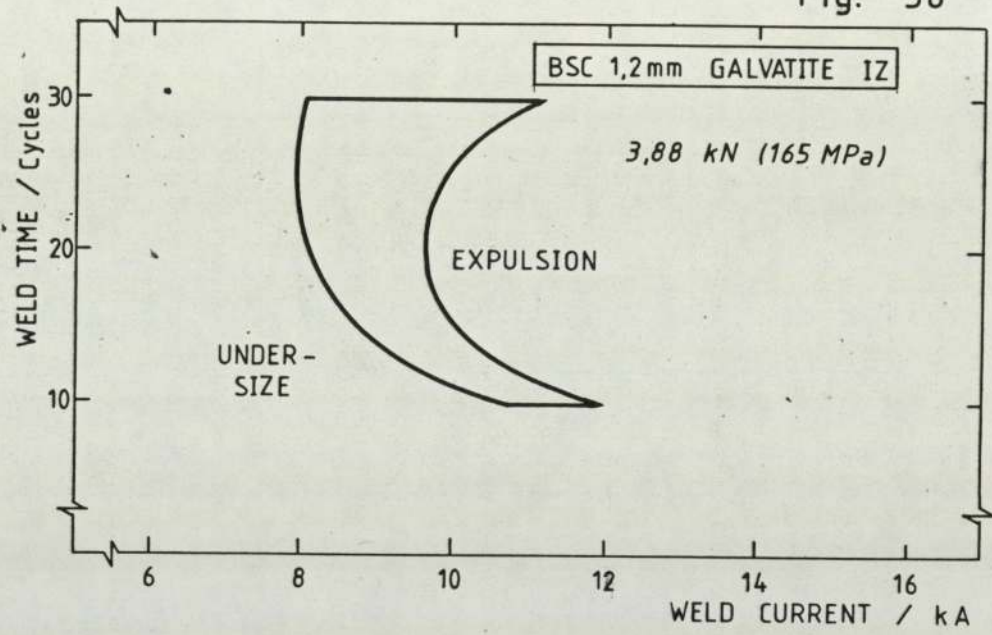
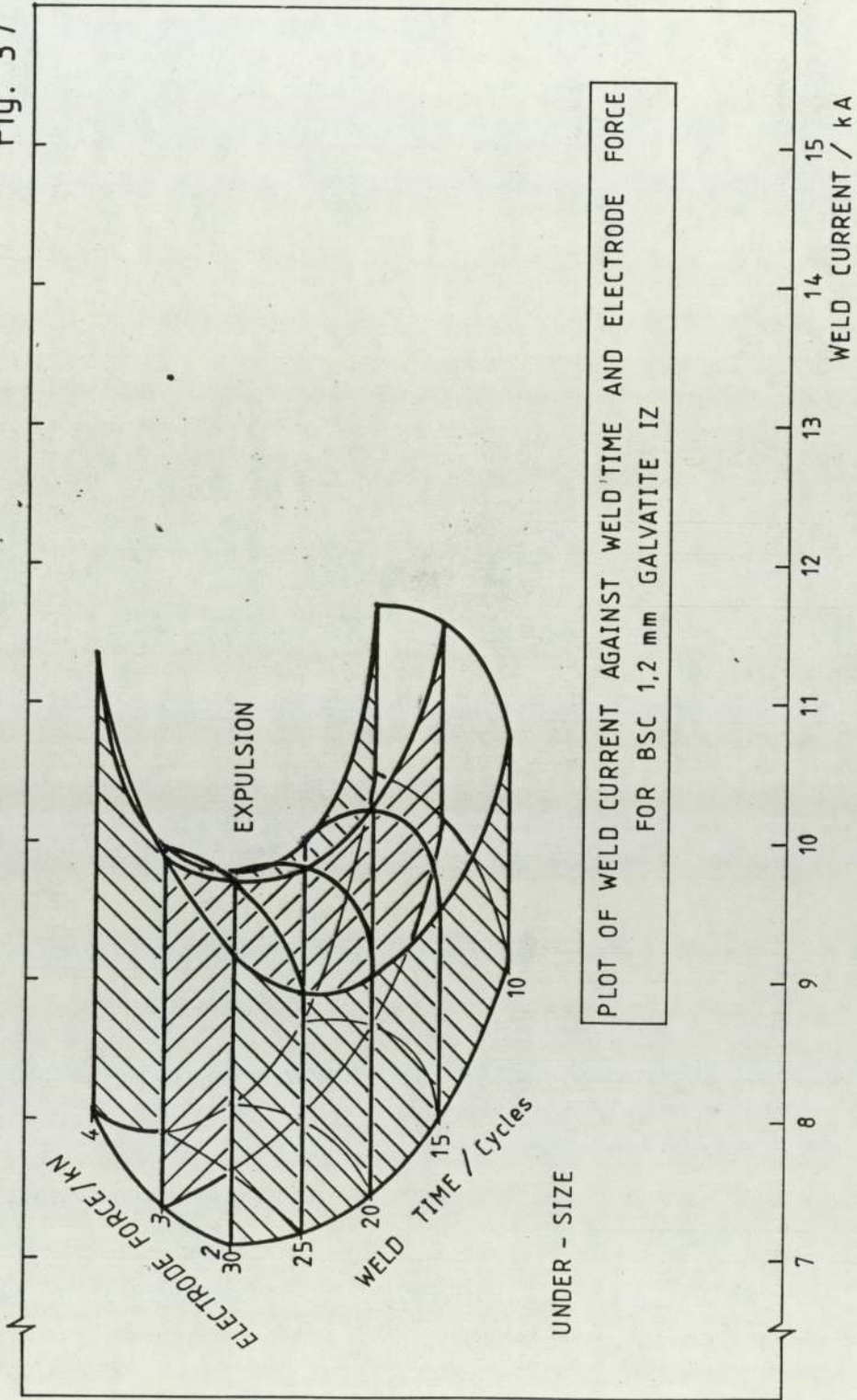


Fig. 37



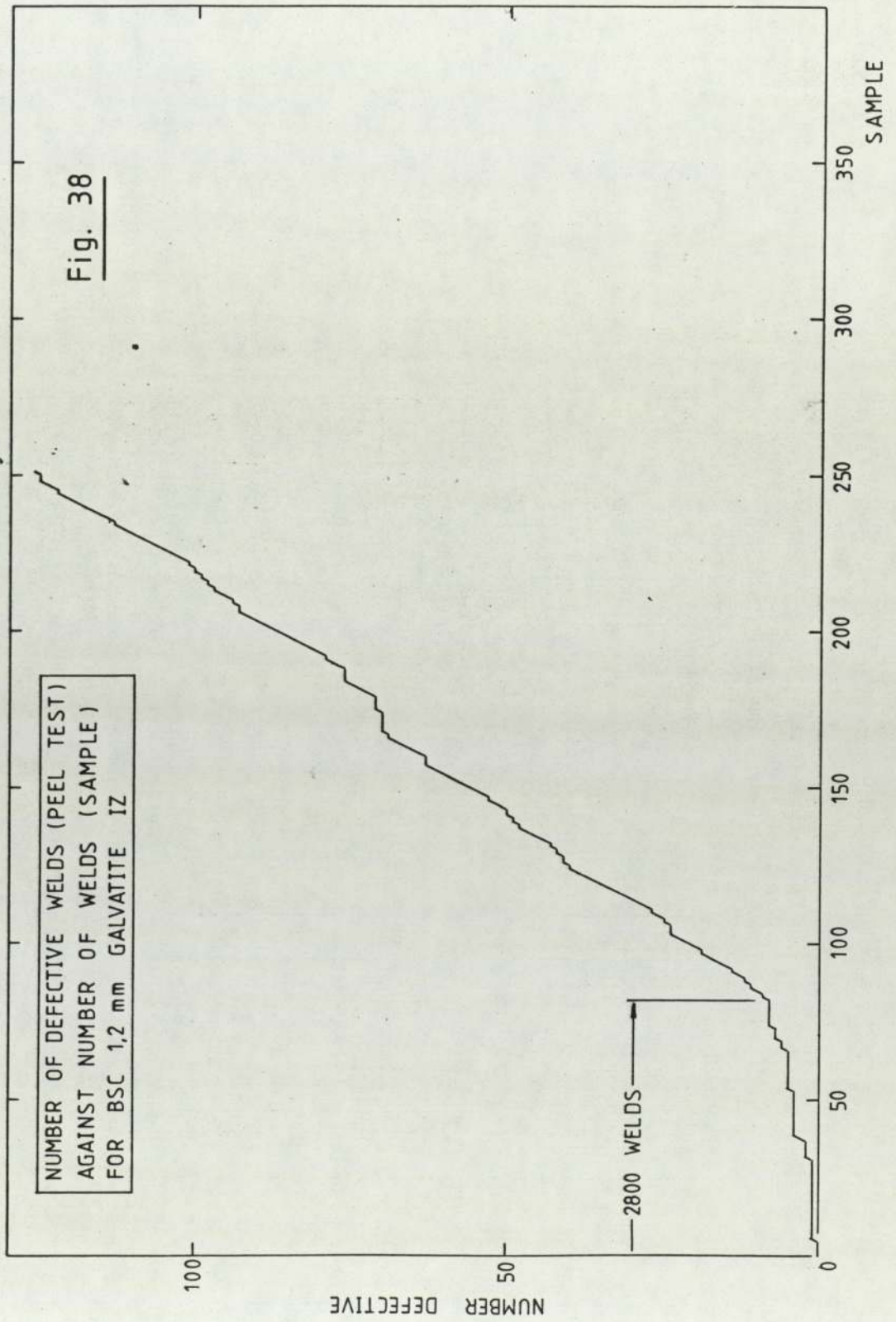


Fig. 39

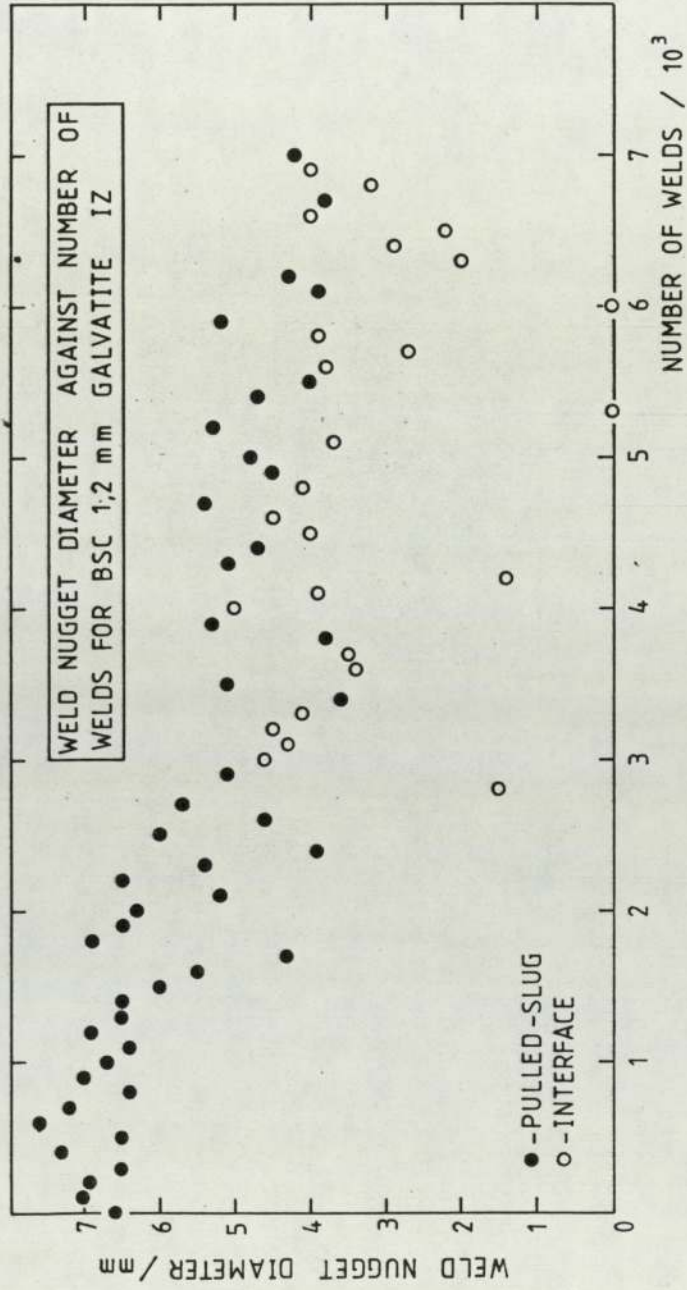


Fig. 40

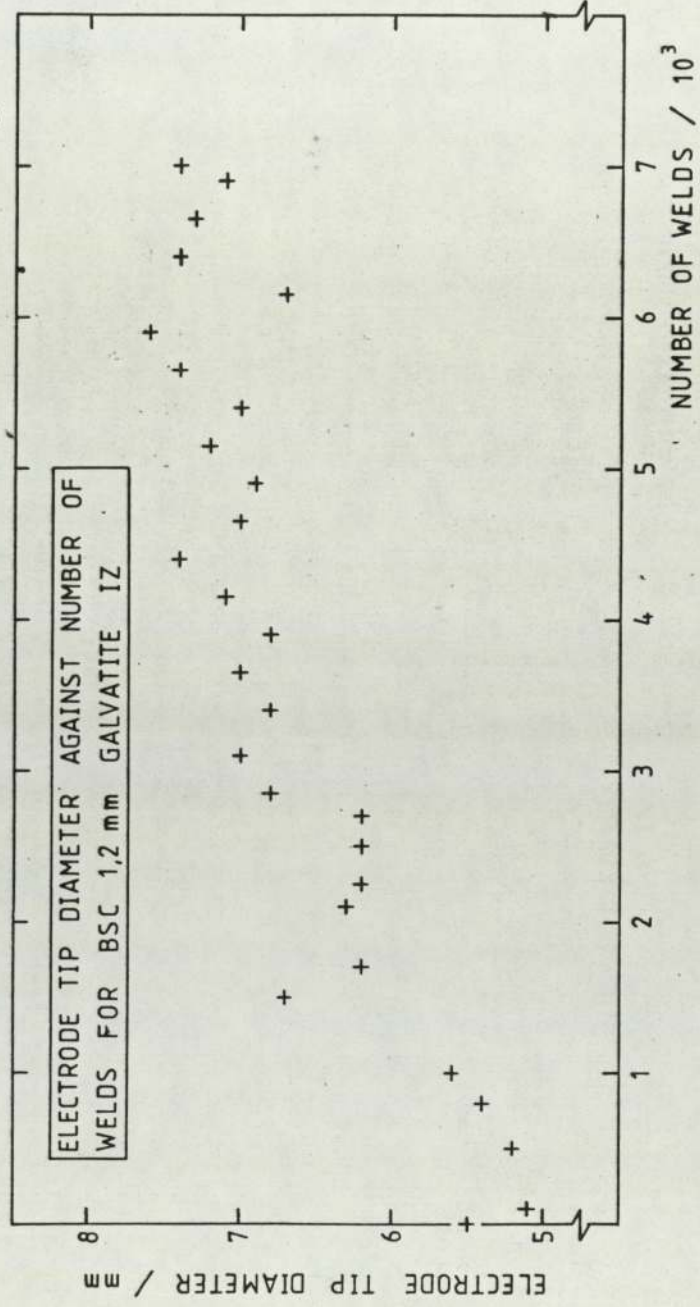


Fig. 41

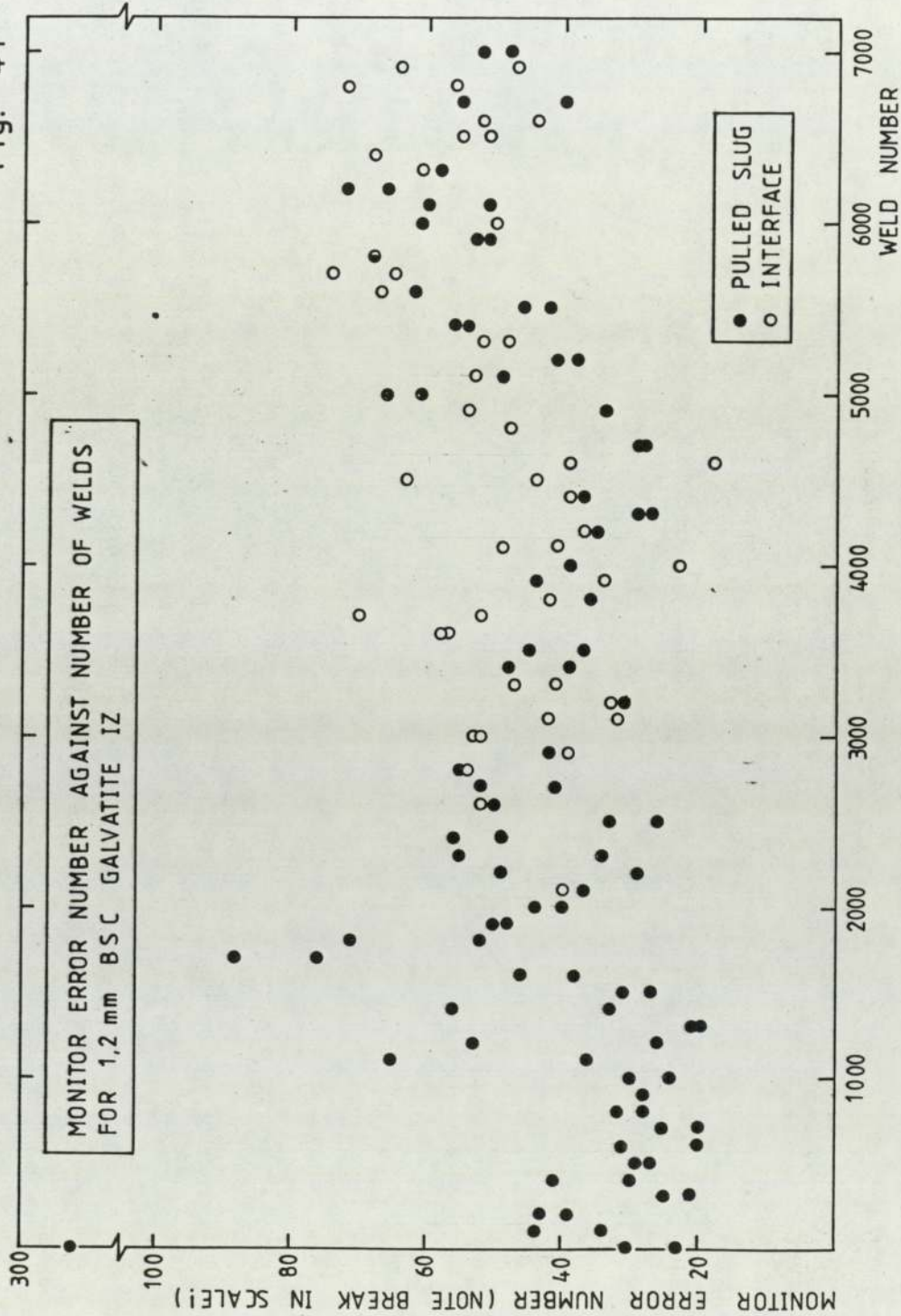


Fig. 42

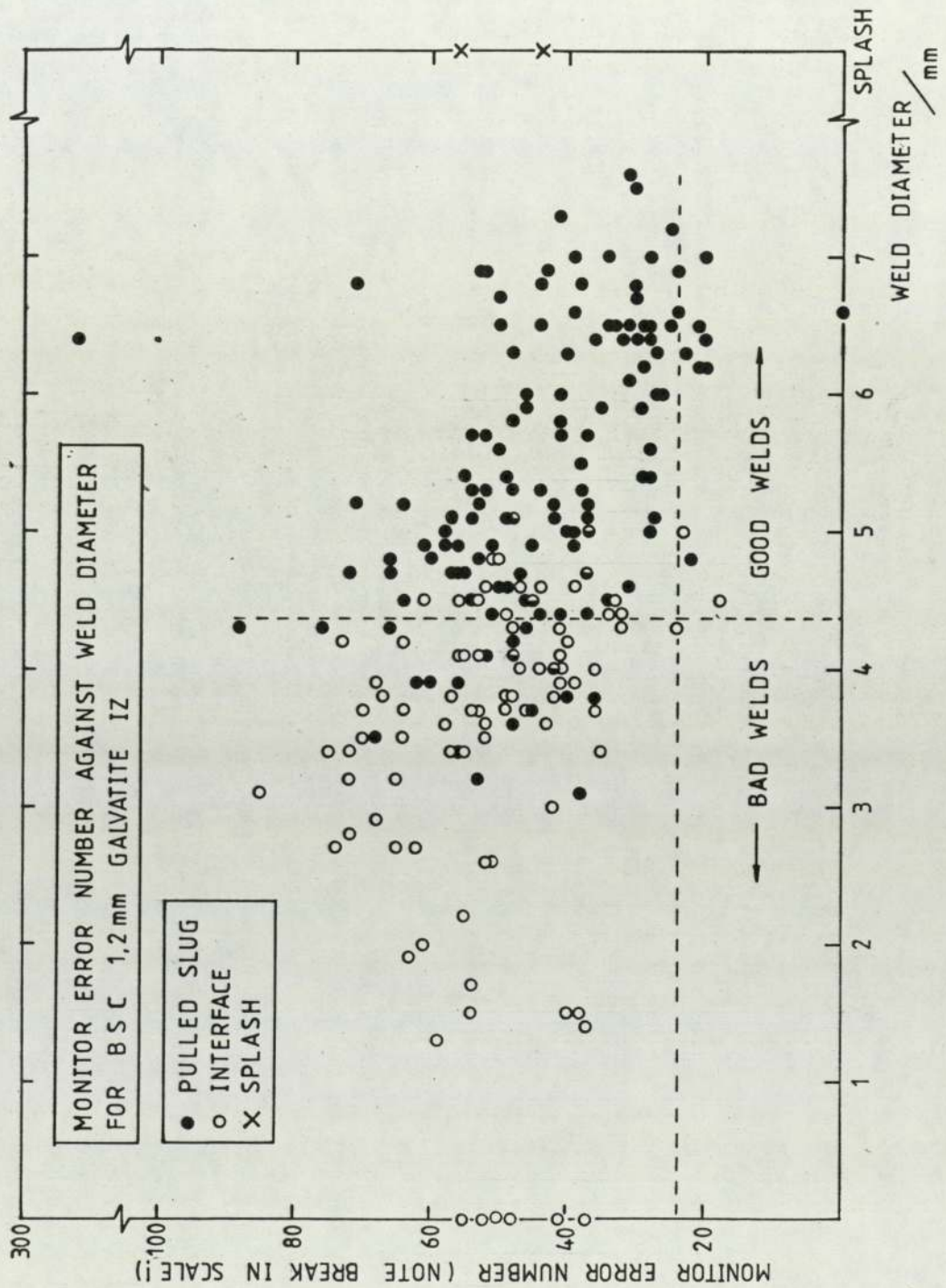


Fig. 43

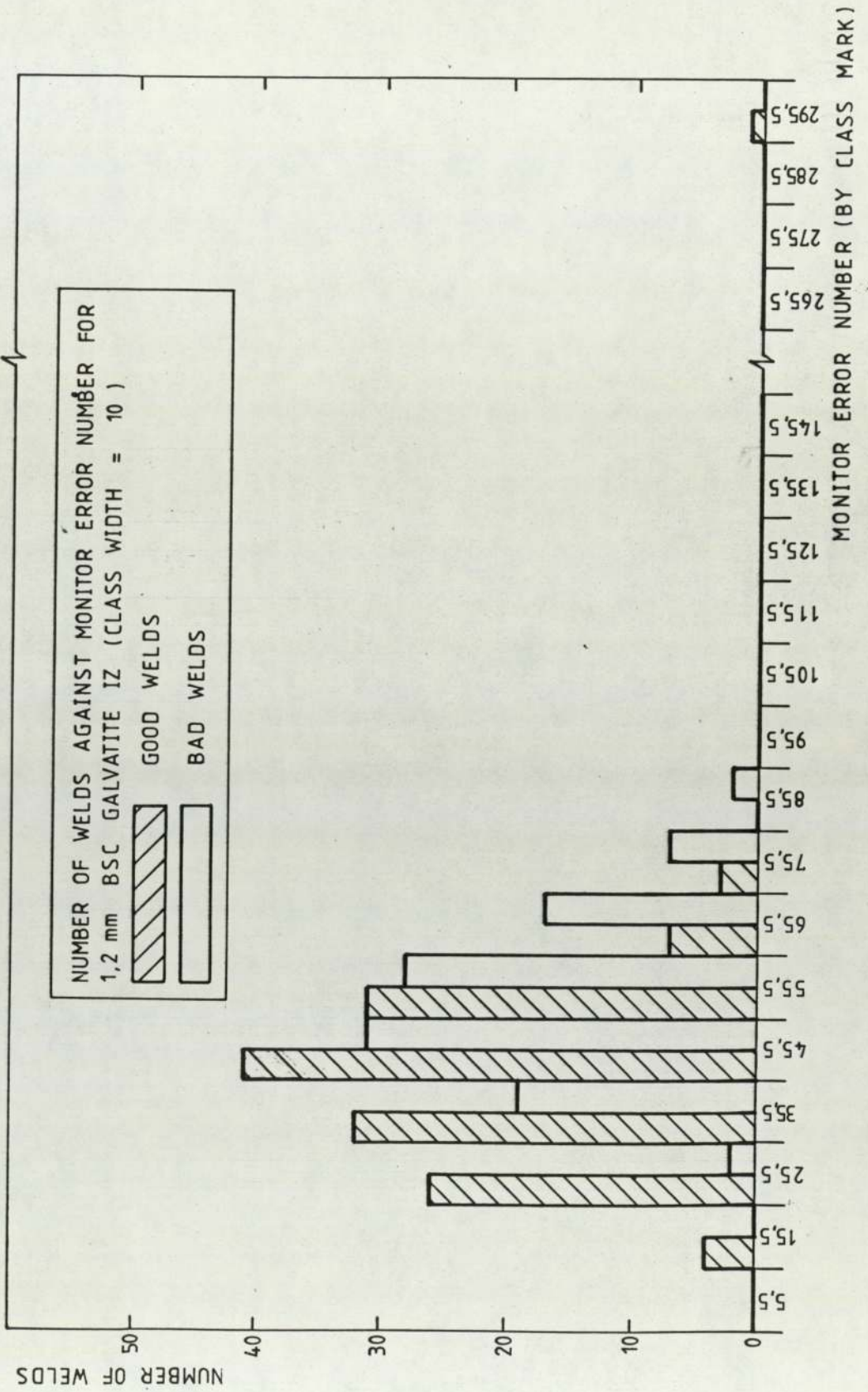


Table 4

Initial Conditions for Electrode Life Test for  
B.S.C. 1.2mm Galvatite IZ

Electrode Force / kN	2.2
Electrode tip diameter / mm	5.5
Inter-electrode gap / mm	10
Squeeze time / cycles	20
Up Slope / cycles	3
Weld time / cycles	18
Weld current / kA	$8.7 \pm 0.23 \sigma_{n-1}$
Hold time / cycles	40
Weld frequency / weld $\text{min}^{-1}$	approx 25-40
Coolant flow / $1 \text{ min}^{-1}$	$\sim 7$

Table 5

Analysis of B.S.C. 1.2mm Galvatite IZ Base Metal

(all weight percent - balance iron)

Carbon	0.029
Sulphur	0.018
Phosphorous	0.005
Manganese	0.28
Soluble Aluminium	<0.01
Nitrogen	0.0032
Silicon	0.001
Carbon equivalent =	0.076

#### Coating

- i)  $195 \text{ gm}^{-2}$  iron zinc alloy including both sides
- ii)  $0.004 \text{ gm}^{-2}$  chromate on each side, no phosphate

### 4.3 Electro zinc "Zintec"

Quantities of 1.2 mm, double-sided zintec were obtained from W.C.M. James. Samples of the material were sent to B.S.C. for analysis (Table 6). Weldability lobes were produced for this material using both truncated cone and pimpel type electrodes at an electrode force of 2.4 kN, (Figures 44a and 44b).

Electrode life tests were carried out (with truncated cone electrodes) with initial conditions as given in Table 7. A plot of the number of defective welds against the number of welds produced allows the usable electrode life to be calculated as 3051 welds with approximately 5% of the welds up to this point faulty. A graph of weld nugget diameter against number of welds shows the way in which the weld quality changes with electrode life (Figure 45). Figure 46 is a plot of the increase in electrode tip size with electrode life. The information obtained by recording the monitor error number is presented in Figures 48, 49 and 50. Figure 48 is a plot of the change in error number with electrode life, whilst Figure 49 shows the relationship between weld nugget diameter and monitor error number. The distribution of error numbers between good and bad welds is given in Figure 50.

Table 6

## Analysis of W.C.M.James 1.2 mm Zintec Base Metal

(all weight percent - balance iron)

Carbon	:	0.028	Sulphur	:	0.008
Phosphorus	:	0.005	Manganese	:	0.31
Nickel	:	< 0.01	Copper	:	0.019
Tin	:	< 0.01	Soluble Aluminium	:	< 0.01
Silicon	:	0.001	Nitrogen	:	0.0028
Niobium	:	< 0.01	Chromium	:	0.010
Titanium	:	< 0.01	Boron	:	< 0.001

Carbon equivalent = 0.08

## Coating

- i) 2  $\mu\text{m}$  electrozinc on each side equivalent to 28.23  $\text{gm}^{-2}$  over both sides
- ii) 0.02  $\text{gm}^{-2}$  of chromate on each side
- iii) No phosphate coating

## WELDABILITY LOBES

Fig. 44a

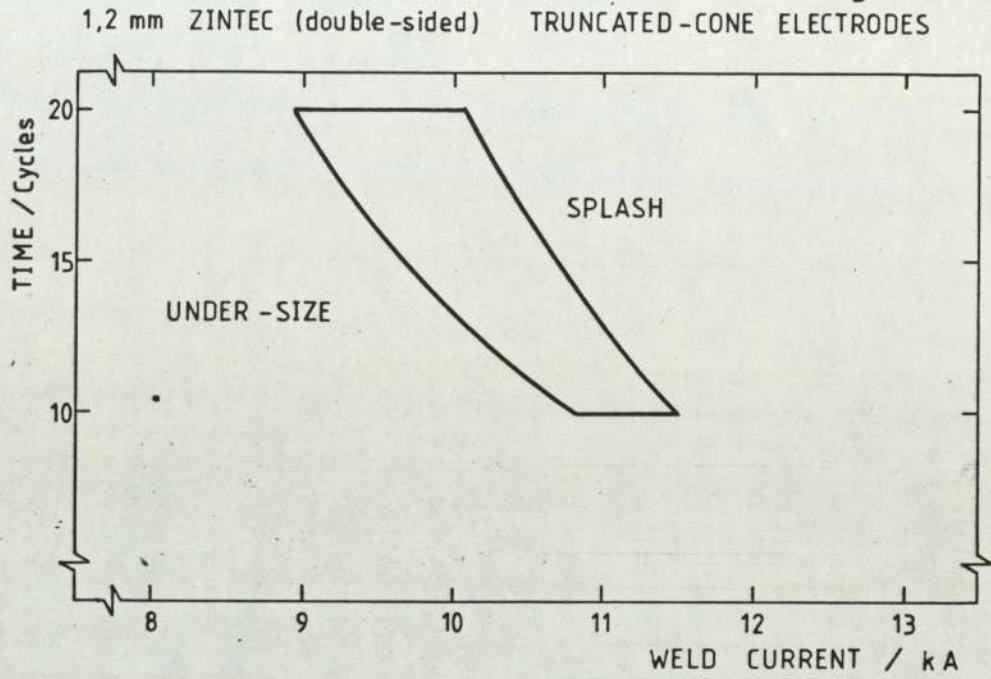


Fig. 44b

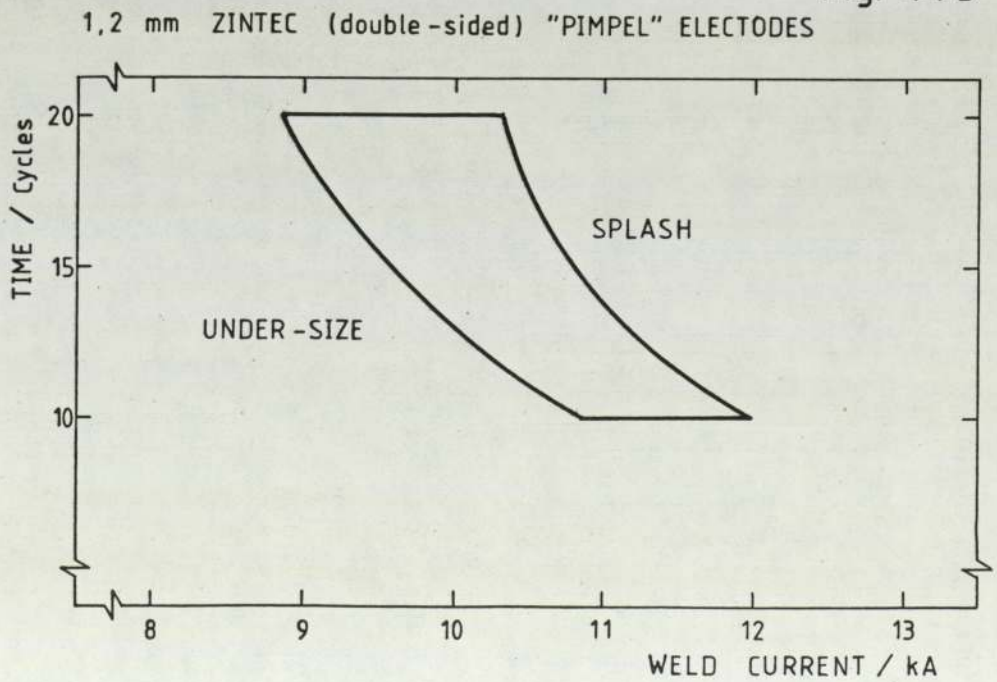


Table 7

Initial Conditions for Electrode Life Test for  
W.C.M.James 1.2 mm Zintec

Electrode force / kN		2.4
Electrode tip diameter / mm		5.5
Inter-electrode gap / mm		10
Squeeze time / cycles		20
Up Slope / cycles		3
Weld time / cycles		15
Weld current / kA		$10.1 \pm 0.39_{\sigma_{n-1}}$
Hold time / cycles		40
Weld frequency / weld $\text{min}^{-1}$	approx.	25 - 40
Coolant flow / $1 \text{ min}^{-1}$		$\sim 7$



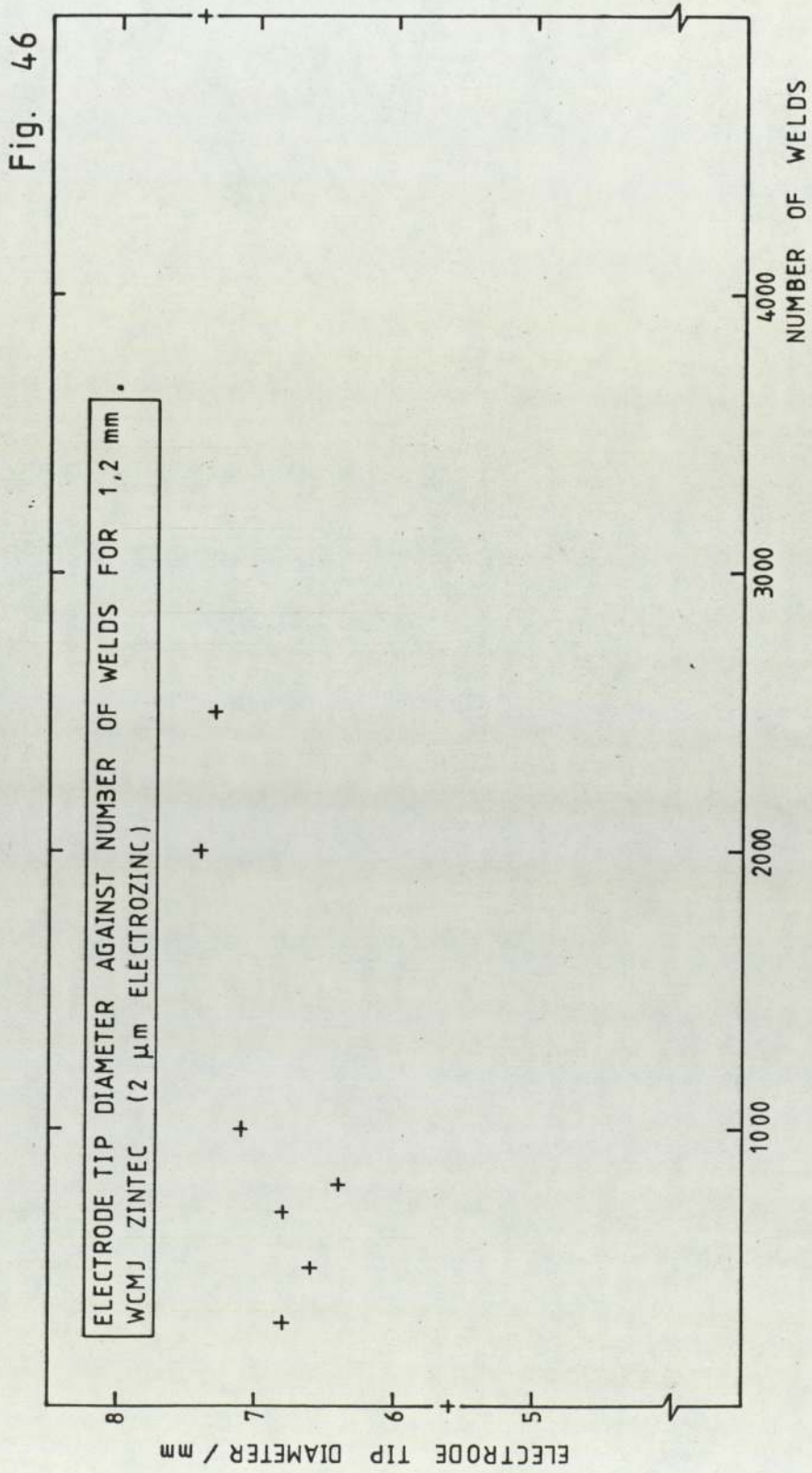


Fig. 47

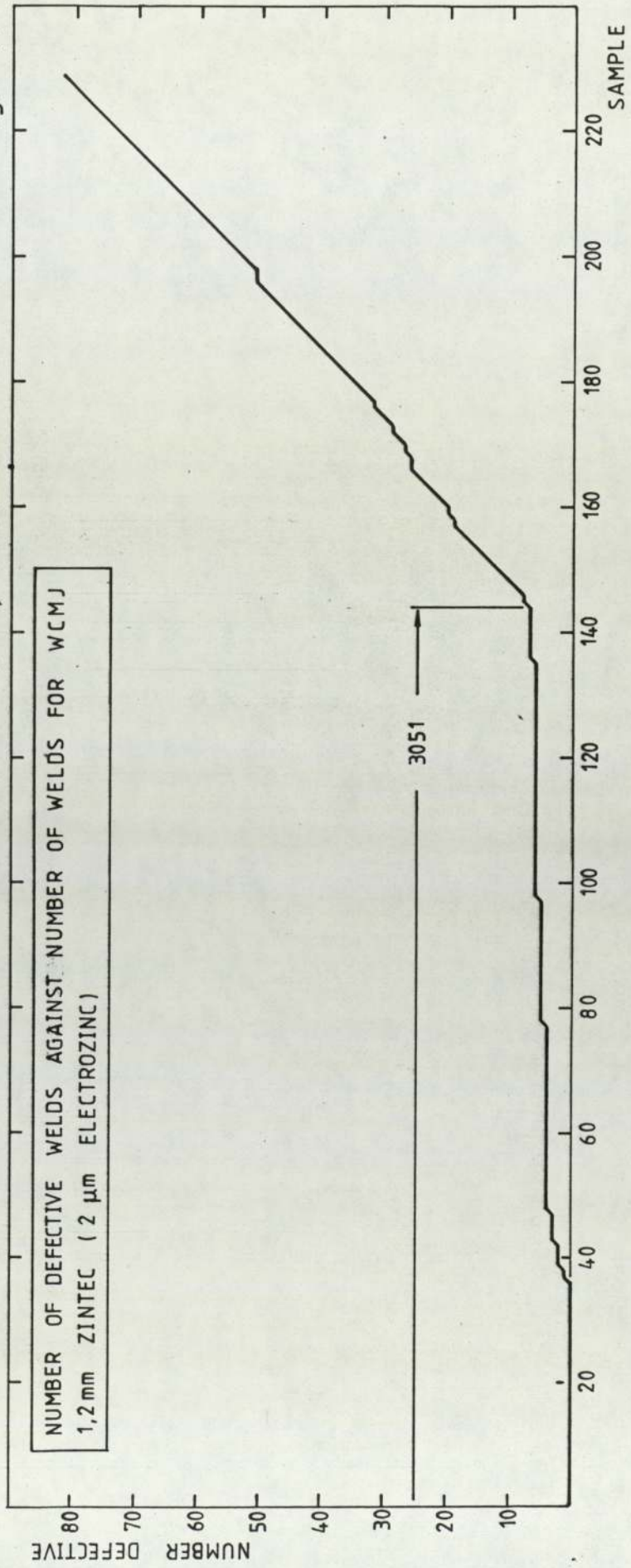


Fig. 48

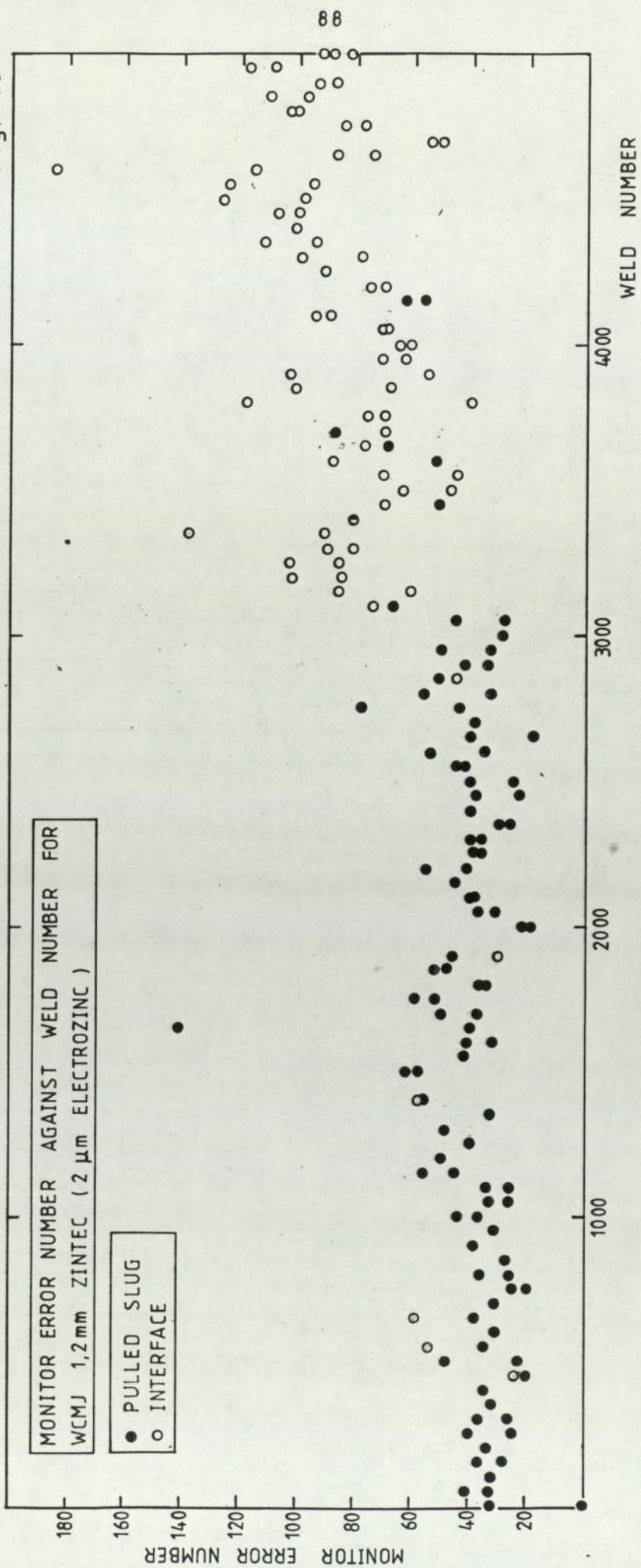
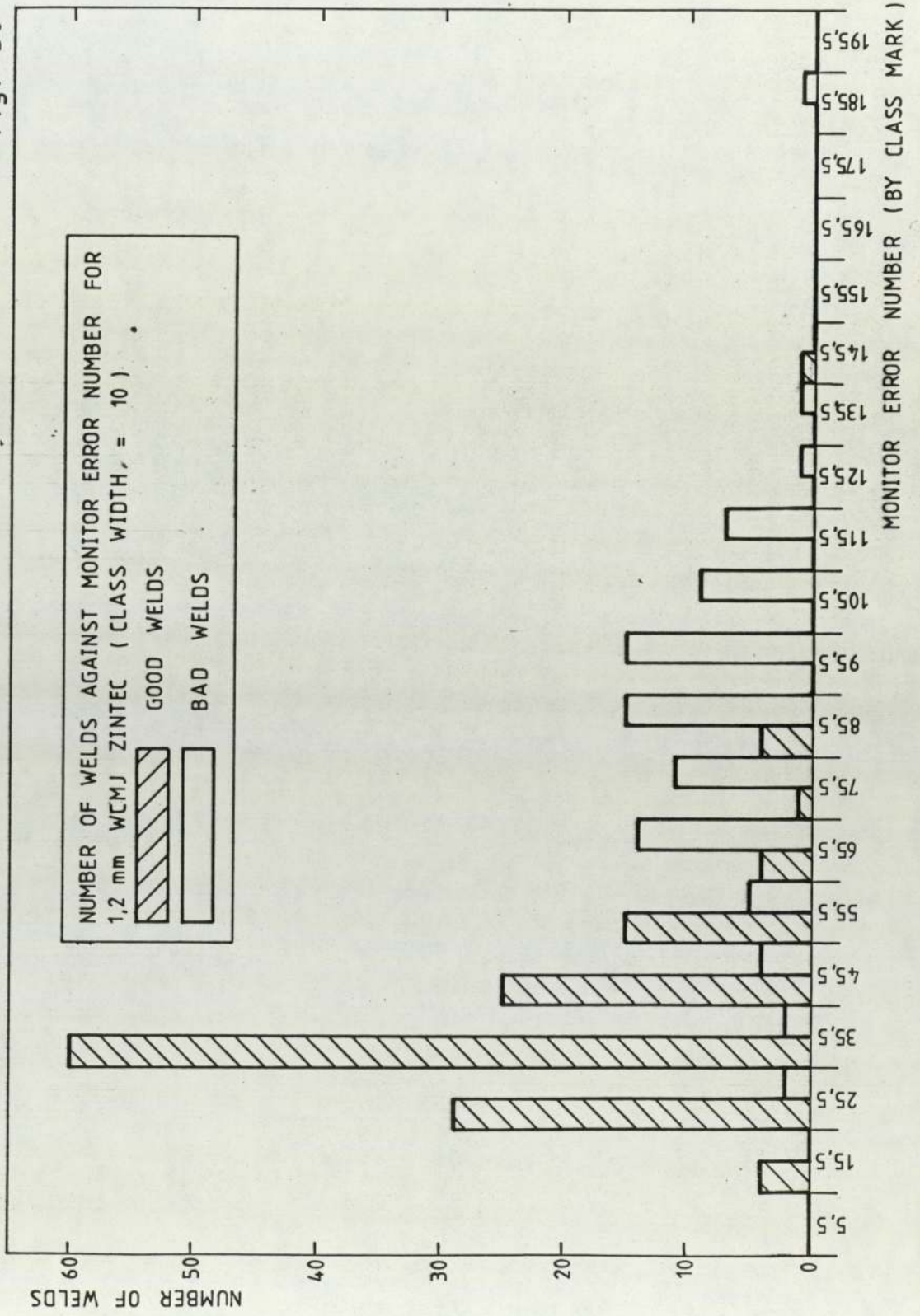




Fig. 50



#### 4.4 Metallographic Examination

##### 4.4(1) Weld quality

During the determination of weld quality by mechanical destructive tests, for the purpose of assessing weldability lobes and electrode life, metallographic sections of sample welds were prepared in order to confirm the quality of welds. It is clearly impractical to present all of the many photomicrographs made but it is felt that a selection of these is important.

A range of weld structures was regarded as acceptable. Plate 9 shows an acceptable weld in spangle coated material, whilst Plate 10 shows a commercially produced weld in an electro-zinc material. This second weld is near the lower limit for acceptability, with its small central cavity and fairly low penetration. The first weld on the other hand exhibits slightly excessive electrode indentation.

Plate 11 shows a substandard weld with a small nugget and low penetration. At the lowest currents or weld times it is possible to find no evidence of fusion at all (Plate 12) although carbide precipitation gives evidence of heating.

At the other extreme some welds showed clear evidence of expulsion of molten metal from the weld (Plate 13). Plate 14 shows an extreme case of this where the thickness of the weld is less than the single sheet thickness. A severe

through-weld crack can also be observed.

Even in welds which did not exhibit expulsion evidence was often found of surface cracks if the weld had been produced at too high a current. These cracks were often associated with excess indentation and sheet separation. (Plate 15).

#### 4.4 (2) Electrode deterioration

Metallographic examination of exhausted electrodes was carried out to study the mechanism of electrode wear. Plate 16 shows the structure of the electrode material itself with chromium-copper particles embedded in an  $\alpha$ -copper matrix.

The surface of the electrode showed a range of phase bands from the copper rich  $\alpha$ -phase which makes up the electrode matrix through the yellow  $\beta'$ -phase to the grey  $\gamma$ -phase and grey zinc rich  $\epsilon$ -phase containing oxides and dross (Plate 17). Both of the two outer layers showed considerable evidence of cracking and this is shown more clearly in Plate 18 a/b. This plate also shows evidence of spalling and thickness variation in the outer layers.

Plate 19 shows the way in which the edges of the electrodes spread, with material flowing radially outward and back along the electrode side. This is shown more clearly in the scanning electron photomicrograph, Plate 20.

Plate 21 is a scanning electron micrograph which shows more clearly than Plate 18 a/b the cracking in the outer layers together with the oxide inclusions.

Line concentration profiles were produced across a similar area (Plate 22), and these show the concentration across the electrode surface of the elements zinc (Plate 23), copper (Plate 24) and iron (Plate 25). These tend to suggest that the outer, grey, layers are of iron zinc alloy rather than copper zinc.

Plates 26 and 27 show the coating morphology for hot dipped and electrozinc coatings. It will be observed that the surface of the hot dipped material is fairly even, but, since the substrate surface is uneven the coating is of variable thickness. The electrozinc material on the other hand closely follows the profile of the substrate and hence has an uneven surface but fairly constant thickness.

## 5 DISCUSSION

### 5.1 Weldability

In general the three materials investigated all exhibited satisfactory weldability, as evidenced by weldability lobe width in Figures 6, 8, 11 and 20 for spangle "galvatite"; Figures 32 and 35b for "galvatite IZ"; and Figures 44a and 44b for "zintec". On the other hand it was found very difficult to produce satisfactory welds in the thinner (i.e. less than 1.0 mm) grades of all three materials without causing excessive indentation and sheet separation (see Figures 4, 5, 31a and 31b). This is almost certainly due to the increased current and weld time required for coated steels (AWS : 1982).

The Galvatite spangle obtained from W.C.M. James Ltd. showed definite anomalies in its welding behaviour compared with Galvatite obtained from other sources in the same thickness (1.2 mm). In addition to the markedly increased electrode force required to produce a weldability lobe of acceptable width (see Figs. 7 and 8), the morphology of the fracture on mechanical testing was such that mechanical strength rather than weld size had to be used as a criterion for weld acceptability.

Analysis of samples of the two materials showed two major differences as shown in tables 1 and 3.

- i) The carbon content of the base metal of the 1.2 mm W.C.M.James Galvatite was 0.142% by weight compared with 0.035% in nominally the same material obtained from British Steel (Carbon equivalents 0.219 and 0.085 respectively).
- ii) The zinc coating on the W.C.M.James Galvatite was considerably wavier than the specification allowed and contained considerable amounts of dross.

Whilst the variation in coating quality seems the most likely cause of differences in optimum welding conditions (N.T. Williams 1973), (for example pressure and width and position of weldability lobes), and differences in electrode life, the marked difference in carbon content between the two steels almost certainly accounts for the difference in weld fracture morphology, and the differences in the results of the modified Erichson cupping test (Figs.10a & 10b). The effect of carbon on the mechanical properties of steels and martensite in particular is widely reported in the literature (see for example E.C.Rollason (1973) and R.W.K.Honeycombe (1981)). The British Standards Institution (BS 1140 : 1980), suggests that carbon contents above 0.15% are likely to cause embrittlement of resistance welds. This is supported by Williams (1981) who has shown that the incidence of interface failure increases with increasing carbon content. It should be noted however that the graphs of tensile shear strength against weld current and weld time for the two materials (Figures 12 a, b and 23 a, b) did not show the expected increase in weld strength with carbon content,

indeed the material with slightly higher strength was that with considerably lower carbon content. Since the test piece geometry in both cases conformed to that recommended in BS 1140 : 1980, the most likely explanation for this discrepancy is the effect of the different welding conditions required for each material due to coating differences.

Comparison of weldability lobes for 1.2 mm zintec material produced with truncated cone and "pimpel" electrodes shows very little difference between weldability with the two types of electrodes (Figs. 44a and 44b). The slightly increased width of the "pimpel" weldability lobe (Fig. 44b) is probably a result of increased elastic spread of the "pimpel" electrode tip during the welding cycle due to electrode geometry.

## 5.2 Electrode Life

The electrode life is probably the single most important factor in a discussion of the resistance welding properties of coated steels. With the exceptions of changes in welding parameters due, for example, to equipment malfunction, or changes in the properties of the materials being welded (which should be under the control of the inspection function), the most frequent, and least controllable, source of defective welds is the deterioration in the electrode tips.

The change in electrode tip diameter with number of welds

followed the same pattern in all cases, with one notable exception. In most cases the electrode tip diameter increased rapidly at the start of the test at a rate which decreased until at around a thousand welds it became level or displayed only a gradual increase in weld size.

The change in weld size or weld strength, however, did not display a trend corresponding to the change in tip diameter. In all cases, again with one notable exception, the weld nugget diameter gradually fell during the entire test. The change in weld tensile-shear strength for the two spangle materials was similar except for a slight increase in the rate of reduction at the end of the electrode life. It should be noted that there is no rapid drop in weld strength or nugget size during the first thousand welds, as would be expected if weld quality were dependent purely on the increase in electrode tip diameter in this region of electrode life.

The exception noted above is that of 1.0 mm Galvatite IZ welded with "pimpel" type electrodes (Figs. 33 and 34). This material exhibited a very rapid increase in electrode tip diameter with an equally rapid reduction in weld size. The trend in both cases was approximately linear and it should be noted that this material was the only one to exhibit a clear relationship between tip diameter and weld size. The electrode lives were determined by examination of the rate of production of faulty welds. The corresponding graphs of number of defective welds against number of welds produced

are given in the results section as Figures 15a, 15b, 38 and 47. The electrode life was determined as the point at which there is a steep increase in the rate of production of bad welds. The electrode lives determined, together with the proportion of bad welds produced during the useful electrode life are given in table 8.

Table 8. Electrode Life Data for Coated Steels

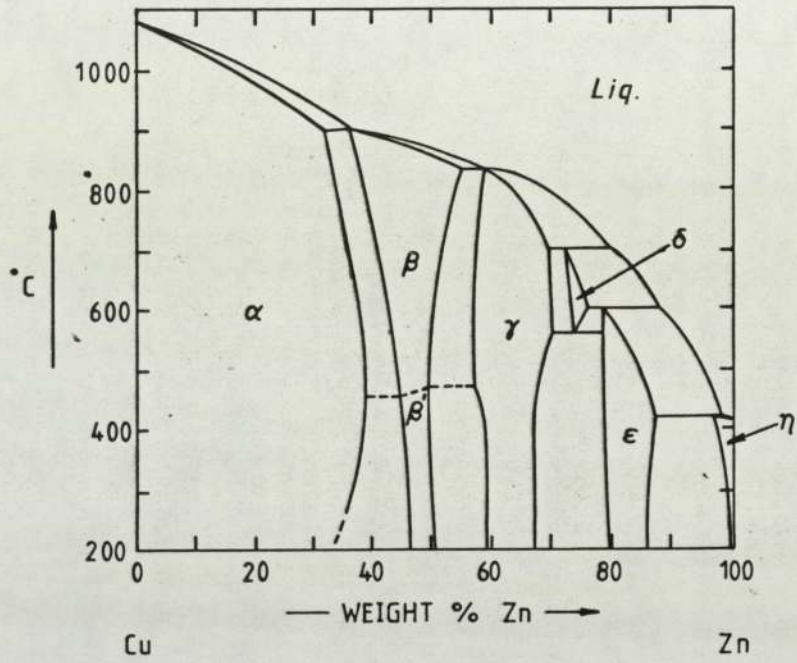
Material	Electrode life	% defective
W.C.M.J. 1.2 mm Galvatite	2975	9
B.S.C. 1.2 mm Galvatite	1775	0
B.S.C. 1.2 mm Galvatite IZ	2800	12
W.C.M.J. 1.2 mm Zintec	3051	5

What is immediately apparent from this table is that the electrode lives for all three materials are remarkably similar. With the exception of the 1.2 mm Galvatite spangle obtained from the British Steel Corporation, all of the electrode lives were in the range 2800 to 3051 welds. In particular it should be noted that the electrozinc "Zintec" material, with a coating weight of only  $28.23 \text{ gm}^{-2}$ , and the iron-zinc alloy coated material, both of which are reported in the literature as giving significantly longer electrode lives (F.J.Ganowski et al (1973), N.T.Williams et al (1971), N.T.Williams (1973) etc.) showed no significant increase in electrode life over the Galvatite spangle obtained from

W.C.M. James, although there is an increase over the Galvatite spangle obtained from British Steel of 58% for the IZ material and 72% for the zintec material. It is probably significant that the B.S.C. Galvatite, although having the shortest electrode life, produced no bad welds during the electrode life, compared with the five to twelve percent bad welds produced in the other materials. Further experimental work would be necessary to establish any correlation between electrode life and the quality of welds produced during that life. It has always been proposed in the literature that the severe reduction in electrode life when welding coated steels results from the increased welding current and weld time necessary because of the reduced contact resistance of soft zinc coatings, combined with the alloying of the copper electrodes with zinc from the coating, both of these factors leading to a greatly increased rate of electrode spread with a concomitant drop in weld size.

Investigation of the mechanism of electrode wear during welding of zinc coated steel by means of microsection (see plates 16 to 25) showed clear evidence of phase bands with cracking and spalling of the outer layers. Reference to the copper-zinc equilibrium diagram (Figure 51) allows identification of the phases present (Figure 52). The majority of the spalling seems to result from cracks which develop in the phase band, of average composition 65% zinc, and this is supported by previous work on copper-zinc diffusion couples by this author (P.N. Whateley (1979) ) which included microhardness surveys of the phases appearing (Table 9).

Fig. 51



PHASE EQUILIBRIUM DIAGRAM FOR THE  
SYSTEM COPPER-ZINC

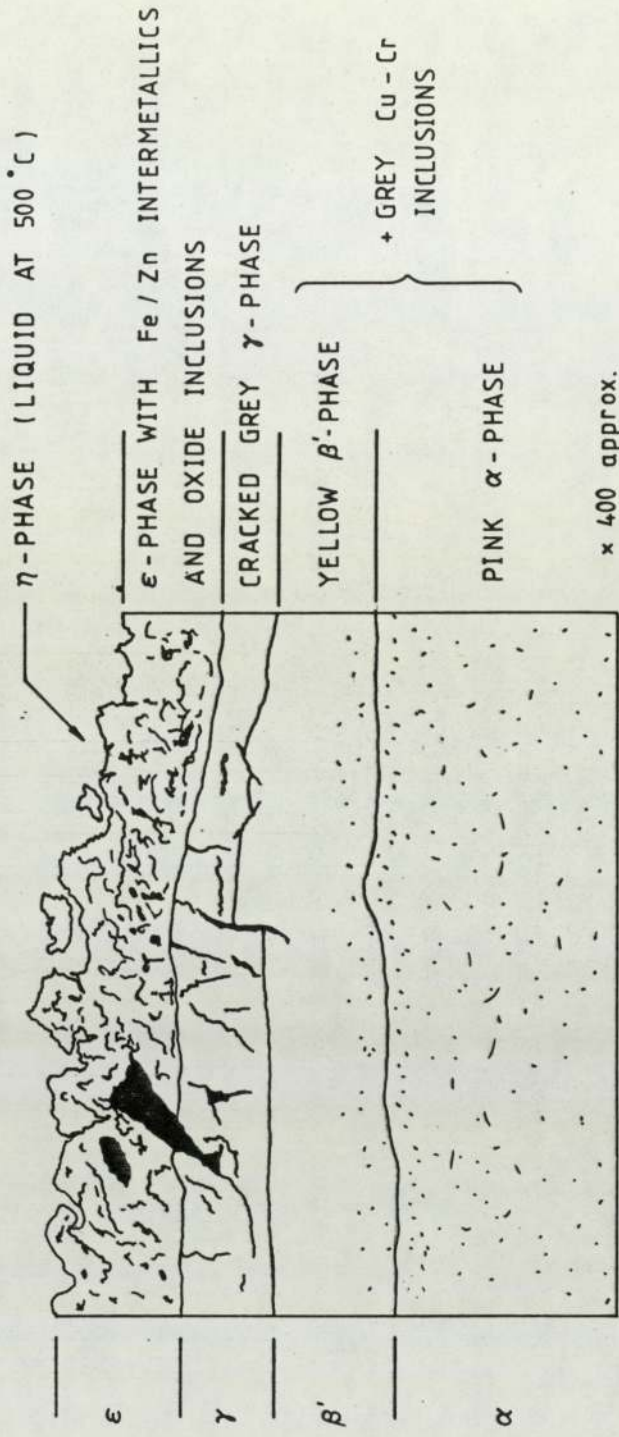


Fig. 52 STRUCTURE OF COPPER-ZINC INTERDIFFUSION LAYER (SCHEMATIC)

Table 9: Microhardness of Phases in Cu-Zn Diffusion Couple. (From previous work)

Phase	mean HV : 20 g
Cu-rich $\alpha$	61.6
$\beta$	126.3
$\gamma$	367.15
$\epsilon$	146.3
$\eta$ (zinc-rich)	56.2

The hardness of the  $\gamma$ -phase tends to confirm the observed brittleness of this phase.

The behaviour of the electrodes during their life can therefore be summarised as consisting of three phases:

- I) An initial period of rapid increase in electrode tip diameter at a decreasing rate of increase. This corresponds to a period in which there is no apparent decrease in weld size or strength.
- II) A secondary, extended period during which there is either a gradual, constant increase in electrode tip diameter or the tip diameter remains constant. During this period the weld size either remains constant or exhibits a cyclic variation which appears to be due to the spalling and rebuilding of alloy layers on the electrode surface. Where this spalling is present there is a marked deterioration in the surface appearance of

welds which may, or may not, be aesthetically acceptable.

III) The final stage during which there is a rapid decrease in weld size and weld strength, the onset of which marks the end of the electrode life. This is sometimes, but not always, accompanied by a rapid increase in electrode tip diameter.

Since, as mentioned before, there appears to be no correlation between electrode tip diameter and weld quality it seems likely that the primary cause of faulty welds is the amount of contamination of the electrode surface, with tip spread only a secondary factor. However, considerable additional work would be necessary to verify and quantify this effect.

### 5.3 Monitor Reliability

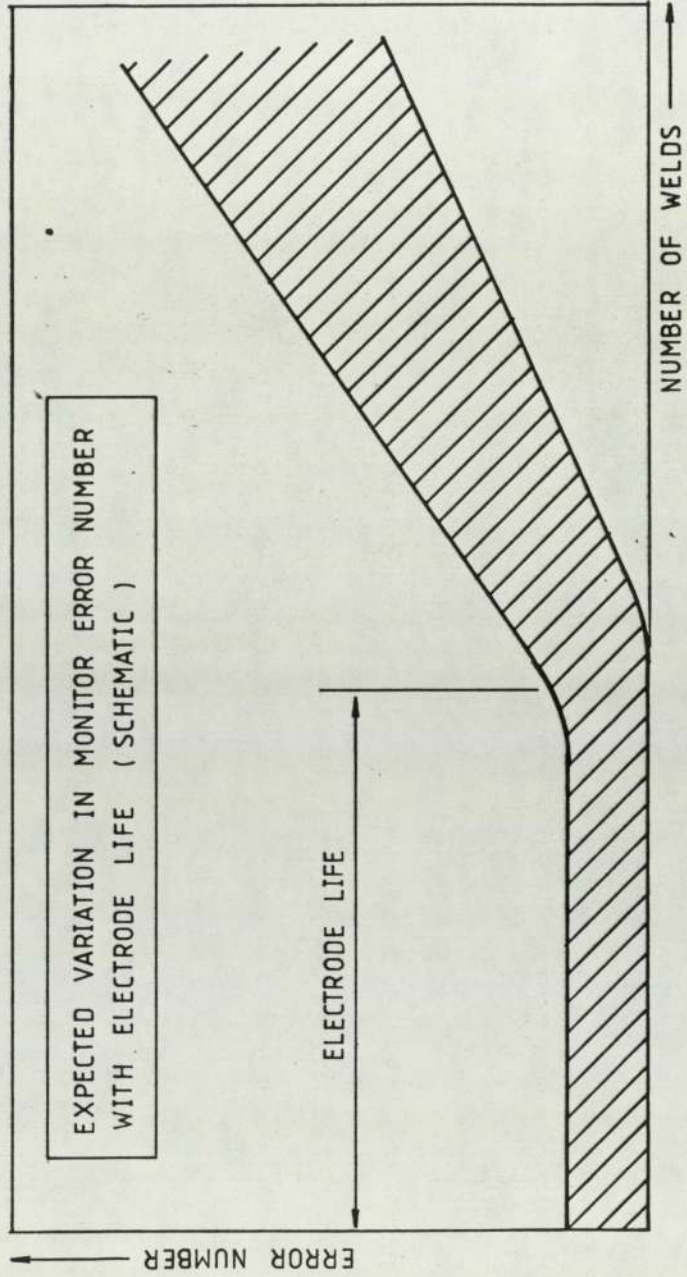
The overriding factor in a consideration of the reliability of an in-process monitor for resistance welding is the ability of the monitor to distinguish between good and bad welds. Random defective welds may be produced during the electrode life due to variations in material surface, for example, and it is important that components containing these welds should not be incorporated into safety critical components. In addition to random defective welds there is a rapid increase in the number of defective welds produced at the end of the electrode life (see Figs.15a, 15b, 38 and

47) and it is important that this trend be both reflected by, and clearly distinguishable in, the monitor error number.

The ideal trend in a plot of monitor error number against number of welds produced would show a low level of monitor error with little scatter during the electrode life (see Fig.53). At the end of the electrode life an increase in monitor error would be expected together with an increase in the scatter range.

Of the materials investigated by the author the hot dipped materials, whether spangle or iron-zinc alloy, showed a slight upward trend corresponding to the end of the electrode life, although in all three cases the trend was all but masked by the wide dispersion of results both during and after the electrode life (Figs.16, 28 and 41). The fourth material, zintec, showed a marked upward trend in monitor error number after the electrode life of three thousand welds (Fig.48). In addition the scatter band prior to this point was narrower so that the effect was not hidden. The two major differences between this material and the three hot dipped materials investigated are the coating thickness and the method of application of the coating. The zintec material has a coating thickness of only  $2\mu\text{m}$  compared with coatings ranging in thickness from  $14\mu\text{m}$  to  $22\mu\text{m}$  for the Galvatite materials. In addition the hot dipped, Galvatite materials are, by definition, subjected to temperatures above the melting point of zinc ( $419.5^{\circ}\text{C}$ ) during the coating process which leads to considerable interdiffusion of iron and zinc,

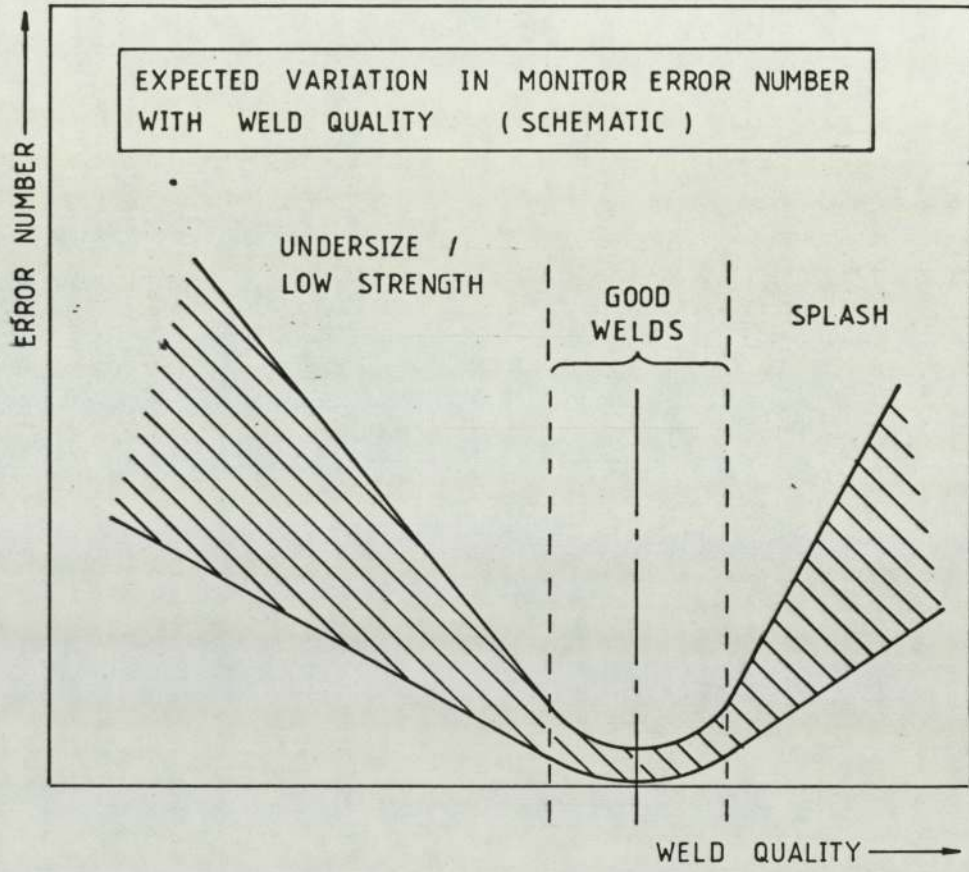
Fig. 53



indeed, in high silicon steels, the activity of the iron is increased to such an extent that no unalloyed zinc remains after hot dipping. In the case of the IZ material the iron zinc alloy coating is produced by subsequent heat-treatment to allow completion of the interdiffusion. The initial alloying due to hot dipping is likely to be uneven due to differences in the surface of the base metal such as orientation of ferrite grains, and this will lead to variation in coating thickness even though the surface is reasonably flat due to the use of air knives for cooling. Metallographic examination of coatings (Plates 26 and 27) showed that although the substrate surface is uneven in both electrozinc and hot-dipped materials the thinner coating in the electrozinc material followed the contour of the substrate so that there was little variation in coating thickness.

The scatter in monitor error number was also observed when the dependence of monitor error on the weld quality was investigated. Assuming that the master weld is chosen to be of optimum or near optimum weld size or strength, then a plot of the error number produced by the monitor against weld quality should ideally be similar to Fig.54 with a low error number within the range of acceptable welds and increased error and scatter for unacceptable welds. Since the change in monitor error with electrode life was largely hidden by the spread in error values, despite the absence of high scatter in a plot of weld quality against electrode life (Figs.13, 25, 27, 39 and 45), it would be expected that a

Fig. 54



clear correlation between weld quality (either nugget size or strength) and monitor error would be absent, and this proved to be the case for the three hot dipped materials (B.S.C. Galvatite, W.C.M. James Galvatite and B.S.C. Galvatite IZ), although some correlation can be observed for the electrozinc "Zintec" material. It should be emphasized that the scatter in error numbers is independent of the quality of the welds, and given the characteristics of the materials involved, appears to be a function of coating variability. This point is important and will be referred to again.

Some idea of the ability of the monitor to discriminate between good and bad welds may be obtained by studying the histograms of the distribution of error numbers between good and bad welds. The ideal here, of course is to have two clearly defined peaks, one for good welds and one for bad. The peak for bad welds would, however, be expected to show more spread than that for good welds. The histograms for the two Galvatite spangle materials (Figs.18 and 20) show reasonably pronounced separation between the peaks but difficulty in distinguishing between good and bad welds is caused by the amount of scatter in the results. On the other hand the histogram for the Galvatite IZ material (Fig.43) shows distinct peaks with little scatter, but in this case the peaks are close together and this also prevents adequate discrimination between good and bad welds by means of error numbers. The histogram for electrozinc "Zintec" material (Fig.50) shows clearly defined peaks with more scatter for bad welds than good, as would be expected. There

is reasonable separation between the peaks which should lead to adequate discrimination given a carefully chosen tolerance band.

In summary the histograms show that the degree of discrimination between good and bad welds is inadequate for all three Galvatite materials due to excessive scatter in the case of the spangle materials and due to insufficient separation for the iron zinc alloy material. The discrimination between good and bad welds for electrozinc material is adequate since the separation between the peaks is greater and there is less scatter.

In order to show the effect of spread and location of the data given in the histograms on the industrial application of the monitor it was decided to plot the data in the form of cumulative distribution curves showing the percentage of bad welds accepted, " $\pi$  (ACCEPTANCE | BAD WELD)", and the percentage of good welds rejected, " $\pi$  (REJECTION | GOOD WELD)" against monitor error number for each of the four sets of data (Figs.55, 56, 57 and 58). It is important at this point to draw a distinction between the percentage of bad welds accepted, for example, and the percentage of welds which were both accepted and were bad welds, i.e.  $\pi$  (ACCEPTANCE, BAD WELD), since the former is independent of the proportion of good and bad welds in the sample, whereas the latter is not.

In an ideal monitor the two values should be equal to zero

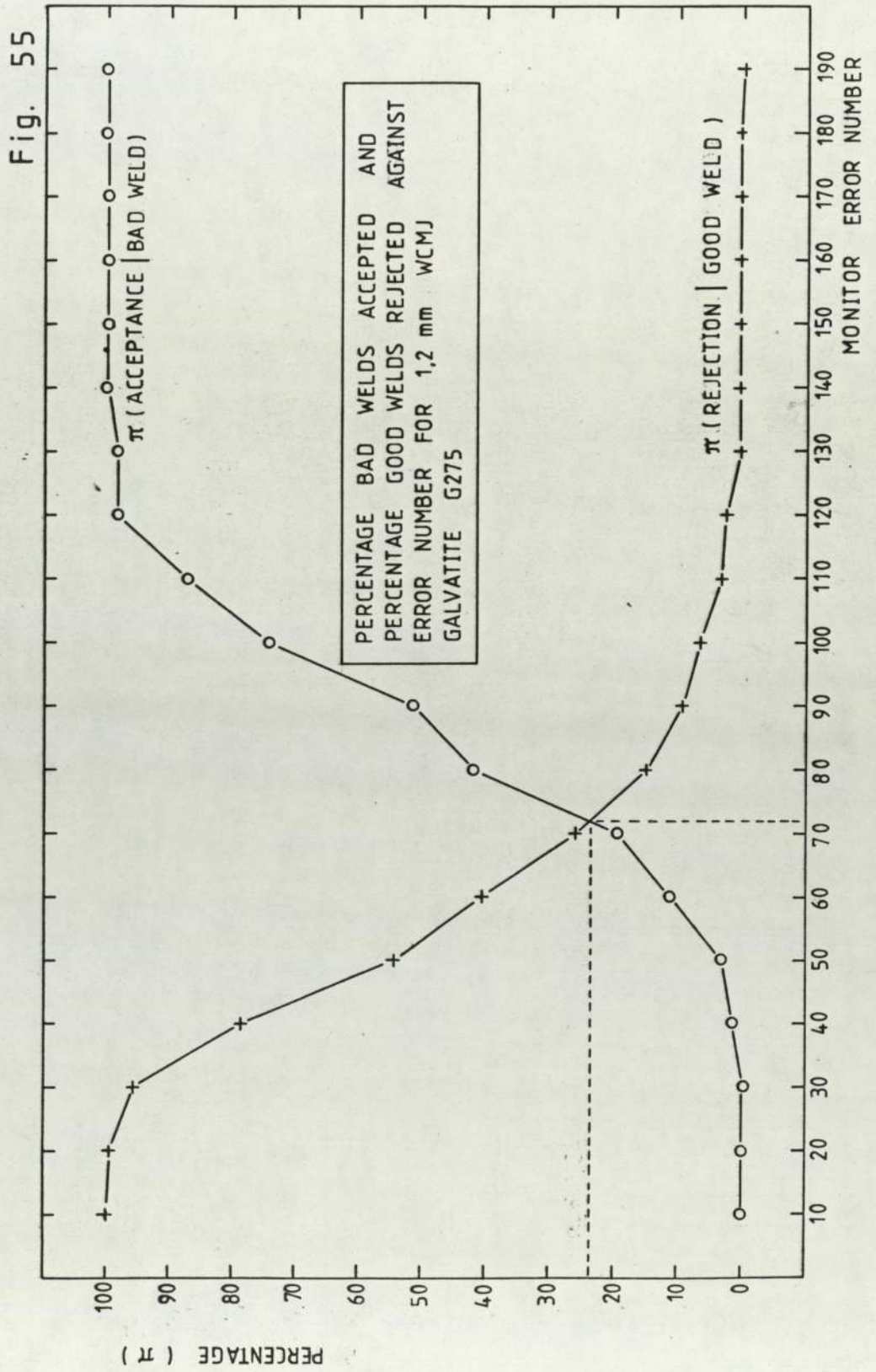


Fig. 56

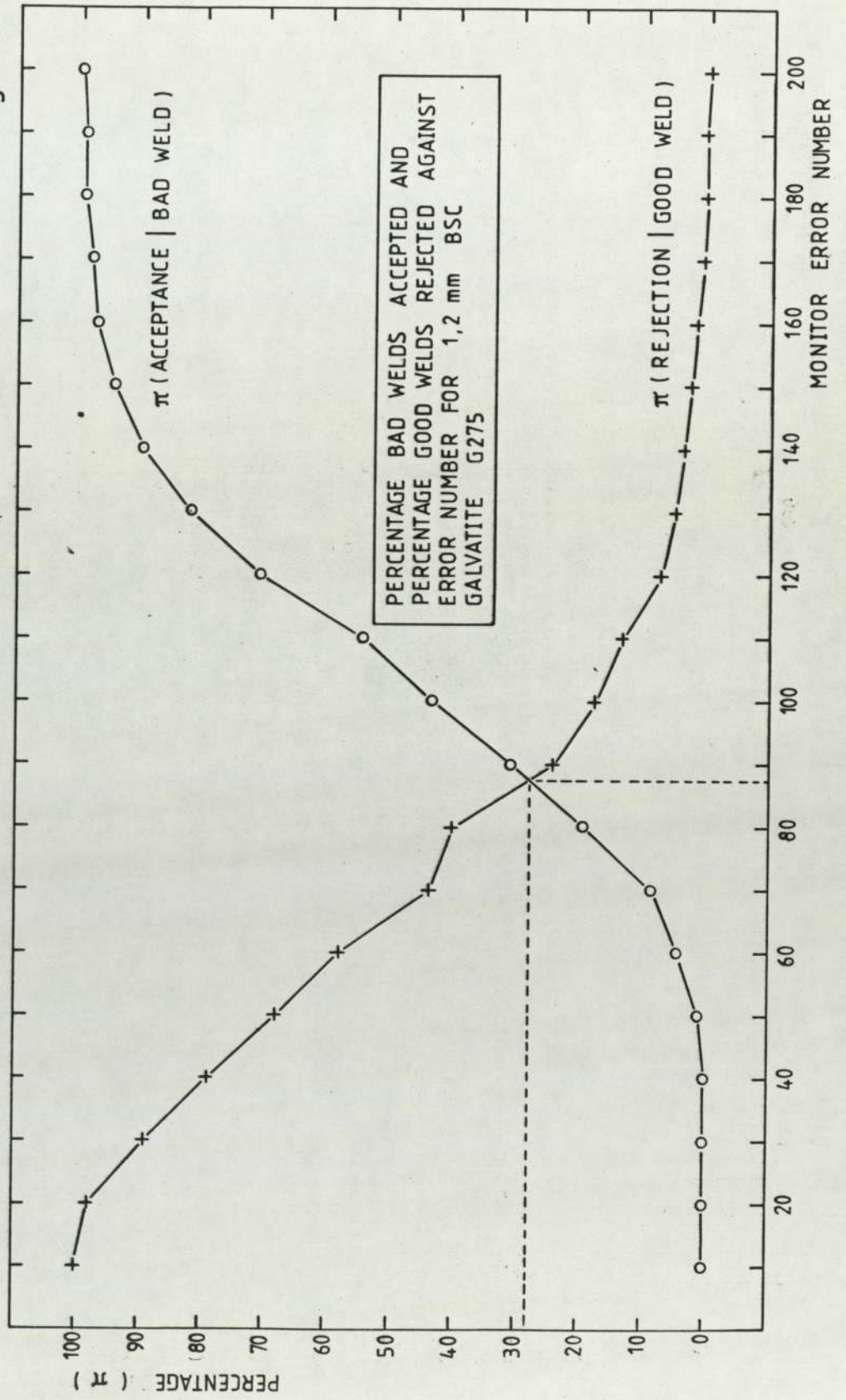


Fig. 57

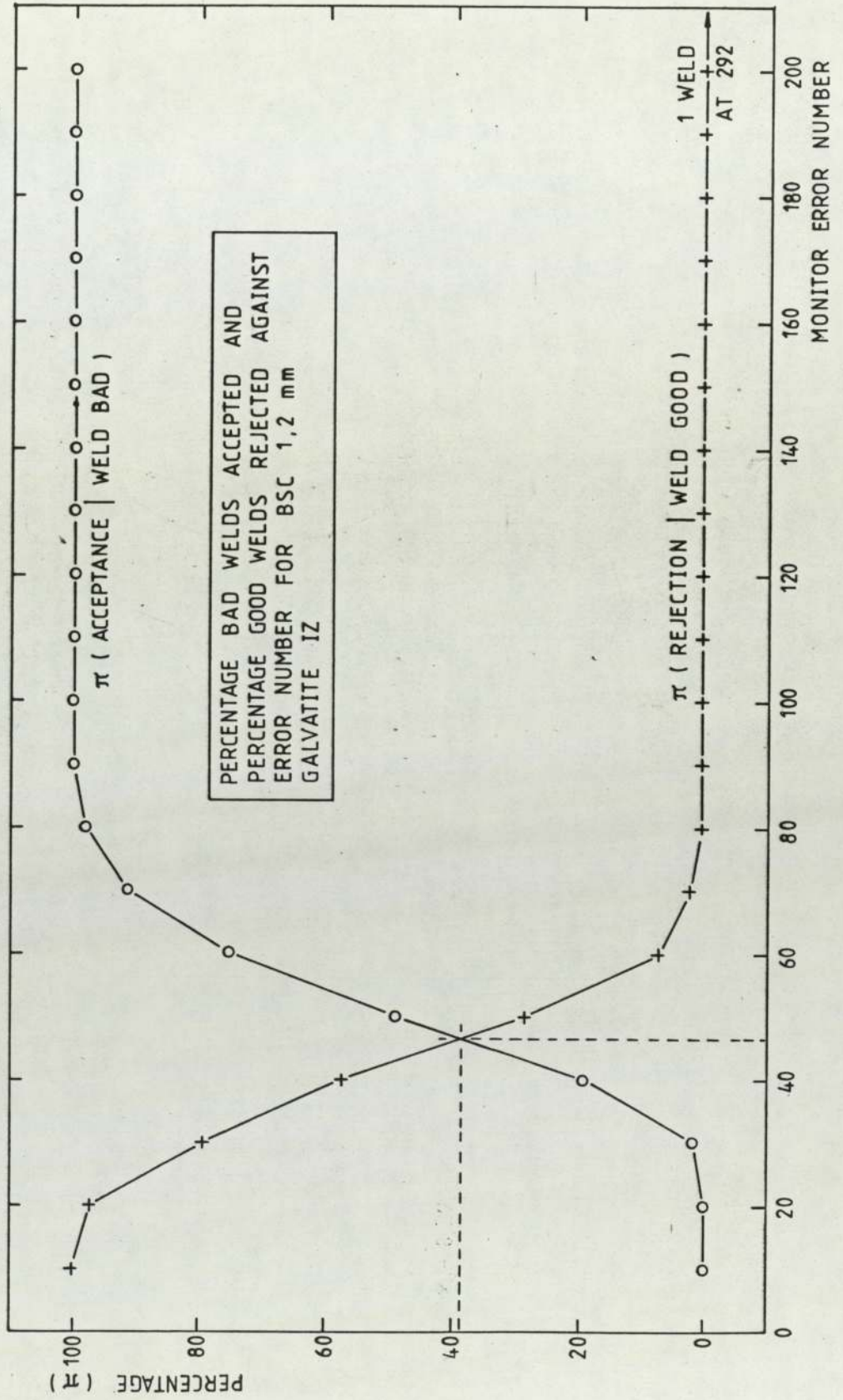
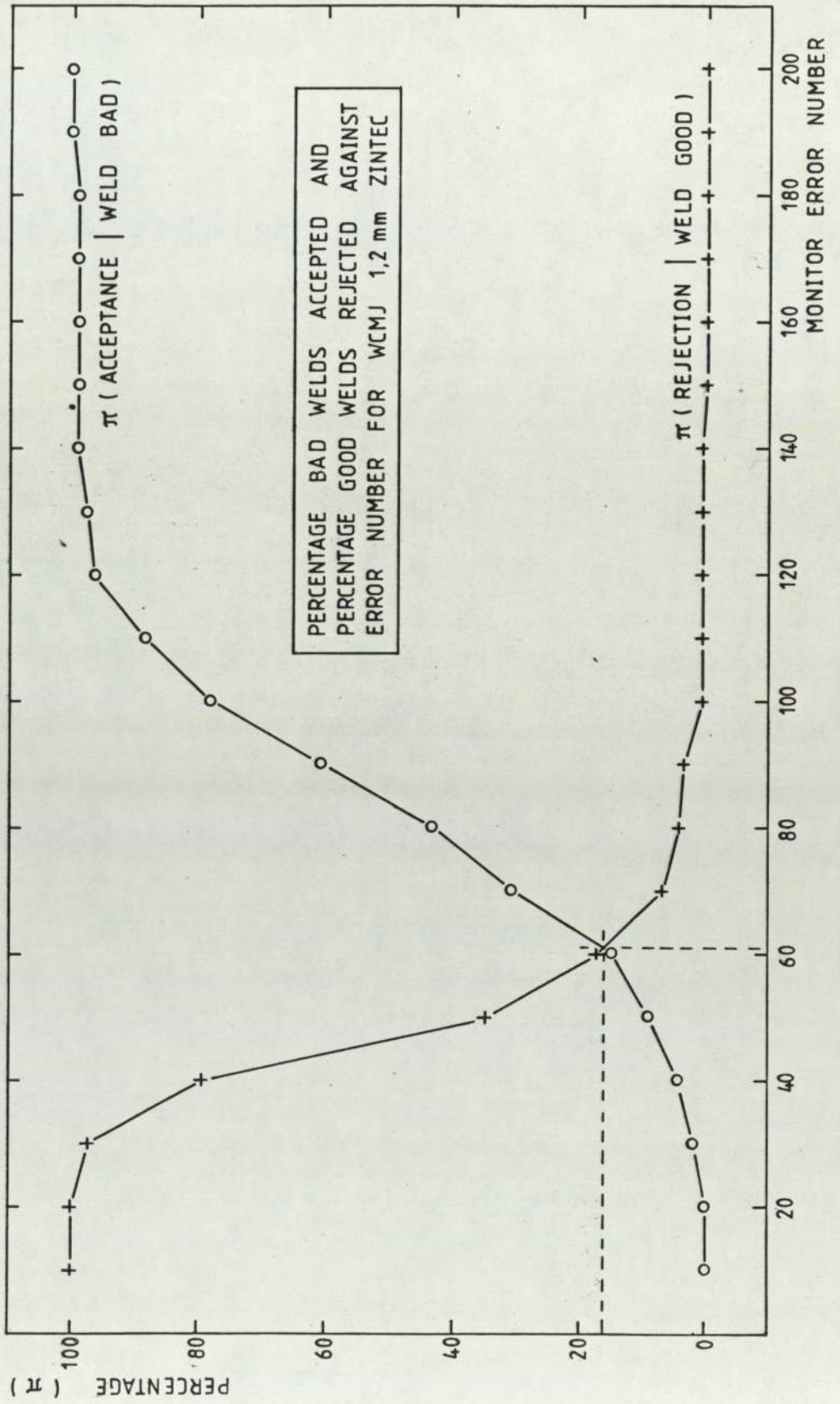


Fig. 58



so that no defective welds are accepted and no good welds are rejected, and in an effective monitor there should be a minimum value on both curves corresponding to a monitor error number which is then used as the tolerance, or fail/pass criterion, for welds.

In an industrial situation, with moderately safety-critical applications, it is reasonable to expect that no more than five percent of defective welds be accepted by a monitoring system. However for these materials the corresponding percentage rejections of good welds are as given in Table 10.

Table 10

Monitor Error Number (A) giving 5% Acceptance of Defective Welds and Corresponding Percentage Rejection of Good Welds (B)

Material	A	B
W.C.M.J. Galvatite G275 1.2 mm	53	51 %
B.S.C. Galvatite G275 1.2 mm	61	55.5 %
B.S.C. Galvatite IZ 1.2 mm	32	74 %
W.C.M.J. Zintec 1.2 mm	41	71 %

This level of wastage is clearly unacceptable from economic considerations alone, but it should also be borne in mind that a rejection of such large numbers of good welds will effectively increase the number of bad welds accepted, as a proportion of all welds produced. Use of a higher error

number for the tolerance value would, of course, reduce the number of good welds rejected but only at the expense of increased acceptance of defective welds. A more quantitative representation of monitor reliability is given by the point at which the two curves cross. These values are given in Table 11.

Table 11

Values of Error Number and Percentage for which  
 $\pi (\text{ACCEPTANCE} \mid \text{BAD WELD}) = \pi (\text{REJECTION} \mid \text{GOOD WELD})$

Material	Error Number	Percentage
W.C.M.J. Galvatite G275	72	24
B.S.C. Galvatite G275	88	28
B.S.C. Galvatite IZ	47	39
W.C.M.J. Zintec	61	16

The percentage values for the three Galvatite materials are clearly unacceptable and even the percentage for the electrozinc "Zintec" material is acceptable only for non safety critical applications.

Whilst the above analysis appears to be of some value in monitor assessment it was felt that a more mathematically rigorous treatment would be of value in future work.

Mean and standard-deviation values for monitor error numbers for good and bad welds for each material were

calculated (Table 12).

Table 12

Mean ( $\bar{x}$ ) and Standard Deviation ( $\sigma$ ) Values for  
Good and Bad Welds

W.C.M.J. Galvatite G275

	Good Welds	Bad Welds
mean, $\bar{x}$	48.13	75.18
standard deviation, $\sigma$	23.90	19.94
number of welds, n	215	62

B.S.C. Galvatite G275

	Good Welds	Bad Welds
mean, $\bar{x}$	68.99	104.44
standard deviation, $\sigma$	35.40	26.88
number of welds, n	205	201

B.S.C. Galvatite IZ

	Good Welds	Bad Welds
mean, $\bar{x}$	44.02	51.62
standard deviation, $\sigma$	25.03	12.56
number of welds, n	123	109

W.C.M.J. Zintec

	Good Welds	Bad Welds
mean, $\bar{x}$	40.26	83.32
standard deviation, $\sigma$	15.58	25.08
number of welds, n	142	87

These values can be used to calculate normal distribution curves for the four materials using the formula

$$f(x) = \frac{1}{\sigma \sqrt{2\pi}} \cdot e^{-\frac{1}{2} \left[ \frac{x - \bar{x}}{\sigma} \right]^2}$$

where:  $f(x)$  is the dependent frequency  
 $\sigma$  is the standard deviation  
 $x$  is the independent variable  
 $\bar{x}$  is the mean of these variables.

The heights of the curves produced using this formula are dependent upon the number of data points,  $n$ , included in calculating the mean and standard deviations of each distribution. Since we are comparing curves produced using different numbers of data points it is important that the heights of the curves be adjusted to show relative rather than absolute frequency. This is achieved by dividing through by  $n$ , so that the area under all the curves is equal to one. In other words:

$$\int_{-\infty}^{\infty} \frac{1}{n \sigma \sqrt{2\pi}} \cdot e^{-\frac{1}{2} \left[ \frac{x - \bar{x}}{\sigma} \right]^2} \cdot dx = 1$$

The four pairs of curves for each of the materials tested are given in this form, see Figures 59, 60, 61 and 62.

It is possible to calculate confidence limits for different percentage degrees of confidence for these curves, these, in other words, are the values of monitor error-number,

Fig. 59

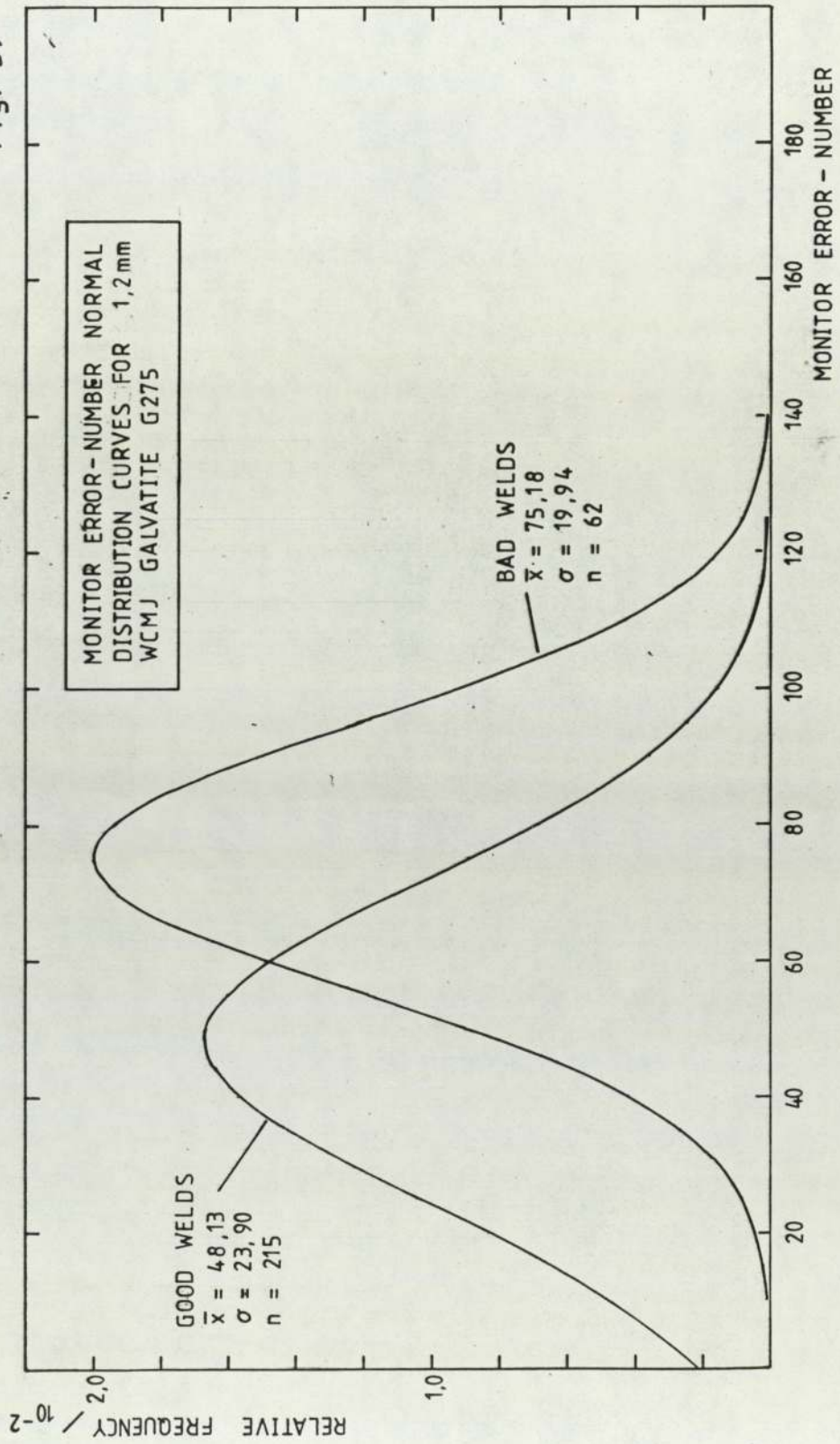


Fig. 60

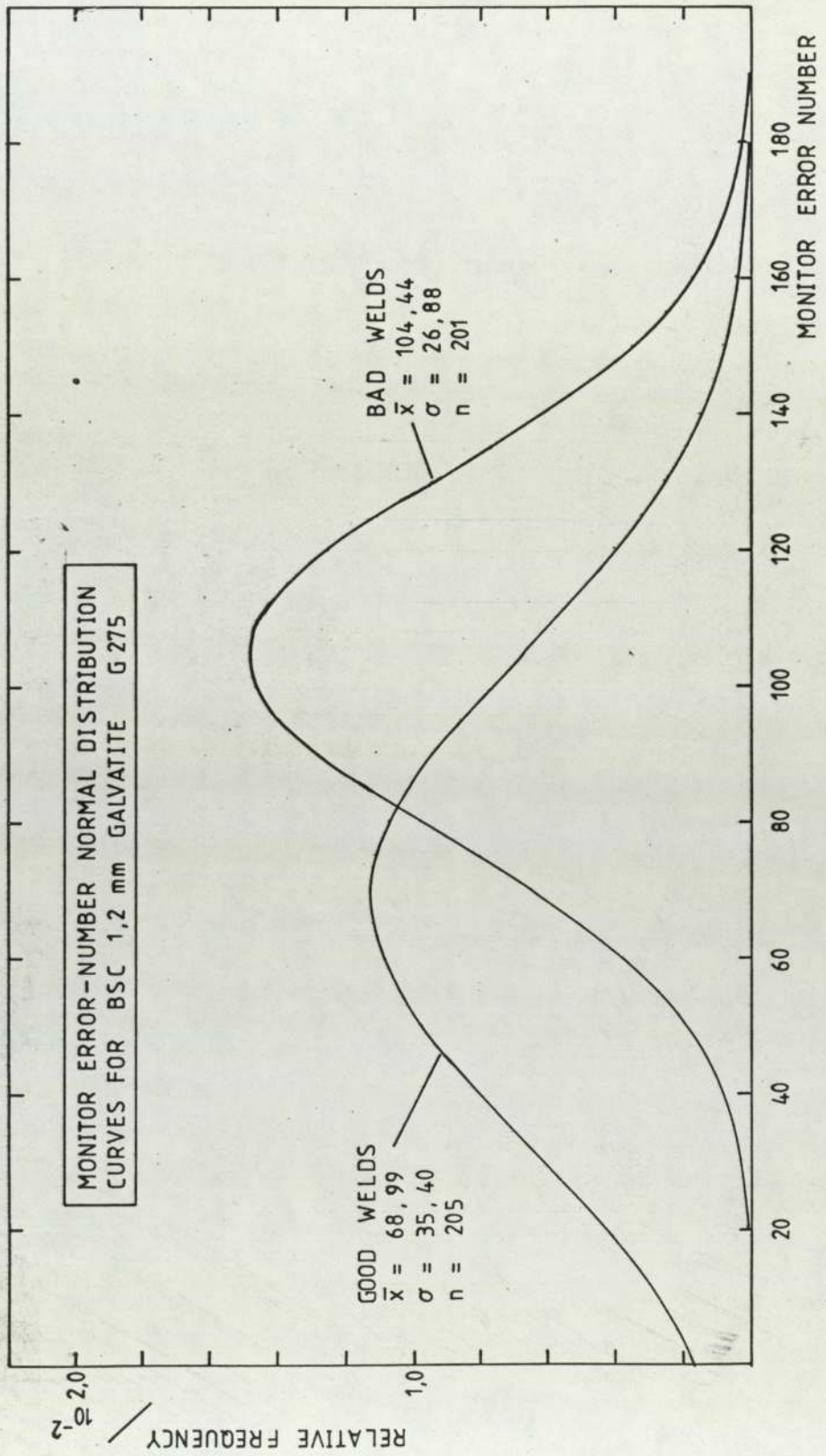


Fig. 61

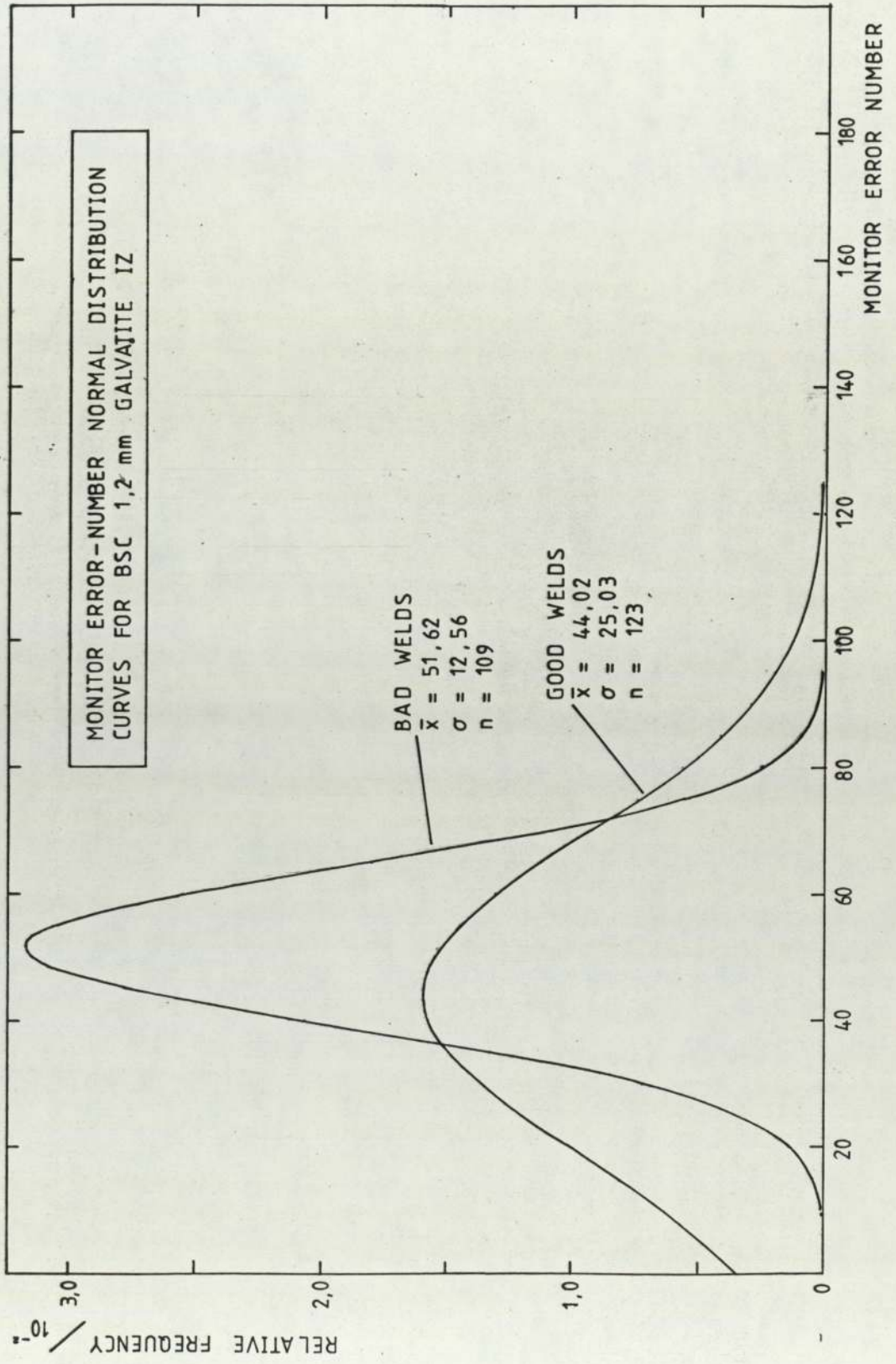
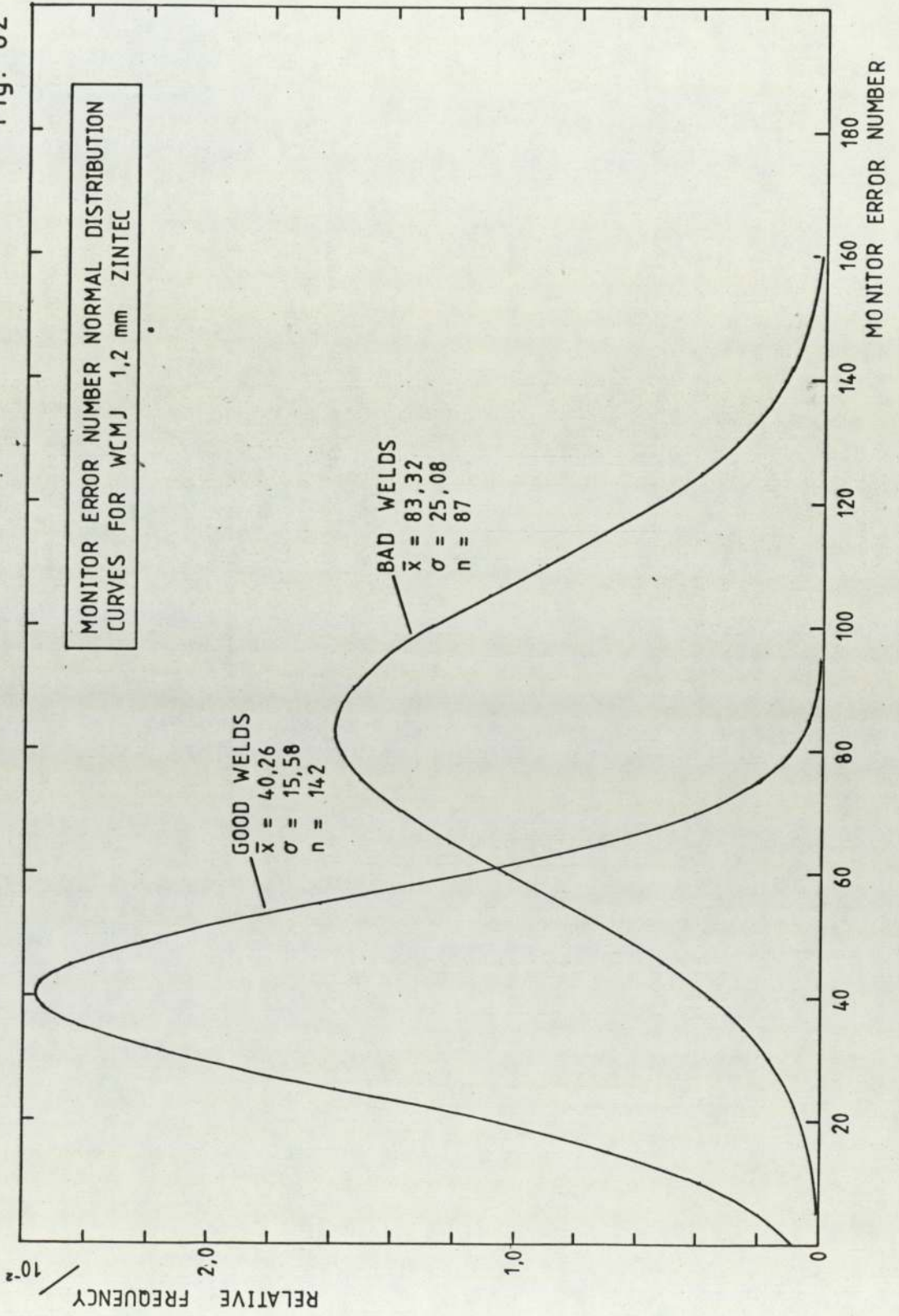


Fig. 62



either side of the mean, within which a certain percentage of error numbers can be expected to fall. Confidence intervals for the normal distribution are given by  $\bar{x} \pm Z_{\alpha/2} \sigma$  where:  $\bar{x}$  is the mean,  $\sigma$  is the standard deviation and  $Z_{\alpha/2}$  is the  $100(1 - \alpha)$  percentage point of the normal distribution. It should be noted that this is used to calculate the confidence intervals for a population, whereas the formula:

$\bar{x} \pm Z_{\alpha/2} \cdot \sigma / \sqrt{n}$  is used to calculate confidence intervals for a sample of size  $n$ . The values of  $Z_{\alpha/2}$  are found from the areas under the standard normal distribution and are usually determined from tables, since there is no analytical solution to the integral of the curve. Sample values of  $Z_{\alpha/2}$  are given in Table 13 to three significant figures.

Table 13 Selected Values of  $Z_{\alpha/2}$

100 (1 - $\alpha$ )	$Z_{\alpha/2}$
95 %	1.96
75 %	1.15
50 %	0.68
25 %	0.32
5 %	0.06

From Abramowitz & Stegun (1972)

The variation in confidence limits with percentage confidence is plotted in Figures 63, 64, 65 and 66. The

Fig. 63

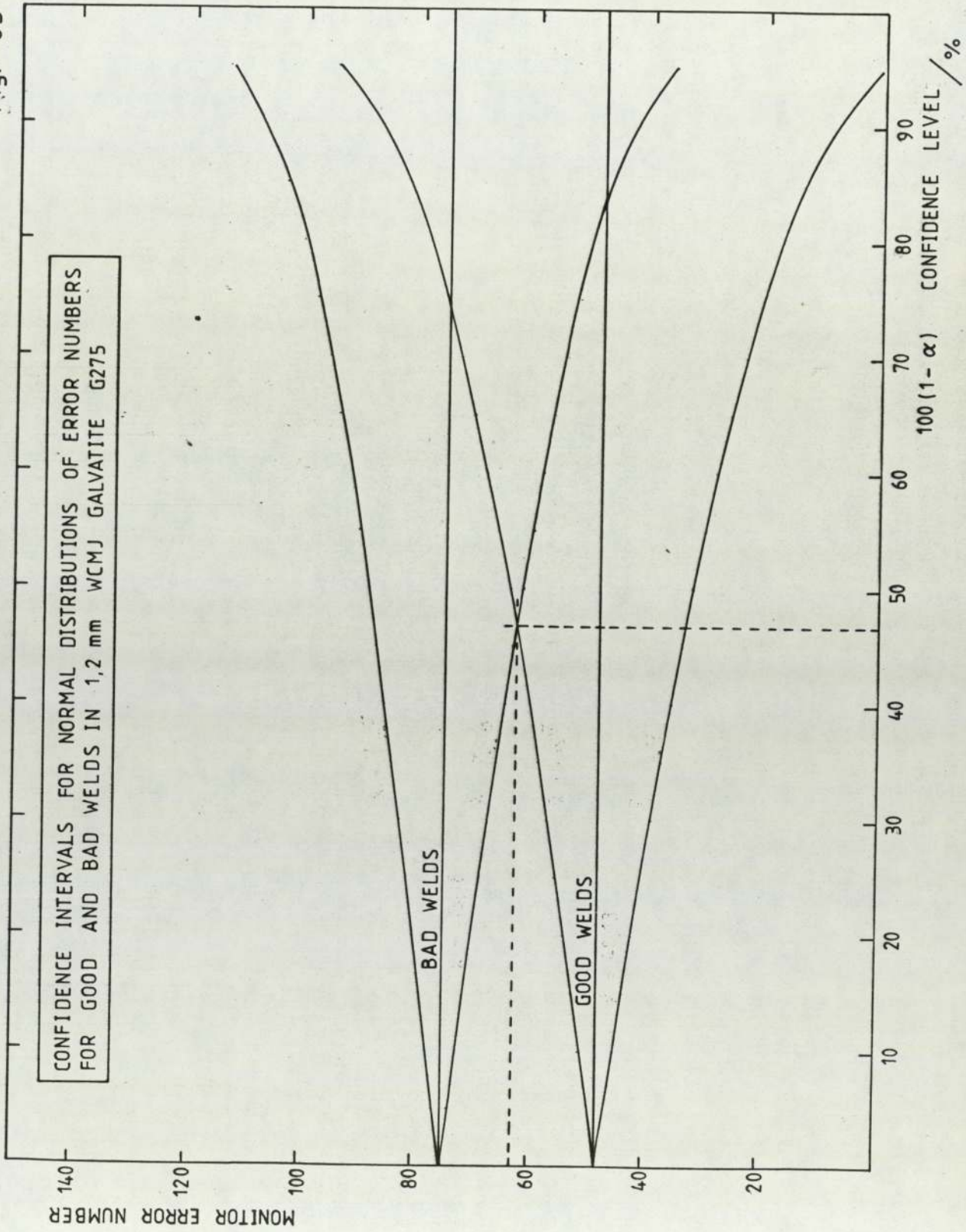


Fig. 64

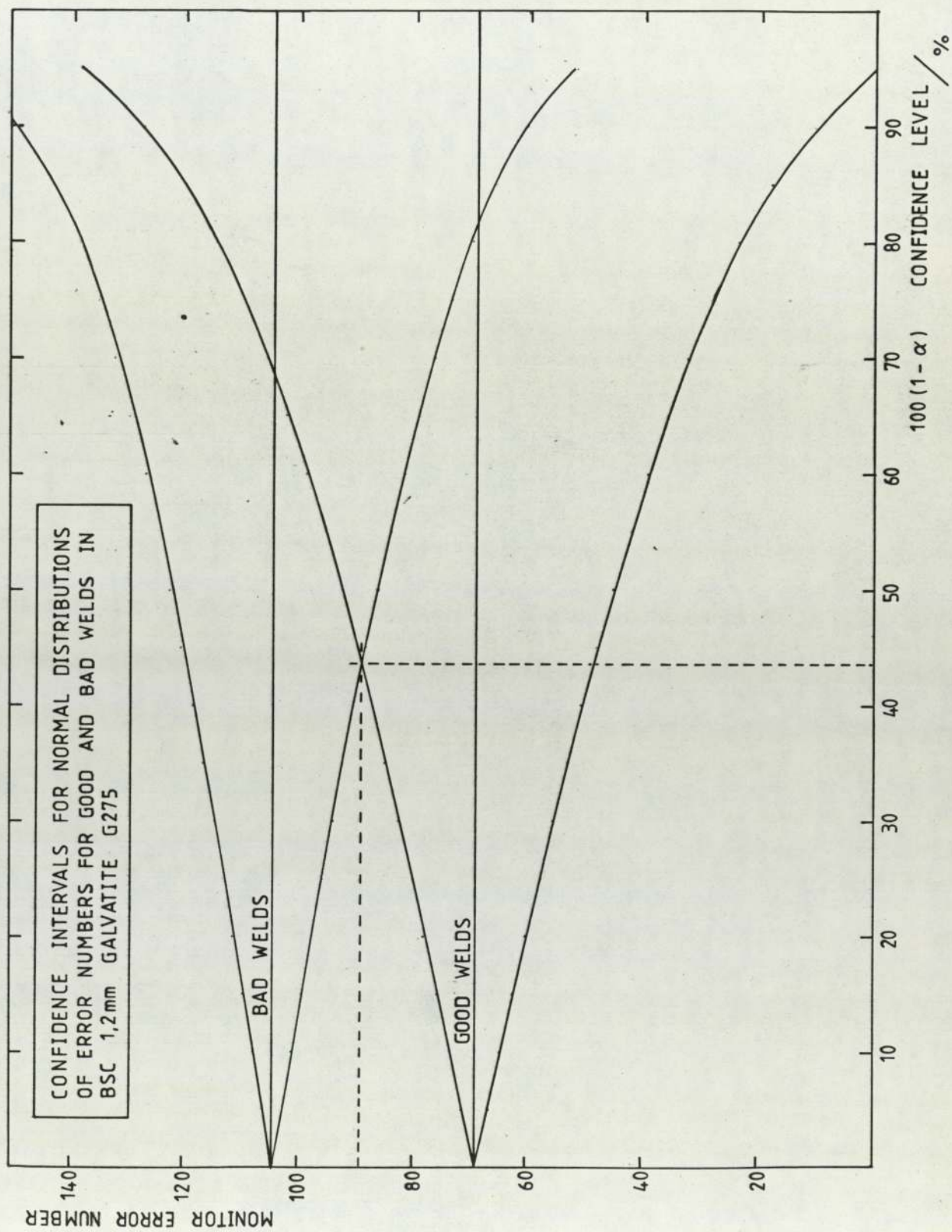


Fig. 65

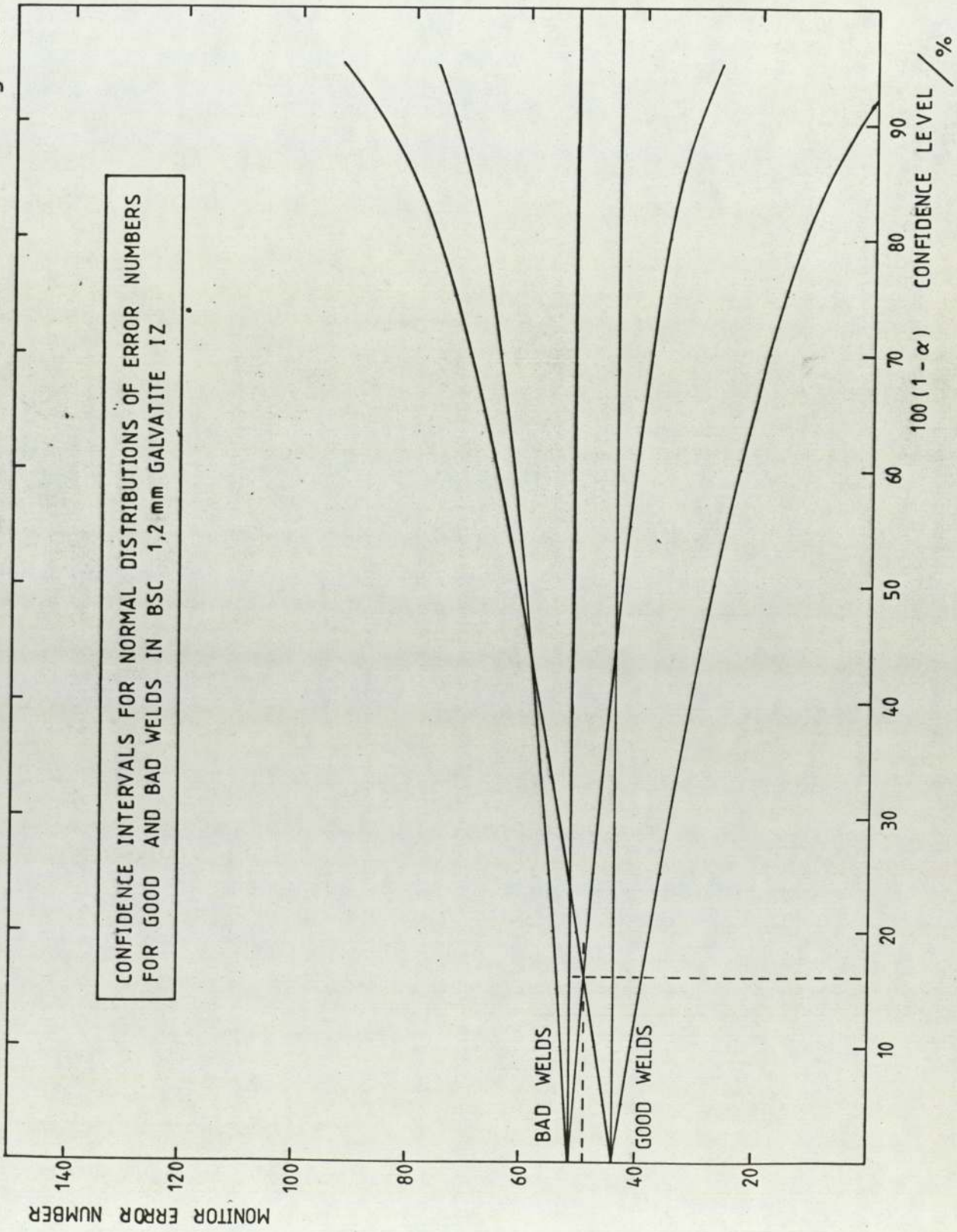
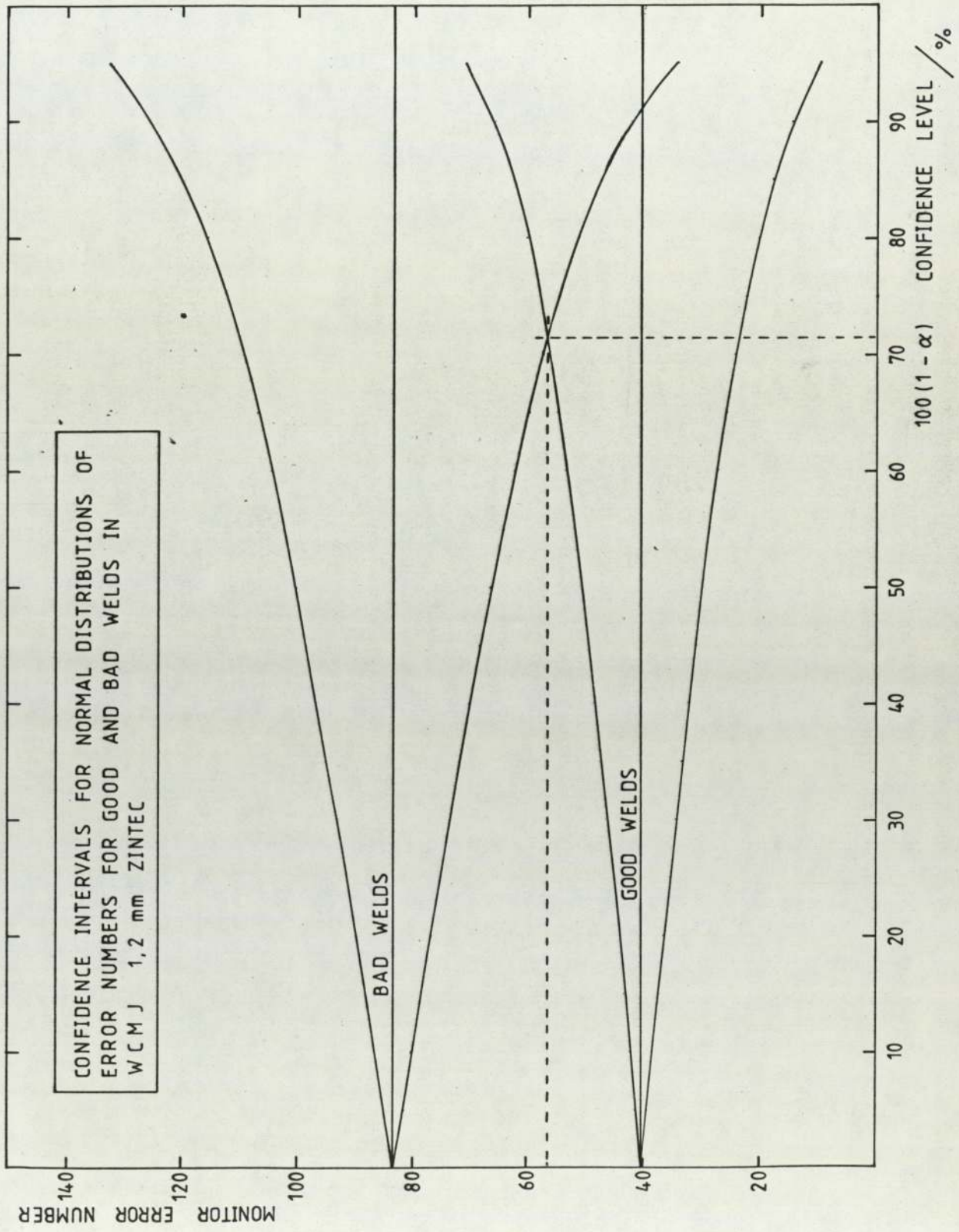


Fig. 66



point at which the upper confidence limit of the good welds and the lower confidence limit of the bad welds cross can be taken as a very good estimate of the reliability of the welding monitor for the particular material. Whilst the reliability of the monitor may be found by inspection of the graph, it is possible to determine the value algebraically. Since, at the point at which the two lines cross:

$$(\bar{x}_g + Z_{\alpha/2} \cdot \sigma_g) = (\bar{x}_b - Z_{\alpha/2} \cdot \sigma_b),$$

then:

$$Z_{\alpha/2} = (\bar{x}_b - \bar{x}_g) / (\sigma_b + \sigma_g)$$

where the subscripts 'b' and 'g' represent bad and good welds respectively. The value of  $\alpha/2$  may be obtained directly from  $Z_{\alpha/2}$  by reference to tables of percentage points of the normal distribution. Hence the percentage reliability,  $100(1 - \alpha)$  may be determined. The values of  $100(1 - \alpha)$  for the materials under investigation are given in Table 14.

Table 14: Percentage Reliabilities for Weld Monitor

Material	$Z_{\alpha/2}$	$\alpha$	$100(1 - \alpha)$
W.C.M.J. Galvatite G275	0.617	0.54	46 %
B.S.C. Galvatite G275	0.596	0.55	45 %
B.S.C. Galvatite IZ	0.202	0.84	16 %
W.C.M.J. Zintec	1.059	0.29	71 %

It is obvious that the reliability of a monitoring system should be as high as possible and it is clear that the 16% reliability when monitoring iron-zinc alloy-coated material is far from acceptable. However it must be remembered that the two peaks for good and bad welds were very close together, and this suggests that the lack of discrimination for this material may result from an incorrect choice of the initial master weld.

The reliability figures for W.C.M.J. Galvatite (46%) and B.S.C. Galvatite (45%) are very similar. This suggests that, despite differences in weldability and electrode life between these materials, the monitoring characteristics are consistent. The only material for which the monitor gave acceptable reliability was the electrozinc coated "Zintec", but even in this case the reliability of 71% is much lower than the 95% or above which would be desirable for any application which was in any way safety-critical.

As was discussed earlier in this section, the amount of scatter in the monitor error number appears to results from variations in coating thickness. Since only the initial portion of the dynamic resistance curve is produced before the coating is displaced from between the electrodes, and that the monitor error number is the numerical value of the maximum deviation of the weld under test from the master weld, it is likely that the scatter can be significantly reduced by ignoring that portion of the dynamic resistance curve caused during coating removal. Recent work at the

University of Birmingham has concentrated on improving discrimination by "weighting" significant portions of the dynamic resistance curve. Whilst reporting this work in detail is outside the scope of this thesis, it can be reported that preliminary results are most encouraging.

## 6. CONCLUSIONS

- 6.1: Anomalies were found between the weldability and electrode life behaviour of the two types of spangle galvanised steel examined. Whilst the poorer quality material required higher electrode force and welding current than the prime material, the electrode life for the prime material was some 40% shorter. However the validity of this result should be carefully assessed by duplication of the experiment before the accepted wisdom that increased current and electrode force play a major role in reducing the electrode lives for coated steels may be dismissed.
- 6.2: If the longer of the two electrode lives for spangle galvanised material is taken as normal, the electrode lives of all three materials were found to lie within  $\pm 3.7\%$  of the mean value of 2942 welds. The similarity of these results strongly suggests that the composition, thickness and surface finish of coatings have no effect on electrode life. Again, this must be subject to confirmation by repetition since it conflicts with received wisdom on the use of iron-zinc alloy coatings in particular.
- 6.3: The use of "pimpel" type electrodes appeared to have a disastrous effect on electrode life. Whilst it may be that the welding conditions used were outside the optimum range for these electrodes, it is considered

that the use of electrodes so sensitive to changes in conditions of use would be impractical under industrial conditions.

6.4: The reliability of the welding monitor under test was determined in terms of percentage reliabilities for each of the four materials. The reliability of the monitor for the iron-zinc alloy material, at only 16% is totally unacceptable, whilst 71% for the electro-zinc coated material is satisfactory but only for non safety-critical applications. The reliabilities for monitoring of welds in spangle galvanised material fall mid-way between the other values at 45% and 46%. When it is considered that a purely random choice between accept and reject for each weld, by tossing a coin for example, gives a "reliability" of 50% it can be seen that these values are also unsatisfactory.

#### 6.5: Post Script

Work on monitor reliability after the end of this author's experimental work has led to a much improved version of the monitor using weighting of the most important parts of the dynamic resistance curve. This suggests that the problems associated with monitor reliability stem from random variations in dynamic resistance at the extremes of the welding cycle.

Plate 1 (overleaf)

British Federal Single-phase Pedestal Welder

Plate 2 (overleaf)

British Federal S3 HUD/3 Welder Control Panel

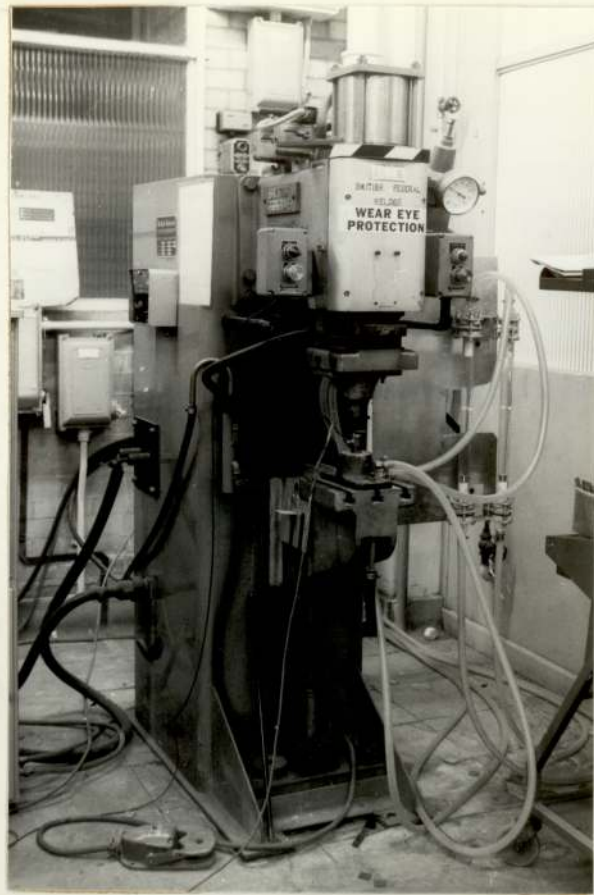


Plate 1



Plate 2

Plate 3 (overleaf)

Position of Voltage Terminals on Electrodes

Plate 4 (overleaf)

Position of Hall-effect Probe in Throat of  
Welding Machine

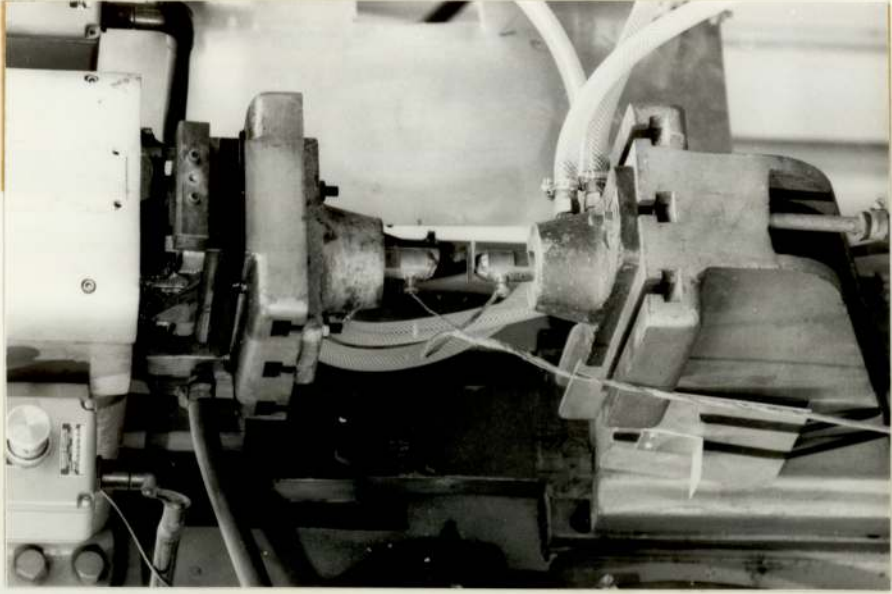


Plate 4



Plate 3

Plate 5 (overleaf)  
Resistance Welding Monitor

Plate 6 (overleaf)  
Pulled-slug Type Failure on Peel-test



Plate 5

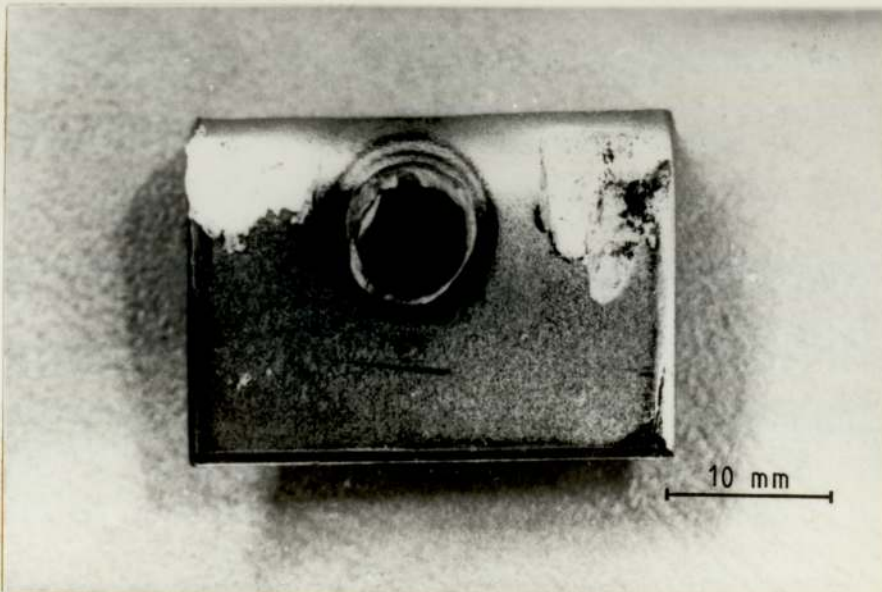


Plate 6

Plate 7 (overleaf)

Interface Shear Type Peel-test Failure

Plate 8 (overleaf)

Pulled-slug Type Peel Test Failure with  
Evidence of Expulsion ("splash")

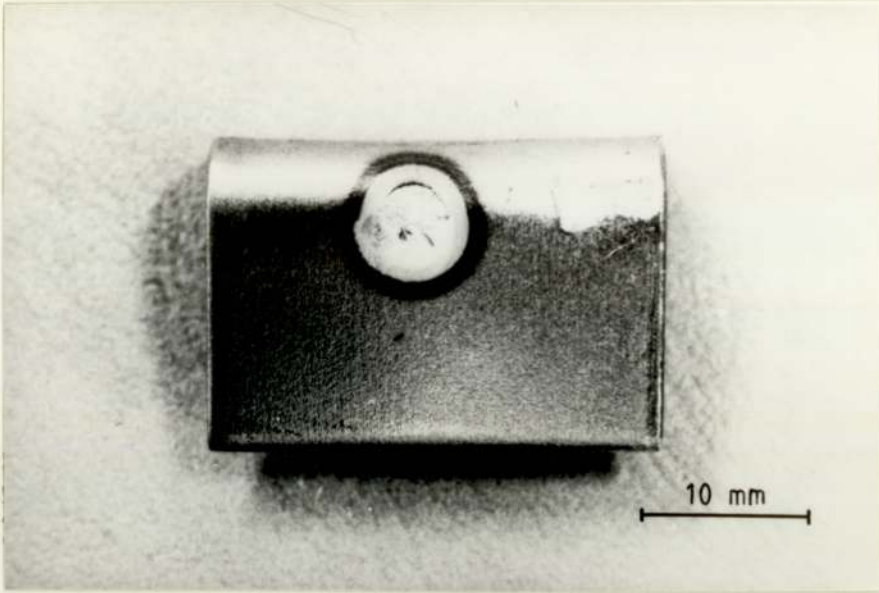


Plate 7

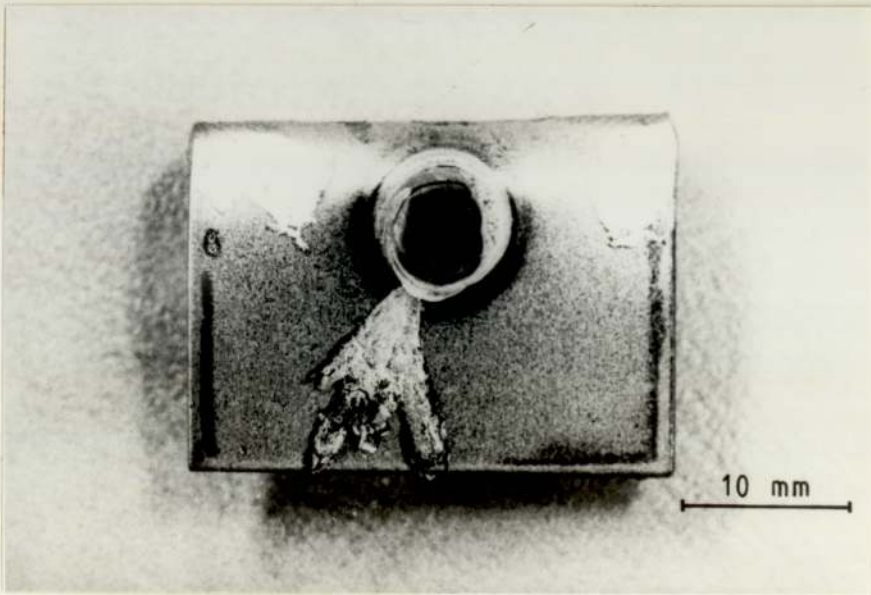


Plate 8

Plate 9 (overleaf)

Acceptable Weld in Spangle Coated Material

Etch ; 0.5% Nital : x10.8

Plate 10 (overleaf)

Commercially Produced Acceptable Weld in

Electrozinc Material.

Note lower indentation and small central cavity

Etch ; 0.5% Nital : x10.8

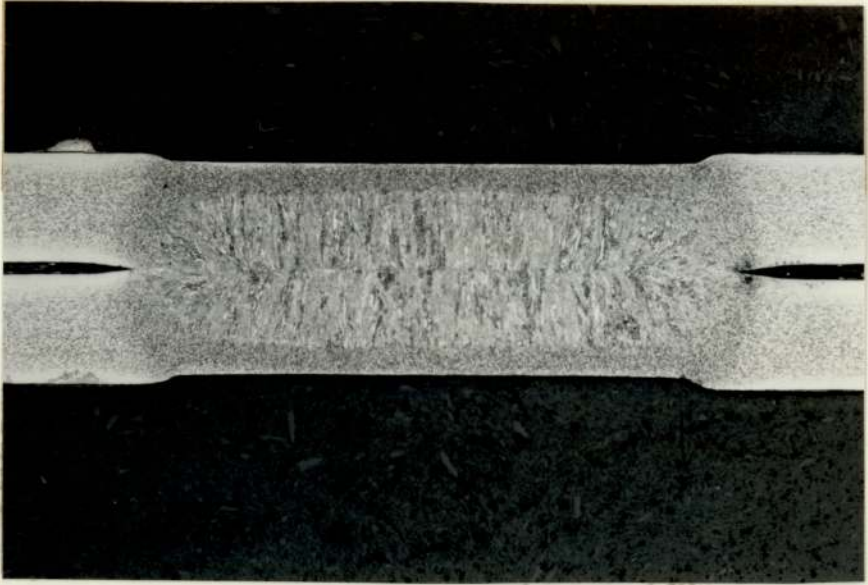


Plate 9

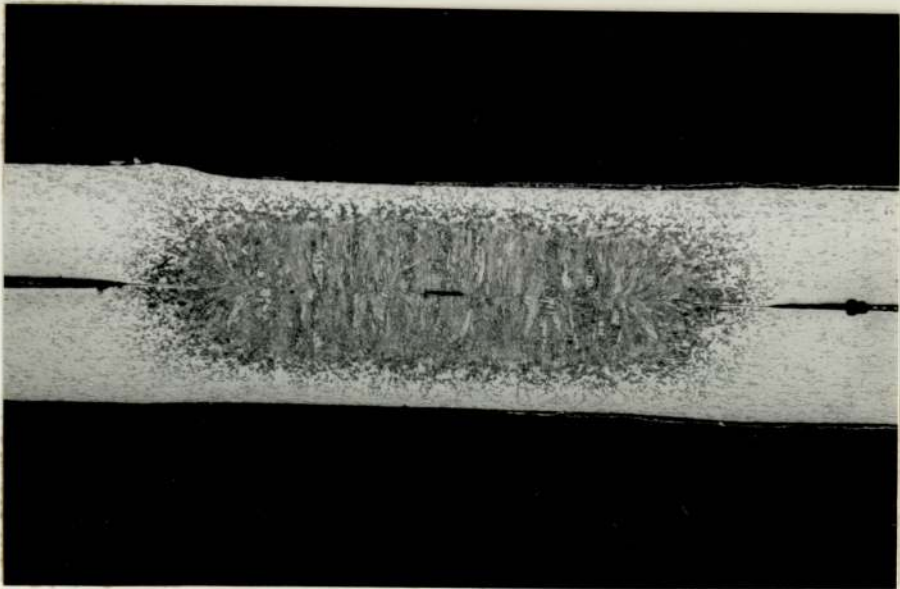


Plate 10

Plate 11 (overleaf)

Substandard Weld Exhibiting Low Penetration with a  
Small Weld and Central Cavity

Etch ; 0.5% Nital : x10.8

Plate 12 (overleaf)

Substandard Weld Showing Complete Absence of Fusion  
Except for Zinc Coating

Etch ; 0.5% Nital : x10.8

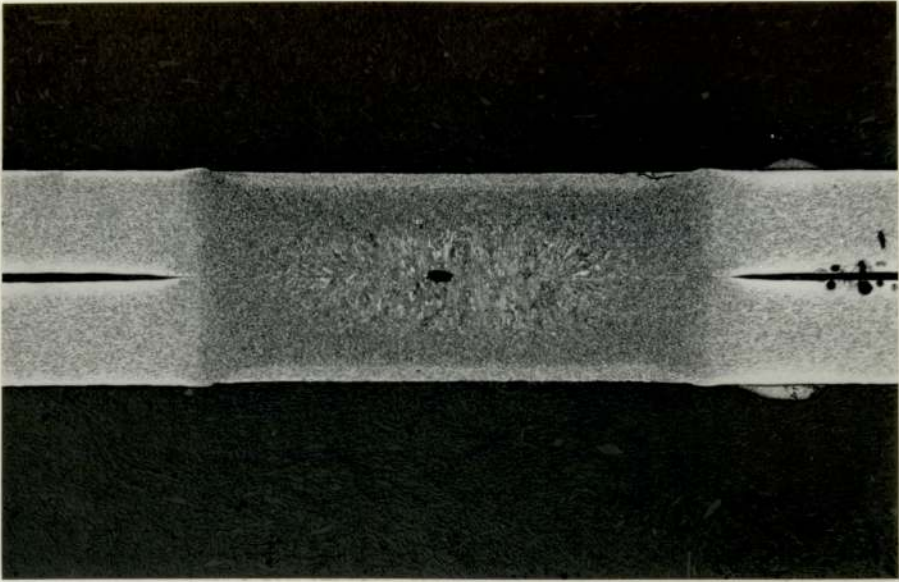


Plate 11

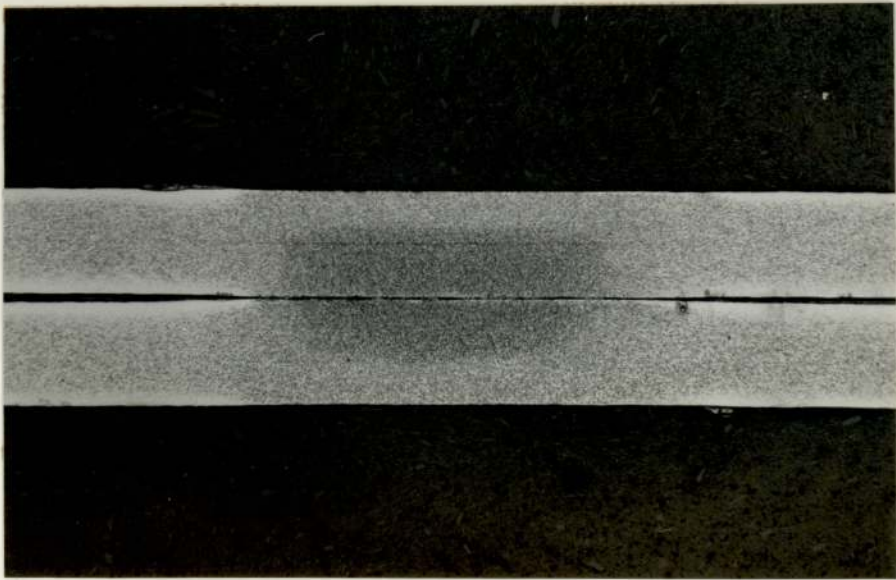


Plate 12

Plate 13 (overleaf)

"Splashed" Weld Showing Evidence of Expulsion  
and Excessive Electrode Indentation

Etch ; 0.5% Nital : x 10.8

Plate 14 (overleaf)

Splashed Weld Showing Extreme Indentation  
and Large Crack

Etch ; 0.5% Nital : x 10.8

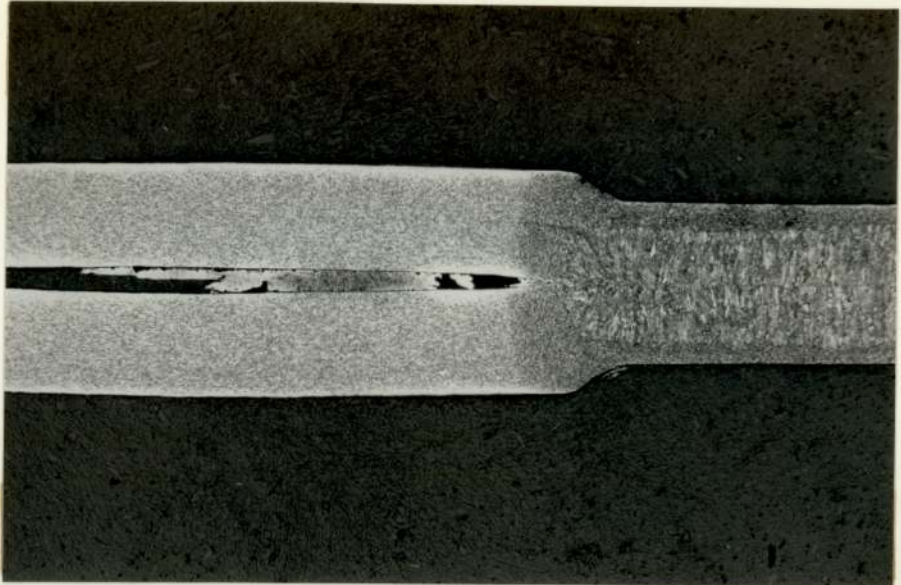


Plate 13

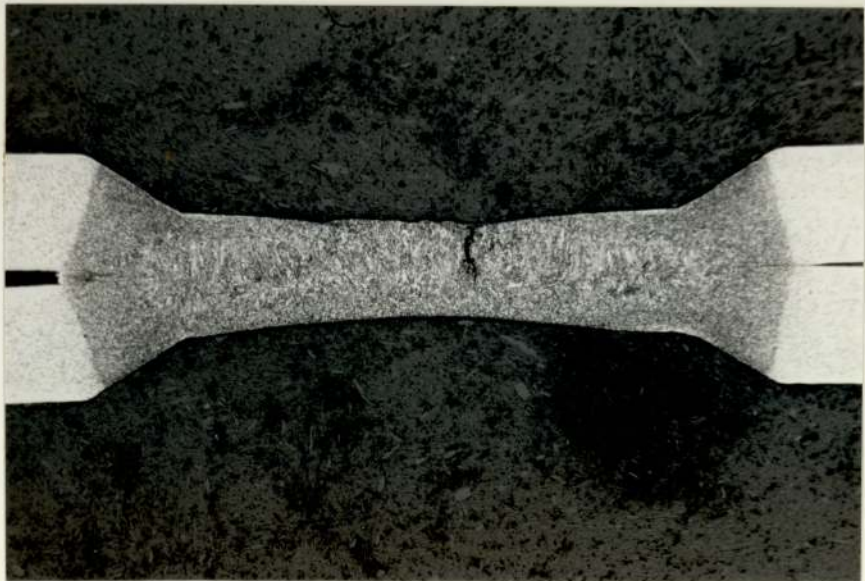


Plate 14

Plate 15 (overleaf)

Weld Produced at High Heat but Without Expulsion  
showing Excessive Indentation and Surface Crack  
Etch ; 0.5% Nital : x 33

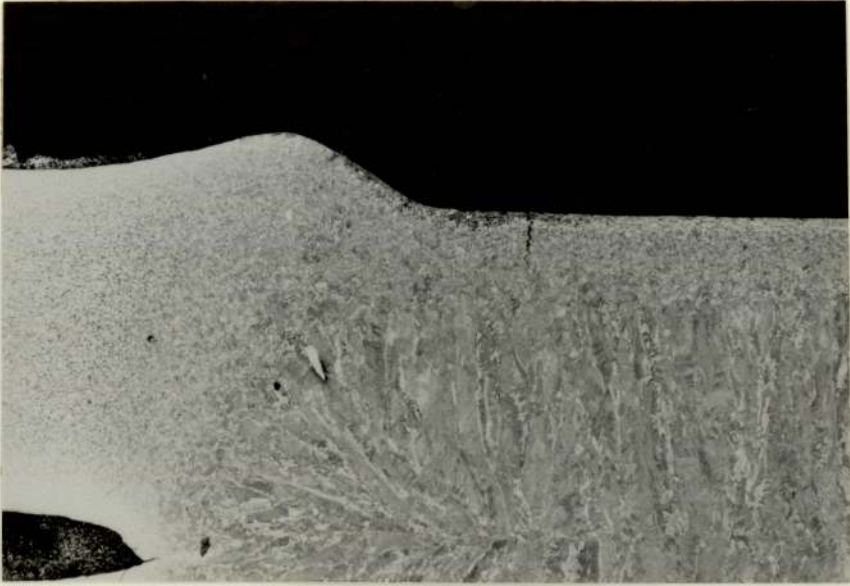


Plate 15

Plate 16 (overleaf)

Structure of Matthey 328 (Cu, 1% Cr, 0.1% Zr)

Electrode Material

Nomarski phase contrast. Unetched x 124

Plate 17 (overleaf)

Surface of Electrode showing Phase Bands

Unetched x 124



Plate 16



Plate 17

Plate 18 a/b (overleaf)

Montage showing Cracking and Spalling of Outer  
Phase Bands and Variation in Thickness

Unetched x 124

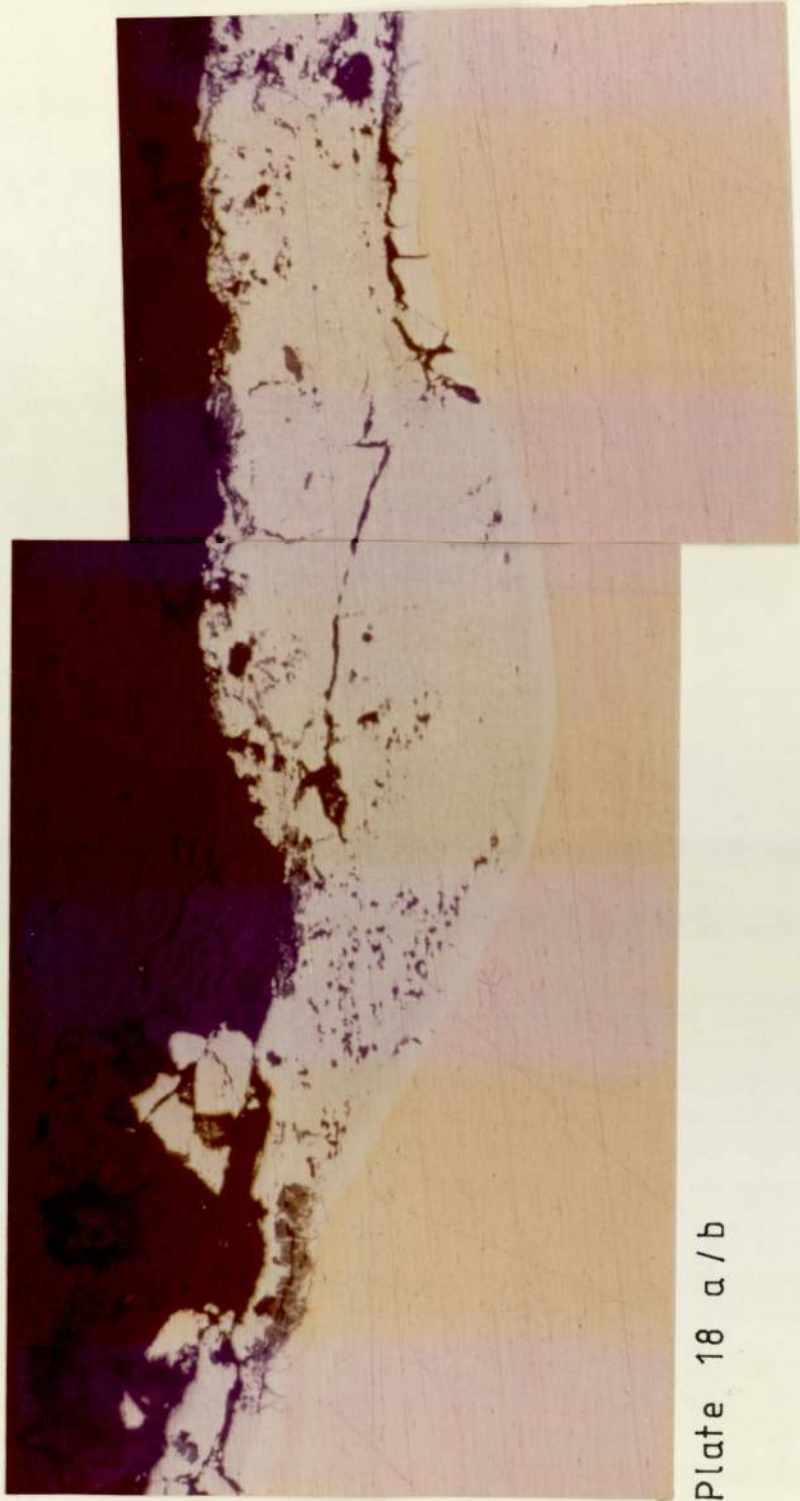


Plate 18 a / b

Plate 19 (overleaf)

Illustrating the Mechanism of Electrode Tip Spread

Unetched x 124



Plate 19

Plate 20 (overleaf)

Scanning Electron Photomicrograph showing Region  
of Electrode Spread

Unetched. Magnification as shown

Plate 21 (overleaf)

Scanning Electron Photomicrograph showing Detail  
of Phase Layers

Unetched. Magnification as shown



Plate 20

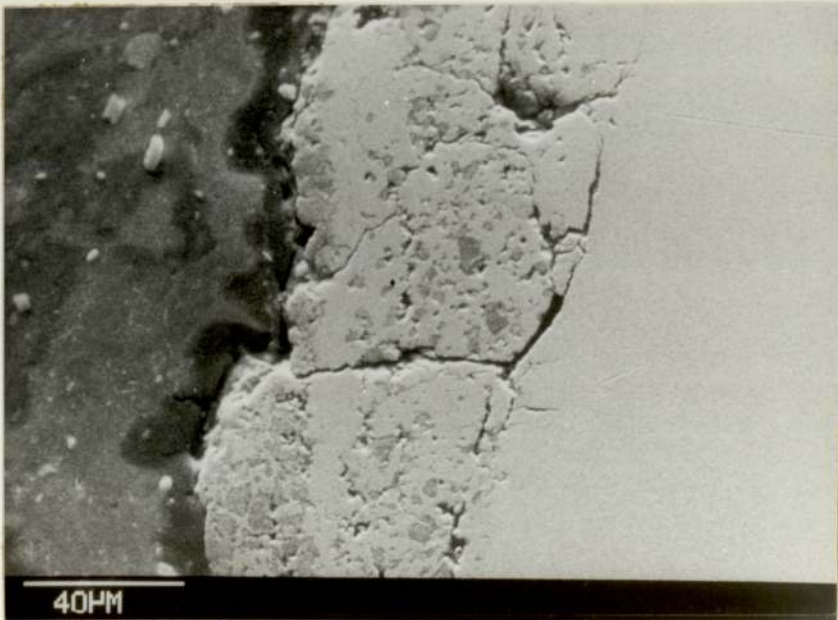


Plate 21

Plate 22 (overleaf)

Scanning Electron Photomicrograph of Phase Layers  
showing Position of Line Concentration Profile  
Unetched. Magnification as shown

Plate 23 (overleaf)

Zinc Line Concentration Profile Corresponding to  
Plate 22

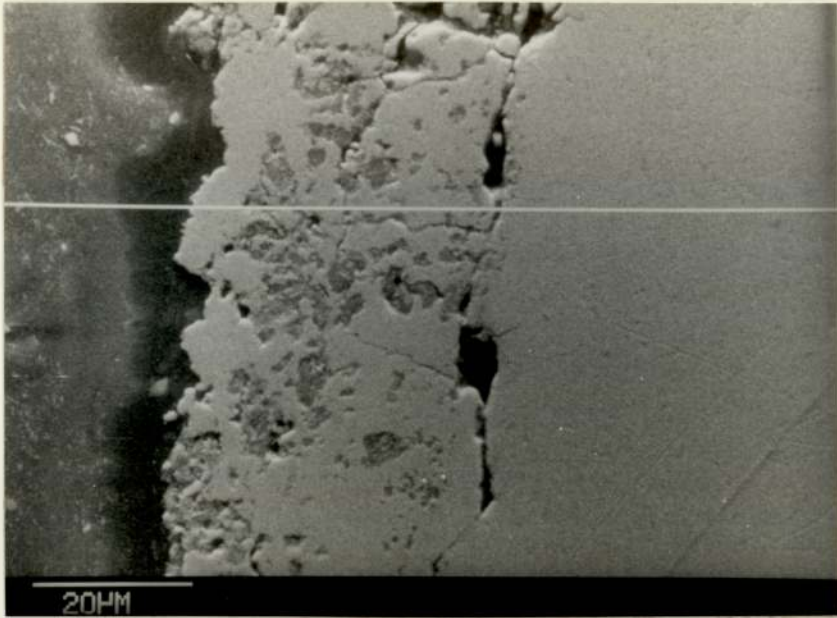


Plate 22

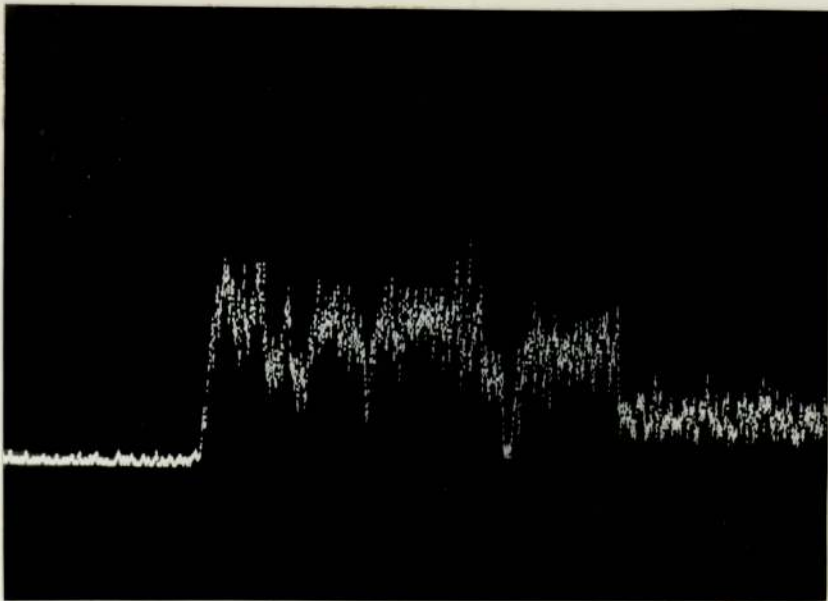


Plate 23

Plate 24 (overleaf)

Copper Line Concentration Profile Corresponding  
to Plate 22

Plate 25 (overleaf)

Iron Line Concentration Profile Corresponding  
to Plate 22

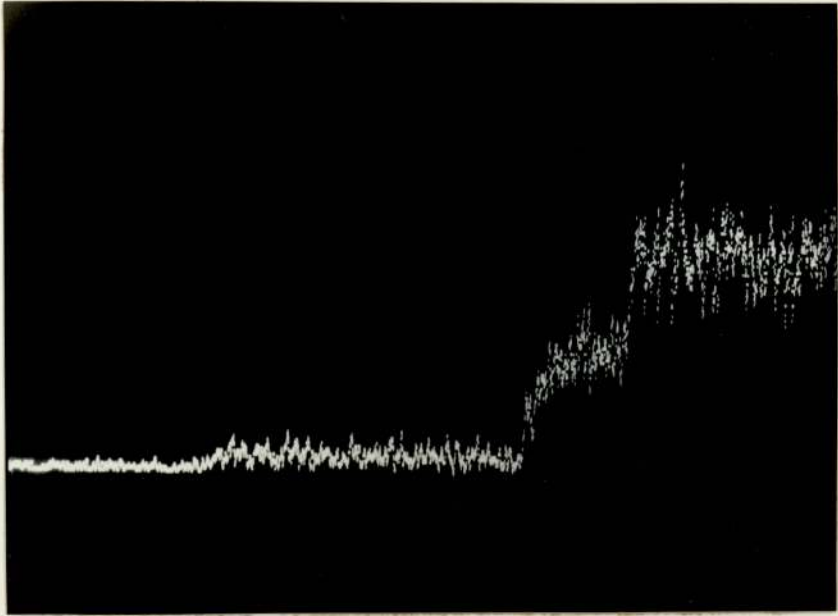


Plate 24

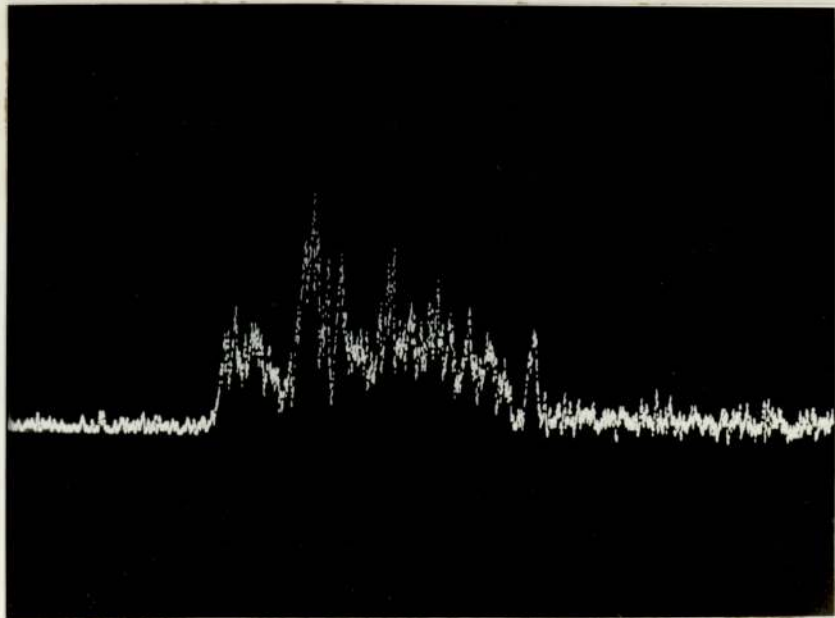


Plate 25

Plate 26 (overleaf)

Coating Morphology for Hot Dipped Galvanised Steel

Unetched. x 500

Plate 27 (overleaf)

Coating Morphology for Electro zinc Coated Steel

Unetched. x 500

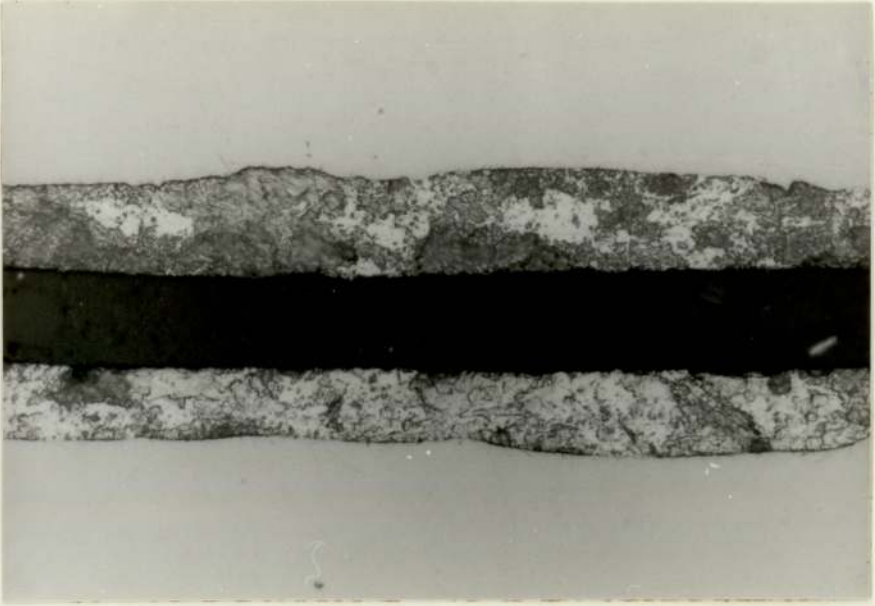


Plate 26



Plate 27

## REFERENCES

- AWS : 1980 : Welding Handbook 7th ed. Vol.3  
(American Welding Society) 1980
- AWS : 1982 : Welding Handbook 7th ed. Vol.4, p.68  
(American Welding Society) 1982
- M.Abramowitz and I.A.Stegun:  
"Handbook of Mathematical Functions"  
(New York: Dover Publications) 1972
- BS 1140 : 1980 :  
"Resistance Spot Welding of Uncoated and  
Coated Low Carbon Steel"  
(British Standards Institution) 1980
- BS 1449: Part 1: 1972 :  
"Specification for Steel Plate, Sheet and  
Strip" Part 1  
(British Standards Institution) 1972
- BS 4215: 1967 :  
"Spot Welding Electrodes and Electrode  
Holders"  
(British Standards Institution) 1972
- B.J.Brinkworth :  
"An Introduction to Experimentation"  
2nd ed. pp.102 - 109  
(London: Hodder and Stoughton) 1973

D.W.Dickinson et al. :

Welding Journal 59 (6) 1980  
pp.170 - S - 176 - S

M.Evrard: Ed. proc. 7th Int. Conf. Hot Dip Galv.  
Paris 1964 pp.317 - 343  
(Oxford : Pergamon) 1967

N.A.Freytag : Ed. proc. 7th Int. Conf. Hot Dip Galv.  
Paris 1964 pp.368 - 390  
(Oxford:Pergamon) 1967

F.J.Ganowski and N.T.Williams :

Conf. Steel Sheet and Strip Wldg., 1, pp.64 - 74  
(Cambridge : Welding Institute) 1973

W.Glage: Ed. proc. 9th Int. Conf. Hot Dip Galv.  
Dusseldorf 1970 pp.321 - 337  
(London : Industrial Newspapers) 1971

Jan Holásek : Compilation of research work accomplished  
in the Welding Research Institute  
(Bratislava) 1974 pp.54 - 62

R.W.K.Honeycombe :

"Steels, Microstructure and Properties"  
(London : Edward Arnold) 1981 pp.98 - 102

F.C.Porter : Metal Construction, 15, (11) Nov.1983  
pp.676 - 679

E.C.Rollason: "Metallurgy for Engineers" 4th ed. p.163  
(London : Edward Arnold) 1973

N.T.Williams and R.C.Lavery :

Ed. proc. 9th Int. Conf. Hot Dip Galv.

Dusseldorf 1970 pp.338 - 354

(London : Industrial Newspapers) 1971

N.T.Williams: Conf. Steel Sheet and Strip Wldg., 1, pp.50 - 57

(Cambridge : Welding Institute) 1973

N.T.Williams : Welding and Metal Fabrication, 45, 5,

June 1977, pp.275 - 288

N.T.Williams : The Metallurgist, February 1981 pp.85 - 89

P.N.Whateley : "Investigation of the Phases Appearing in a  
Copper - Zinc Diffusion Couple" (unpublished)

1978